# THE DESIGN AND TESTING OF A VAPOUR PUMP IN THE ABSORPTION REFRIGERATION CYCLE

BY

E. KRAFFT

April 1995

Submitted to the University of Cape Town
in partial fulfilment of the requirements
for the degree of Masters of Science

Supervisor: G. Vicatos

# Acknowledgement

The author wishes to sincerely thank the following:

Mr G Vicatos, supervisor of the project, for his invaluable assistance, encouragement throughout the thesis and the many hours revising the manuscript.

Mr H Emmerich for the professional manufacture of the vapour pump.

Mr M Jolivet for his assistance with the construction of the experimental apparatus.

Mr L Watkins for his friendly assistance in overcoming all sorts of technical problems.

# Synopsis

This thesis presents a new pumping method in absorption refrigeration. A vapour pump, powered by a fraction of the high pressure refrigerant, is proposed to replace the conventionally used electric pump. The only energy required to power the cycle is the heat supplied to the generator. The system thus becomes completely independent of the availability of electricity and can be driven by low grade energy such as waste heat.

The literature review reveals that pumping has been a central problem to the development of absorption refrigeration. Since its inception early in the 18th century, many designs of absorption machines were put forward to overcome the pumping problem. They include the three fluid system ('candle' fridge), systems where circulation is based upon gravity and the thermosyphon effect and some more recent systems (thermal pump, membrane separation). Though having been successful to a varying degree in domestic refrigeration, above systems do either not work reliably or do not have a large refrigeration capacity. For larger applications an externally driven pump (usually electric) has to be relied upon.

The absorption cycle -vapour pump system is modelled by a computer simulation. The simulation investigates the thermodynamic stability of the cycle and predicts how the cycle behaves when changing the operating conditions (generator-, evaporator and sink temperature). The design of a prototype vapour pump is presented together with the results of the experimental investigation

The pump is of the positive displacement type with two 180 degrees opposed pistons doing the pump work. Movement of the

pistons is achieved by exploiting the pressure difference between generator and absorber. A control mechanism regulates the direction of piston movement.

The simulation shows that the coefficient of performance (COP) is typically around 0.47 as compared to the ≈0.60 for an absorption machine using an electric pump. The maximum COP for the vapour pump system occurs at higher generator temperatures compared to the electric pump system. The experimental tests confirm in principle that the vapour pump system works and that the COP decreases when changing from an electric pump to the vapour pump.

Future experimental work to verify the simulation predictions is recommended. Various improvements on the cycle and pump, aimed at obtaining more accurate results, are proposed.

# Table of Contents

**Appendices**

# List of Illustrations

## List of Tables

# NOMENCLATURE

| | |
|---|---|
| A | area |
| D | diameter |
| E | energy |
| F | force |
| H | enthalpy |
| I | moment of inertia |
| L | stroke length |
| P | pressure |
| T | temperature |
| V | volume |
| Q | volume flow rate; power |
| | |
| freq | stroke frequency |
| h | specific enthalpy |
| m | mass flow rate |
| x | solution refrigerant concentration |
| y | vapour refrigerant concentration |
| st | denotes strong solution |
| we | denotes weak solution |
| | |
| $\Delta$ | difference |
| $\eta$ | efficiency |
| $\rho$ | density |
| $\sigma$ | tensile/compressive stress |
| $\tau$ | shear stress |
| $\upsilon$ | specific volume |

# CHAPTER 1

## 1.1 Introduction

A new pumping method in absorption refrigeration is introduced in this study. In conventional absorption refrigeration an externally driven pump returns the strong solution from the absorber to the generator. The proposed new pump, replacing the conventionally used one, is termed 'vapour pump' as it is powered by a fraction of the high pressure vapour mixture that is liberated in the generator. This thesis presents the design and experimental investigation of a vapour pump in the absorption refrigeration cycle.

Absorption refrigeration has to a large extent, especially in domestic refrigeration, given way to compression refrigeration; mainly because of the latter's superiority in energy efficiency and ease of control. With the ever increasing cost of high grade energy, absorption refrigeration is regaining interest, especially where low grade waste heat is available. However, its applicability becomes questionable in areas where electricity is not available because of its externally driven pump. The introduction of the proposed vapour pump allows for an exclusively heat powered cycle, rendering the refrigerator independent of the availability of electricity.

The objectives of the thesis were to design, construct and test a vapour pump for use in absorption refrigeration machines. Testing of the vapour pump was done:

i) by experimentation with the prototype vapour pump. The experiments were conducted in the Mechanical Engineering

department and therefor limited to the absorption refrigeration plant facilities available.

ii) theoretically by a computer simulation. Vicatos [24] has developed a model for the ammonia-water cycle. This simulation, amended to include the vapour pump, is used for the theoretical prediction of the cycle behaviour.

The absorption refrigeration machine in the department was subsequently altered to operate with Freon R22 and tetra ethylene glycol dimethyl ether (E181). Only very limited thermodynamic data has been published on the R22-E181 binary system (Mastrangelo [14] and by Kriebel et al [12]) and it proved beyond the scope of this thesis to produce a simulation for the R22-E181 absorption machine. The refrigerant flow rates of the two systems for equal refrigeration capacity, and the corresponding coefficient of performances, are similar (Pearson [16]). The vapour pump (material, sealing) is designed to operate in a R22-E181 environment.

Refrigeration history with emphasis on absorption refrigeration is presented in the remainder of chapter 1. The development of the absorption refrigeration machine is traced from its origin to modern time. Chapter 2 deals in more detail with the conventional absorption cycle and the working fluids commonly used. Chapter 3 introduces the vapour pump, describing its principle of operation and the modified absorption cycle. A detailed design of the vapour pump is presented in chapter 4, followed by a discussion of the theoretically predicted pump behaviour in chapter 5. Chapter 6 is concerned with the experimental testing of the vapour pump and the performance of the cycle with the vapour pump.

## 1.2 History of absorption refrigeration

### 1.2.1 General

The practice of cooling bodies below the temperature of the atmosphere has been followed for centuries. In earlier times the means of cooling was provided by nature itself: ice that formed on rivers and lakes in the cold winter months and snow. A bulletin entitled "The Romance of Ice", published by the National (American) Association of Ice Industries tells of some very early refrigeration: the early Greek poet Simonides observes at a banquet that the liquor served to guests is cooled by snow; Alexander the Great had trenches dug for storing snow, in which hundreds of kegs of wine were cooled; Emperor Nero had slaves bring down snow from the mountains, also to cool his wines. The bulletin also claims that the ancient Egyptians knew the secret of cooling by evaporation as still practised by the natives of India today (shallow trays of porous material filled with water, exposed to the night winds, produce a thin film of ice on the surface). Up to the last half of the nineteenth century ice, that was harvested in the winter, was stored in caves in the ground for use during the warm summer months. Hull [10] reports that the first record of American delivery of ice to the home was in 1802. In 1805 Frederick Tudor of Boston exported a shipment of natural ice to Martenique in the West Indies to help stay the ravages of yellow fever. It was only around the middle of the nineteenth century that means were devised whereby ice for refrigeration purposes could be manufactured in commercial quantities. And it was only in this very century that machines for direct -that is without having to produce ice first- home refrigeration have been developed. Inventors of the past have proposed a number of cooling machines; the 'Gorrie Air Machine', the 'Kirk Air Machine', the Allen Dense Air Machine', 'Absorption Machines' and 'Vapour

Compression Machines' to name a few. All machines function upon the same physical phenomenon, namely cooling by expansion and/or evaporation. Basically all modern day refrigeration machines are either of the compression or absorption type and it is the latter with which this thesis is concerned.

### 1.2.2 Development of absorption refrigeration

In 1824 Michael Faraday, working in the Royal Institution of London, succeeded in condensing ammonia gas to a liquid ,which until then was believed to only exist as a vapour. Faradays experimental apparatus consisted of a closed inverted 'V' tube. One end of the tube contained silver chloride crystals, which had absorbed some ammonia gas. The other end was immersed into cold water. The silver chloride crystals were then externally heated by a flame. The ammonia gas, that was liberated and driven off, turned into liquid at the opposite end after being cooled by the cold water. Then Faraday removed both the heat source and the cooling water. As a result the liquid ammonia rapidly evaporated back into a vapour which was then reabsorbed by the crystals. The end that had contained the liquid was found to be extremely cold, as the ammonia had drawn heat from the environment while evaporating. It is the latent heat that the surrounding supplies to the substance. And so, while the liquid evaporates at constant pressure and temperature, the environment looses some of its (heat) energy and consequently drops in temperature. It is this experiment of Faraday that is often named as the origin of absorption refrigeration.

Although Ferdinand Carré is usually credited with the development of the first absorption refrigeration machines (about 1858-1860), both Hull [10] and Macintire [13] mention that Professor Leslie already employed the principle in 1810. Those early machines made use of a liquid absorbent; sulphuric

acid to absorb water (Leslie, Carré and Windhausen (1878)) or water to absorb ammonia (Carré). Carré's continuous absorption refrigeration system is schematically shown in the figure 1.1.

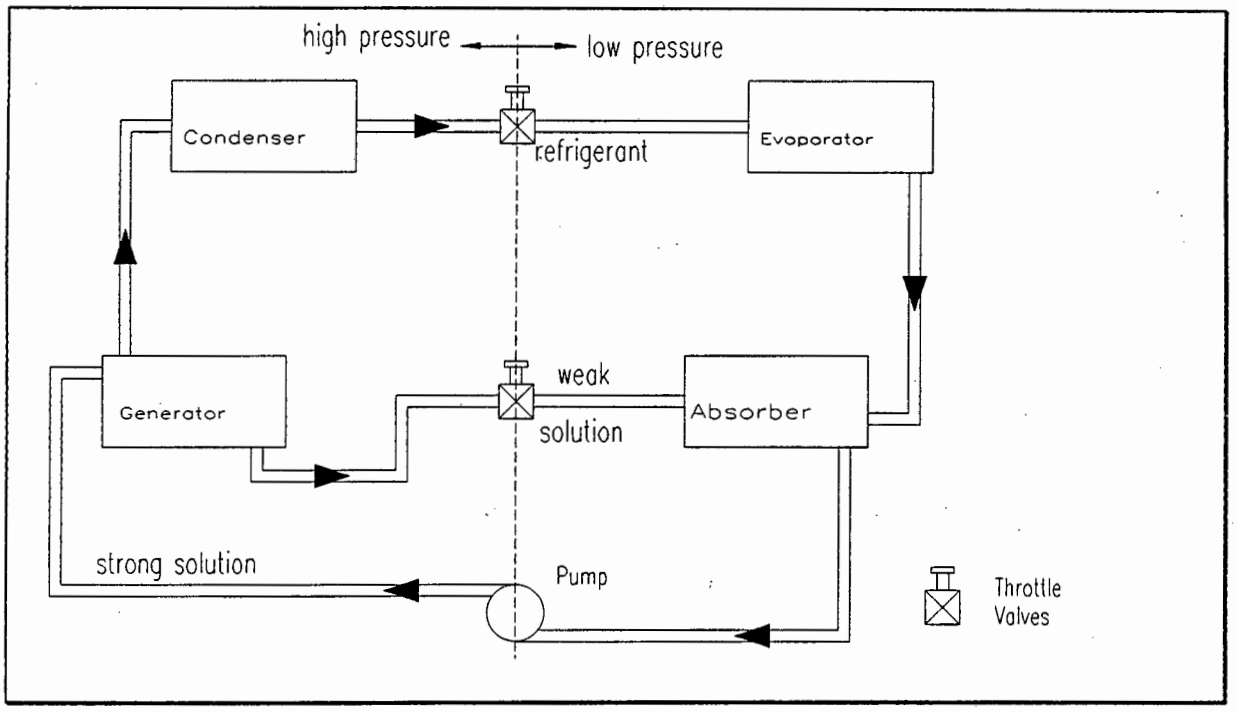


**Figure 1.1** Schematic diagram of the Carré absorption refrigeration machine (continuous operation type)

The machine works on the principle of ammonia dissolving in water. Ammonia, having a high affinity for water, is absorbed at low temperature and a pressure considerably above atmospheric. The mixture is returned to the generator by means of a pump. Heat is supplied to the generator and ammonia boils off at high pressure. The ammonia vapour is liquefied in the condenser, then passes the throttle valve to enter the evaporator. Here heat is drawn from the environment to sustain the evaporation process. The remaining liquid in the generator, of low ammonia concentration (weak solution), returns to the absorber, driven by the pressure difference. Once inside the absorber it absorbs the ammonia vapour coming from the evaporator and the cycle repeats itself.

The original Carré machine of 1859 was somewhat more primitive, but was subsequently improved by himself, Mignon and Rouart in France, Vass and Littmann in Germany and Reece, Mort and Nicole in England.

One characteristic problem inherent in the absorption machine since its inception is that of *continuity in operation.* To ensure uninterrupted cooling a liquid pump is required to return the strong solution (refrigerant dissolved in absorbent) to the generator on a continuous basis, that is from a low to a high pressure. At the time this was no easy task and continuous absorption machines tended to be bulky and technically complicated. Plank & Kuprianoff [11] report that for this reason the continuous absorption machine remained in the domain of large industrial application, but was replaced by the absorption machine of the intermittent type on the smaller scale (e.g. home refrigeration). The intermittent machine was not a new idea; in fact both Leslie`s (1810) and Faraday`s (1824) apparatus was of this type. In machines of this kind a period of heating, during which the refrigerant was driven off the absorbent and then liquefied, was followed by a period of cooling, during which the liquefied refrigerant was evaporated and then reabsorbed by the absorbent. The process was distinctly two- staged, often requiring human presence to change from the one to the other (removing of heat source, closing and opening of valves). While this type of machine could not operate continuously, a liquid return pump was not necessary. Machines of this nature were built on a industrial scale around 1910 in the USA and in 1920 in Germany (by E. Rumpler).

On the whole, absorption refrigeration went out of fashion around the turn of the century. It lost considerable ground to its major competitor, the compression refrigeration machine.

Compression refrigeration proved to be more energy efficient and less bulky.

Around the nineteen thirties the continuous absorption machine experienced a revival, when ways and means were found to avoid the use of a liquid pump. Its development is closely associated with the names of H. Geppert, E. Altenkirch, B. von Platen, C.G. Munters and G. Maiuri. In 1899 Geppert introduced an inert (non-condensing) gas (Geppert used air) into Carré's two-fluid absorption machine to compensate for the pressure difference in the cycle. Because of the generator's higher pressure the air accumulated in the evaporator and absorber, where its partial pressure balanced the previously existing pressure difference. No pump work was required to return the strong solution to the generator since the same total pressure was prevalent throughout the system. The pressure compensating air, however, seriously suppressed evaporation of the refrigerant in the evaporator, thereby stifling the refrigeration effect. The rate of diffusion, and so of evaporation, can significantly be increased when using hydrogen instead of air. According to the kinetic gas theory, the rate of diffusion is related to the average pathlength and velocity of the molecules. Hydrogen is more suited on both accounts. Platen and Munters in Stochholm took up Geppert's idea but used hydrogen as the inert gas. The system in its most basic form is shown in figure 1.2. Heat is supplied to the generator by the electric element or flame (many flame powered absorption machines of this kind remain in operation to this day). The refrigerant, that is driven off, passes through the condenser into the hydrogen filled evaporator

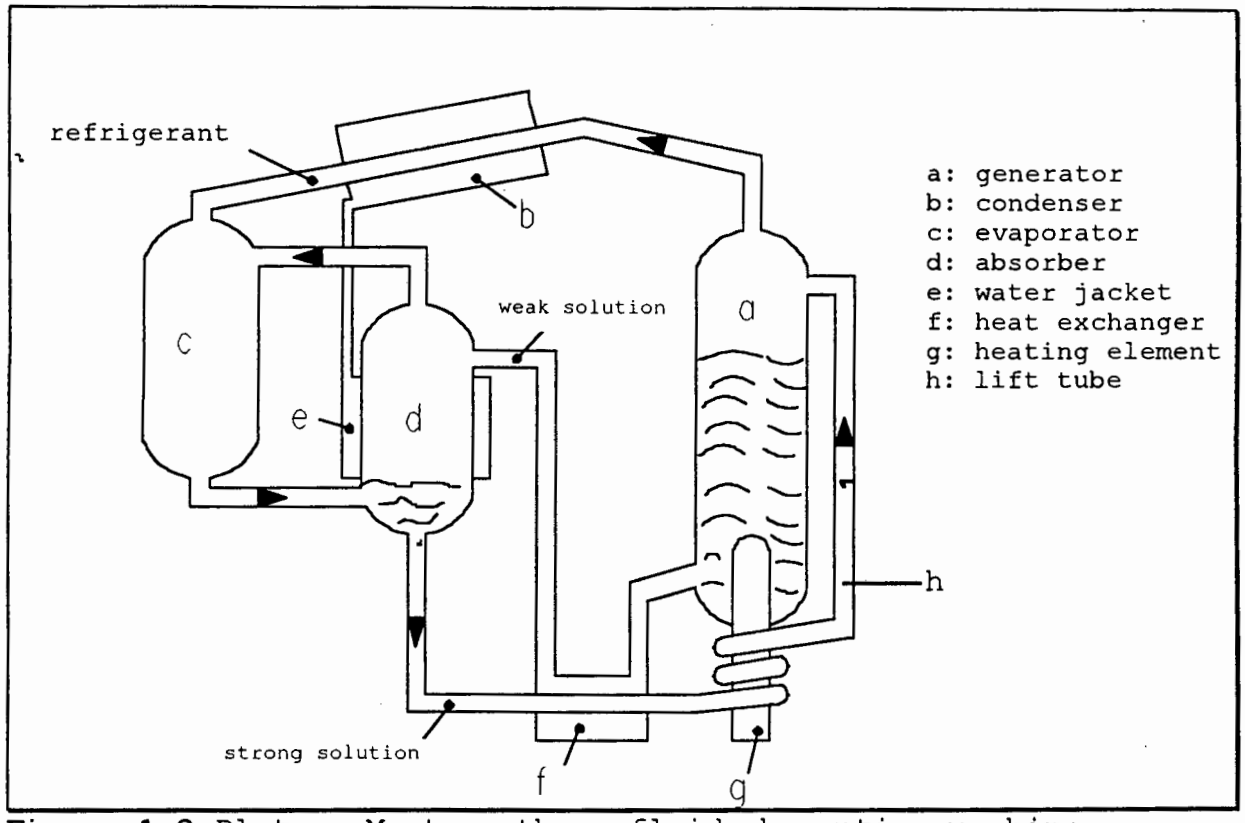


**Figure 1.2** Platen- Munters three fluid absorption machine

The evaporator is arranged above the absorber and since the ammonia rich vapour in the evaporator is heavier than the hydrogen rich vapour in the absorber circulation from one to the other is by gravity and in the direction as shown by the arrows.

With the hydrogen gas cancelling the pressure difference between absorber and generator, circulation of the weak and strong solutions is based upon a percolator type pump. The weak solution flows to the absorber under action of the liquid column in the generator, the top level of which is at the same height as the weak solutions entrance to the absorber. The weak solution absorbs the ammonia (which now becomes the strong solution) and is then returned to the generator after passing through a heat exchanger. The liquid column in the absorber pushes the strong solution into the vertical percolator pipe (h) of the generator. Here liquid is lifted into the generator container (a) under action of rising vapour bubbles (thermosyphon effect).

Machines of this type, also known as *cryotherms* because of the absence of mechanical work input, established themselves in domestic refrigeration. The larger industrial application demand a greater rate of circulation, which can not be met by thermosyphon action alone. Other limitations are that these refrigerators depend on a finely tuned arrangement. They are not very reliable and do often not function properly, especially when not standing upright or when having been transported.

Other absorption machines built around that time used a solid absorbent. They were of the intermittent type and never able to obtain a significant share of the market. Modern time has seen many improved versions of the two fluid absorption machine. While essentially still the Carré machine, successful efforts have been made to increase efficiency, incorporate automatic temperature regulation, decrease the size of the apparatus and exploit various forms of energy as powering source. Recent attention has been focused on systems being powered by waste heat and solar energy (direct or via photovoltaic cells). However, even though the greatest part of the energy input goes to the generator, the pump remains an essential part of the cycle.

## 1.3 Pumping in Absorption Refrigeration

The necessity of circulating the absorbent- refrigerant mixture is a fundamental problem to absorption refrigeration. It hindered development of absorption refrigeration for long periods of time. The already discussed Platen- Munters three fluid system originated from an effort to avoid mechanical pumping. It makes use of a pressure equalising inert gas and achieves circulation by gravity and the thermosyphon effect. Altenkirch

is credited with first having proposed this well known effect for use in absorption machines. Vapour bubbles that rise up the pipe, after some heating by the same source that powers the generator, carry and push the liquid with them.

Plank & Kuprianoff [11] report that Altenkirch has also devised a method to achieve circulation without mechanical pumping in two fluid absorption. Such a system is shown in figure 1.3. The pressure difference between generator and absorber is overcome by the height difference between the two. The absorber is arranged far above the generator, so that the pressure of the liquid column of rich solution is sufficient to bridge the pressure difference. This method only functions in machines with a relatively small pressure difference. Ammonia machines of this kind have not been built, but the principle has successfully been tested using water as refrigerant with $H_2SO_4$ as absorbent. The generator consists of the pipe coiled around the heat element b and the vessel c, in which the vapour is separated (but not formed) from the remaining (weak) solution. The pipe coiled around the heat source b serves the dual purpose of not only boiling off the refrigerant but also of acting as a percolator-type pump (making use of the thermosyphon effect already encountered in the Platen- Munters system). Machines of this type have been manufactured after the second world war (mainly for air conditioning), but again were severely limited by their small refrigeration capacity.

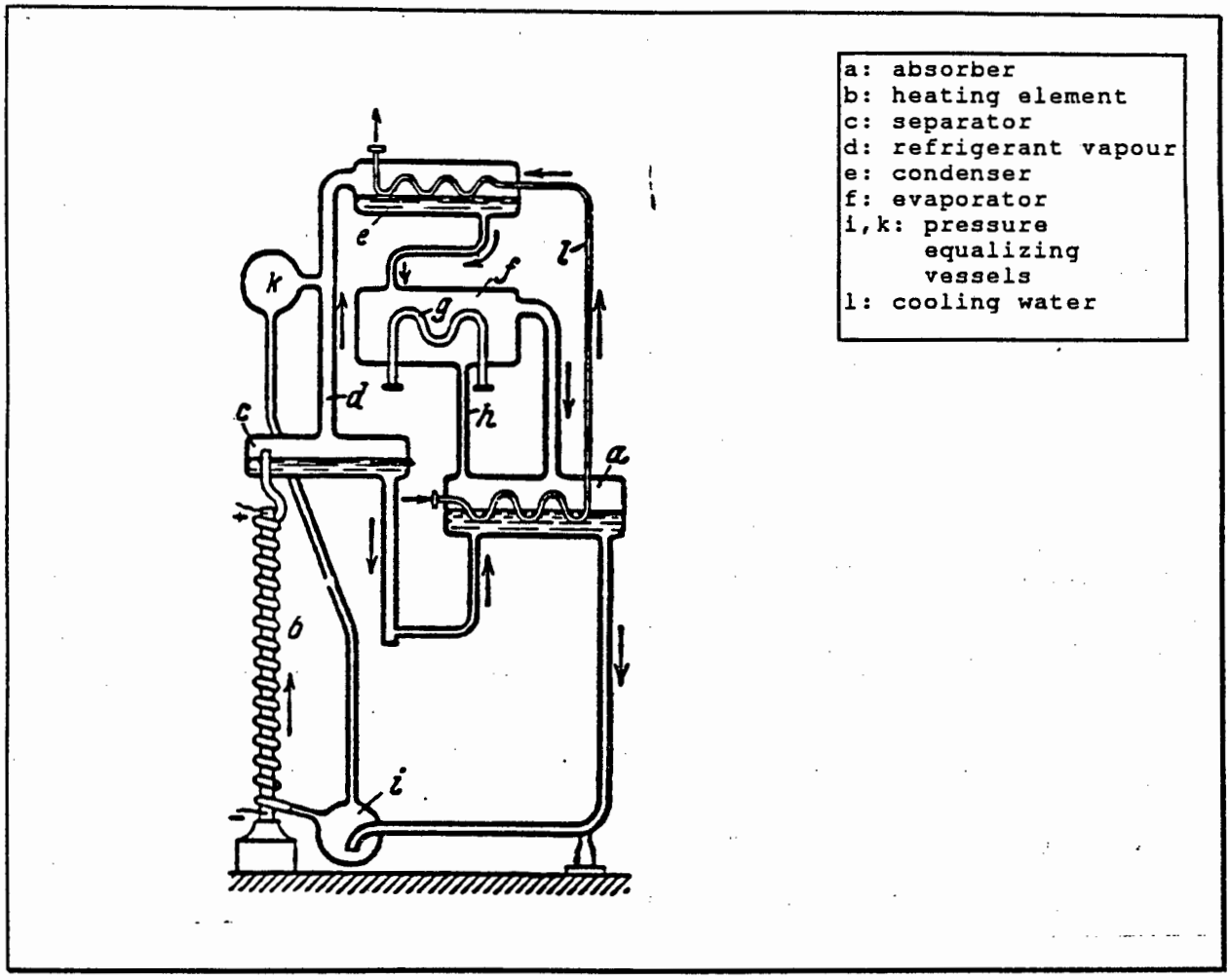


**Figure 1.3** Continuous absorption machine of the Altenkirch system (reproduced from Plank & Kuprianoff [11] (page 388))

A more recent invention has been published by Szücs [22]. He proposes to replace the pump with a radiator that is heated by the same source that powers the generator. The radiator is first flooded by the rich solution coming from the absorber. After some heating the pressure in the radiator increases to a level where more of the rich solution is prevented from entering. Once the pressure inside the radiator exceeds the one of the generator, the rich solution will be passed on to the generator. The radiator pressure drops after discharge; rich solution from the absorber floods the radiator once again, and the process repeats itself. Szücs states that the major

advantages of the cycle are the absence of any moving parts and the independence of electrical power. Vicatos [24] has experimented with a thermal pump of this kind. Electrical sensors were used to activate valves and to regulate the heating periods. Vicatos [24] reports that operation of the pump was troublesome. It did work in principle, but the COP was not observed to improve.

A design by Beasley & Hester [4] achieves absorbent- refrigerant separation by a membrane (hyperfiltration). They further recommend that some work should be recovered by the returning weak solution (high to low pressure) and envisage a work recovery turbine (driven by the weak solution) that helps to pump the rich solution. However, a secondary pump is still required and the cycle remains dependent on the availability of electricity. A great number of machines have been proposed where the whole absorber- pump- generator arrangement is replaced with some other mechanism. These machines go beyond the scope of absorption refrigeration and are not dealt with here.

To the present day two-fluid absorption refrigeration requires the presence of a liquid return pump, which means the cycle needs two energy sources (usually of different nature) to function continuously.

# CHAPTER 2

## 2 The conventional absorption refrigeration cycle

### 2.1 Principle of operation

The absorption cycle shown in figure 1.1 is in its most basic form. In practise a modified cycle is employed to achieve better efficiency. Figure 2.1 shows such an cycle arrangement.

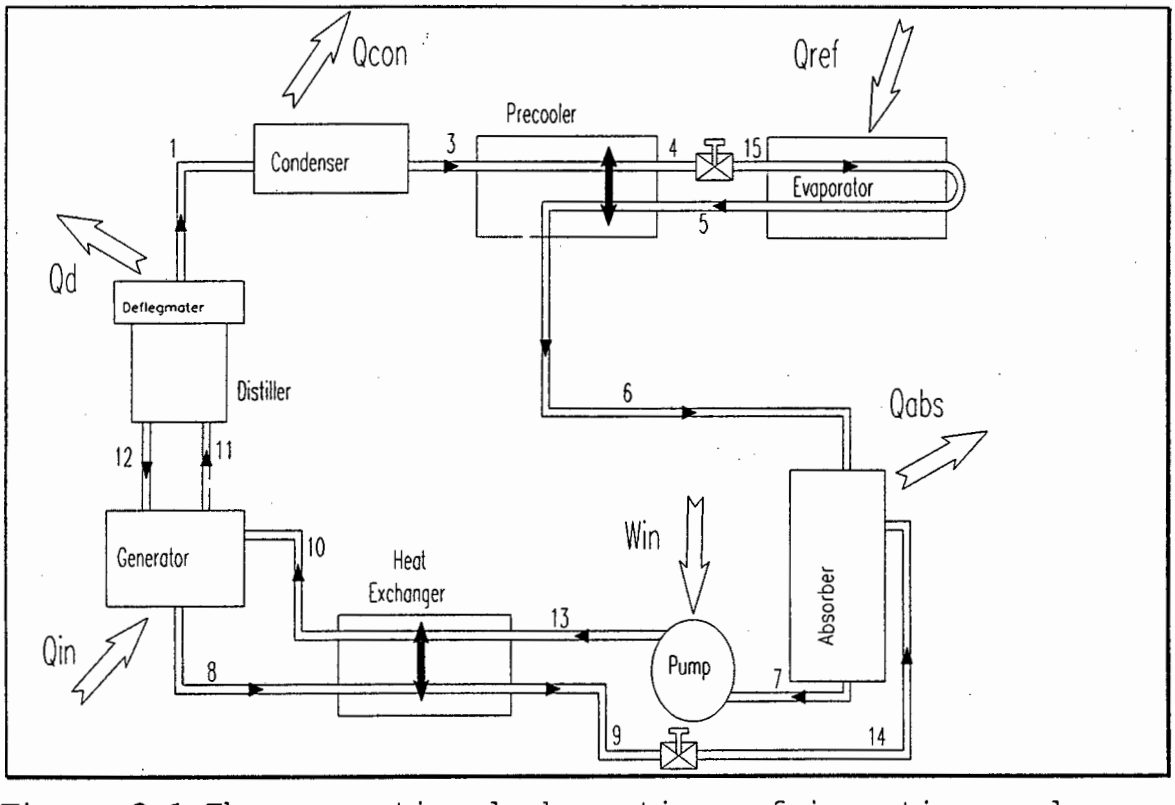


**Figure 2.1** The conventional absorption refrigeration cycle

Two distinct pressures exist throughout the system. The generator, heat exchanger, distiller and condenser are on

high pressure side; the evaporator and absorber on the low pressure side. The throttle valve, solution valve and pump separate the high from the low pressure in the respective connection lines. Heat is supplied to the generator (Qin) in the form of an electric heating element, a flame, waste heat or solar energy. The generator is filled with a liquid mixture of the absorbent and refrigerant. The energy supplied serves to separate the absorbent-refrigerant pair; the more volatile refrigerant is driven off as a vapour. The liquid remaining behind, of relatively low refrigerant concentration and therefor termed weak solution, returns to the absorber driven by the pressure difference that exists between the two. The vapour driven off in the generator, though of high refrigerant concentration, contains some absorbent, the amount of which depends on the volatility of the absorbent. In the case of the ammonia-water combination a fairly large amount of water vapour is carried along with the refrigerant, which is removed in the distillation column. The refrigerant mixture condenses in the condenser at constant pressure by rejecting heat to the cooling environment (Qcon). The precooler is a type of heat exchanger, where some heat energy is passed to the cold refrigerant leaving the evaporator. The precooled liquid refrigerant passes through a throttle valve before entering the evaporator. The energy for the evaporation is drawn from the surrounding (Qref), also known as the refrigeration capacity. The vapour refrigerant is drained off to the absorber, where it is reabsorbed by the weak solution. The heat generated during the absorption process (heat of mixing) together with the heat energy of the weak solution is rejected to the medium that cools the absorber (Qabs). A pump, usually powered from an external electrical source, returns the resulting rich solution to the generator. Before reaching the generator, the rich solution passes through a

heat exchanger, where heat is transferred from the weak to the rich solution. The dual purpose of this is that less heat has to be supplied to the generator and less heat has to be removed from the absorber. As a result the cycle efficiency increases.

## 2.2 The working fluids

Among the many absorbent-refrigerant pairs that have been experimented with to date the most consistent and widely used are:

Ammonia-Water: Ammonia is the only one of the original classical refrigerants to retain its position. Ammonia is cheap and has excellent thermodynamic properties. Water can absorb vast amounts of ammonia and therefor a relatively low volume of liquid mixture has to be circulated per fixed refrigeration capacity. Ammonia has a very high latent heat (1313.3 kJ/kg at -15° C) and a low density as liquid (600 kg/$m^3$ at 30 C). Its low liquid density is of practical advantage in that static heads due to liquid ammonia columns are minimal.. The disadvantages of the pair are that ammonia is corrosive to copper (in the presence of water or oxygen), zinc, most rubbers and plastics. Iron and steel can safely be used. In addition system leaks have to be prevented as ammonia is highly toxic. Thermodynamically the most important disadvantage of the pair is that a relatively large amount of the water evaporates together with the ammonia during generation. This is undesirable as water (absorbent), reaching the evaporator, holds some ammonia

(refrigerant) in solution, that would otherwise have contributed to the refrigeration capacity. The evaporation of water also increases the heat input to the generator. This necessitates the use of a distiller/ deflagmator to prevent significant amounts of water reaching the condenser. Thermodynamic data for ammonia and water are given in appendix B.

Freon R22-E181: E181, the tradename for tetraethylene glycol dimethyl ether ($CH_3(OCH_2CH_2)_4OCH_3$), serves as absorbent, R22 ($CHCLF_2$) as refrigerant. R22 is, together with ammonia, the most common of the primary refrigerants. Although R22 belongs to the chlorofluorocarbon group of refrigerants (CFC's) to be phased out because of their contribution to ozone depletion it is still widely used. Because of the single chlorine atom in the R22 molecule (other CFC's carry two) R22 is considered only minimally damaging to the ozone layer and therefor takes a transitional role in the change from CFC's to new refrigerants (R134a, R152a etc.). R22 has a lower latent heat than ammonia (217.69 kJ/kg at -15 C) but a higher liquid density (1175.15 $kg/m^3$ at 30 C). The refrigerant vapour flow rate to be circulated is similar to the one for ammonia at the same refrigeration capacity. R22 is non-toxic but corrosive to some rubbers and plastic (Pearson [16] reports a softening effect on electrical insulation). The Parker catalogue [15] states that both chloroprene and ethylene-propylene rubber seals are resistant to R22 while normal nitrile-butadiene seals are not recommended for use with R22. Zellhoefer [26] suggested in 1937 E181 as absorbent, initially in combination with R21. R22 was found to be a more suitable refrigerant for E181

as also reported by Mastrangelo [14] and Kriebel et al [12]. Plank et al [11] state that the R22-E181 pair is harmless to copper, steel and aluminium for temperatures under 175 C. The boiling point of E181 at 1.013 bar is 275 C, that of R22 -40.8 C. The difference of 315.8 C implies that only very small amounts of E181 are driven off in the generator; thus no rectification (distiller) is required. E181 is very expensive and is also known to attack a large range of polymers (sealing rings etc.). The Parker catalogue [15] suggests ethylene-propylene seals for use with E181. Data for R22 and E181 is given in appendix B.

Water-Lithium Bromide: Lithium bromide acts as absorbent, water as refrigerant. The pair is low in cost, chemically stable and non- toxic. Lithium bromide absorbs large quantities of water, therefor only a relatively small amount of liquid must be pumped from the absorber to the generator. It is easy to separate the two in the generator as the boiling point of water is considerably lower than that of lithium bromide. The vapour pressure-temperature characteristics of water are such that the pressure in the evaporator and absorber will be extremely low. This is undesirable as any non-airtight joints will cause air to leak in, increasing the pressure and temperature in the evaporator. Also, water cannot be used as refrigerant for temperatures below zero degrees. Another problem with the pair is what is known as crystallisation. If strong solution at a high temperature is cooled, crystals precipitate out of the liquid. The resulting slush-like liquid is difficult to circulate through the cycle.

## 2.3 Uses and advantages of absorption refrigeration

The early refrigeration machines, of both the compression and absorption type, were mainly designed for large industrial applications. During the first sixty years of this century much attention was focused on the development of smaller refrigeration machines for domestic use. Plank et al [11] report that around the time of the second World War absorption machines were very popular in household refrigeration. The reason given is that simplicity and safety was rated more important than energy efficiency in domestic refrigeration. Absorption machines had no moving parts and did not emit much noise. Compressors at that time were technically challenging, unreliable and seldom leak free. The production costs of compressors did not decrease proportionally with the decrease of displacement volume and it was difficult to regulate refrigerating machines with the small flow rates involved. It was economically not viable to build compression machines below a certain size. For that reason very few compression machines below 100 W cooling capacity were built. The production costs of absorption machines, however, could be lowered considerably by decreasing the cooling capacity from 100 W to 35 W. The picture has since then changed considerably. With the advancement of technology the manufacture of reliable compressors of all sizes does not constitute an obstacle any longer. With the capital cost of compression refrigeration machines having become less than that of an equivalent absorption type refrigerator, the compression refrigerator has entrenched itself firmly as the dominant force in the household market.

Besides production cost, another important criterion is the operational cost. Compression refrigeration is more energy efficient than absorption refrigeration. Pita [17] reports that while the COP of a typical lithium bromide-water chiller is around 0.65 to 0.70, an equivalent vapour compression machine chiller has an COP of 3 to 4. This comparison is not a true reflection of performance and has to be moderated by taking into account the type of input energy used. Considering the energy source for the electric driven compressor improves the situation somewhat. Only about one third of the heat energy of the primary fuel (coal, oil, nuclear) in the power plant is converted into electricity. The absorption machine thus requires approximately twice as much heat energy of primary fuel as does the compressor driven machine. Even though the efficiency of absorption machines can be improved by using the two-stage system (refrigerant is boiled off in two stages in two generators), it remains less efficient than its compression type competitor.

The most important advantage of absorption refrigeration is that it does not require high grade energy as input. Solar energy or industrial energy sources such as otherwise wasted low pressure steam or hot combustion gases can be used to power absorption refrigeration machines. At present, absorption refrigeration is mainly restricted to industrial applications where a free energy source is available or where very large units are required.

The absorption cycle as described above, however, still needs electricity to drive the rich solution return pump. The introduction of a vapour pump renders the cycle independent of the availability of electricity. Absorption refrigeration then gains the added advantage that it can be used in areas where no electricity is available (e.g. clinics, farms and schools in remote areas).

# CHAPTER 3

## 3 The vapour pump in the absorption refrigeration cycle

### 3.1 Cycle arrangement with vapour pump

The vapour pump takes the place of the electrically driven one. All other parts of the cycle remain as shown in figure 2.1. A fraction of the high pressure, hot vapour mixture (11) is channelled to the pump via stream 16. The vapour mixture leaving the pump, after having done work, is purged to the absorber via stream 17. The proposed cycle is schematically shown in figure 3.1.

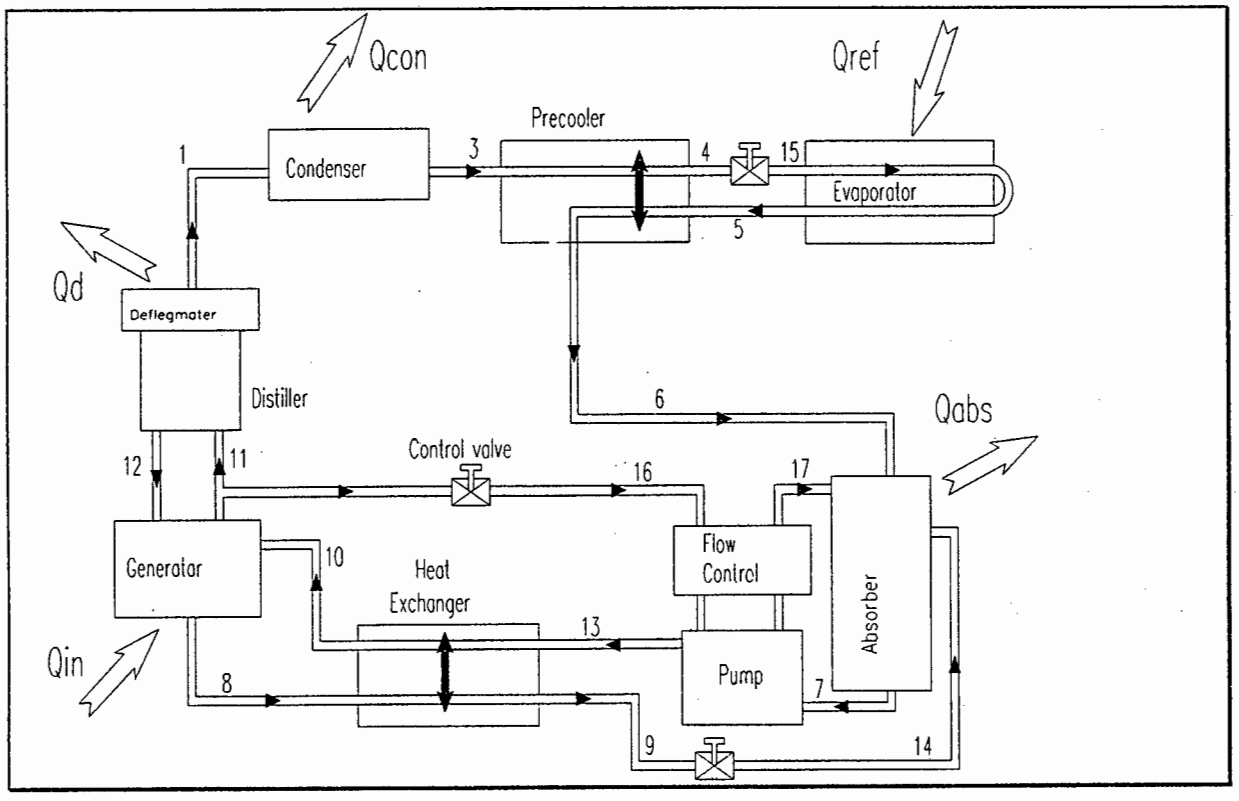


**Figure 3.1** Schematic arrangement of cycle with vapour pump

## 3.2 Principle of operation of the vapour pump

Since the pump is driven by the high pressure vapour mixture it draws its power from the heat supplied to the generator. For the refrigeration effect to remain unaffected by the change of pumps the flow rate through the evaporator has to stay constant. An additional amount of vapour mixture -the amount required for the pumping operation- has to be driven off in the generator. This vapour mixture, together with the refrigerant coming from the evaporator (6), is absorbed by the weak solution in the absorber. The mass balance around the absorber shows that the flow rates of both the weak (9) and the strong solution (7) must increase accordingly in order to absorb the surplus vapour to the absorber and supply it to the generator. The additional amount of heat supplied to the generator is exclusively rejected in the absorber. The vapour pump consists of essentially two parts (figure 3.2):

- a pumping mechanism
- a control mechanism

Figure 3.2 shows an assembly view of the pump. Pumping is done by two opposed synchronised double acting pistons. The two pistons are connected by a steel shaft. Each piston has two vapour sides and a liquid side. Each liquid side has a supply line from the absorber and a delivery line to the generator. Non-return valves are fitted to these lines to restrict flow in the directions intended. High and low pressure vapour is applied to the appropriate piston vapour sides. Pumping is achieved by

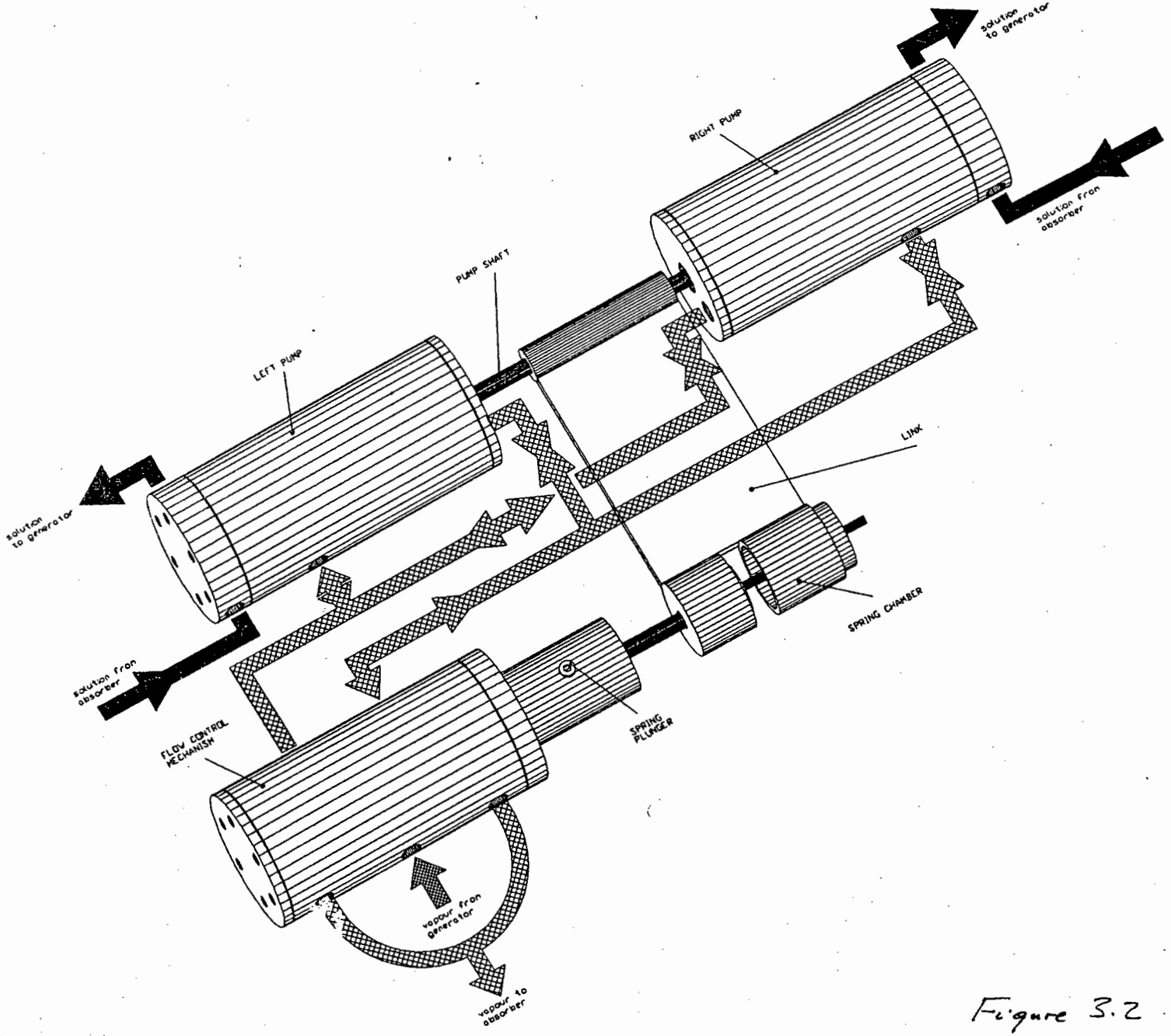


Figure 3.2 The pump assembly

the net force due to the difference in piston area between liquid and vapour sides. The net force exerted by the vapour exceeds the net resisting force of the liquid solution. As the piston arrangement moves, say to the right, the right pump is in delivery mode and the left in suction mode. On the return stroke the reverse action takes place. The double piston arrangement aims at supplying the rich solution to the generator as continuous as possible. To reverse the direction of motion of the pistons the high and low pressure lines are interchanged. This is the function of the control mechanism, that regulates the direction of the flow of the high pressure vapour to the appropriate sides of the pistons in the pumps. Figures 3.3a & 3.3b depict the principle of operation. The shaft in the control mechanism has two distinct positions, one at either end. At these positions the shaft opens and closes the respective channels for forward and return movement of the pistons. The control shaft is held in either of these positions for the duration of the stroke by a spring plunger. A link mechanism (figure 3.2) that is rigidly fixed to the piston shaft, but spring mounted to the control shaft, provides motion to the control mechanism. This enables the control shaft to oscillate between the allowed positions while the pistons undergo reciprocating motion. With the control shaft initially held, say in the 'left' position (figure 3.3a), the vapour is channelled to push the pistons to the right. While the pistons move continuously to the right, the control shaft remains in position until the force, exerted by the increasingly compressed spring in the link, overcomes the force of the spring plunger. Then the control shaft 'jumps' to the 'right' position, switching

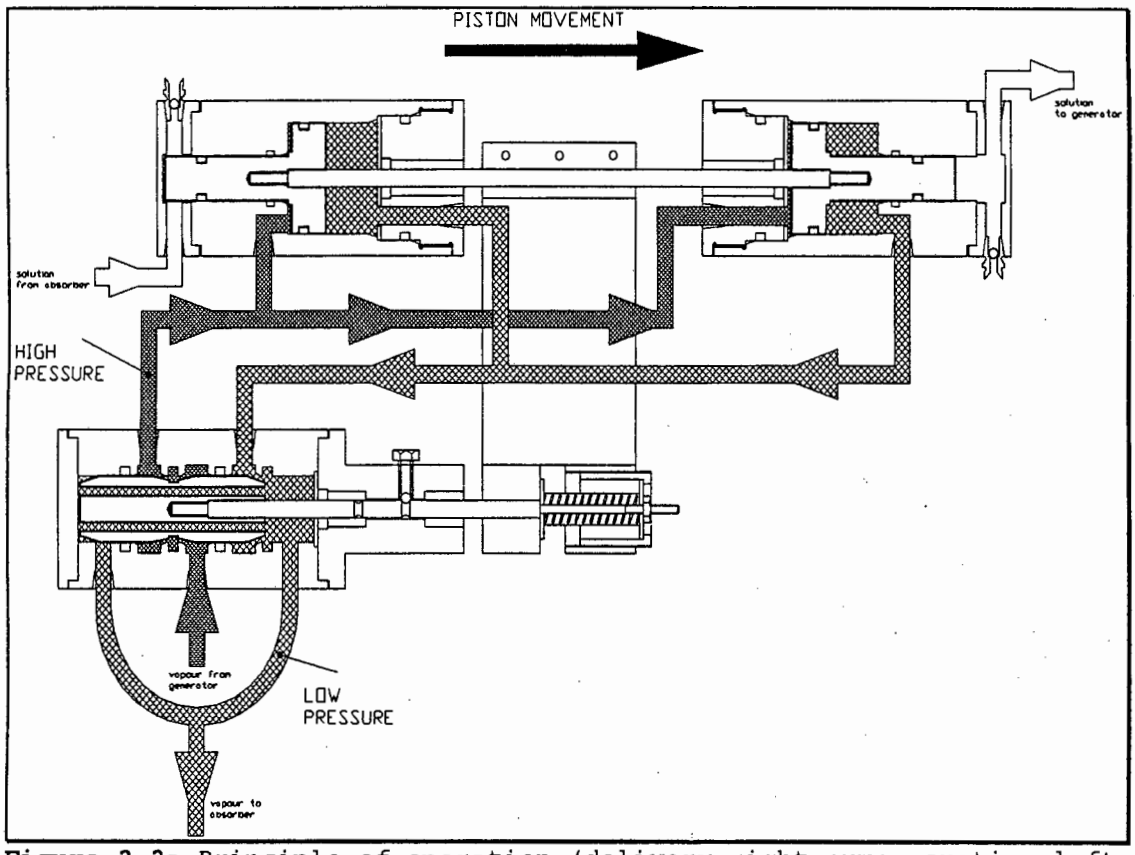


**Figure 3.3a** Principle of operation (delivery right pump, suction left pump)

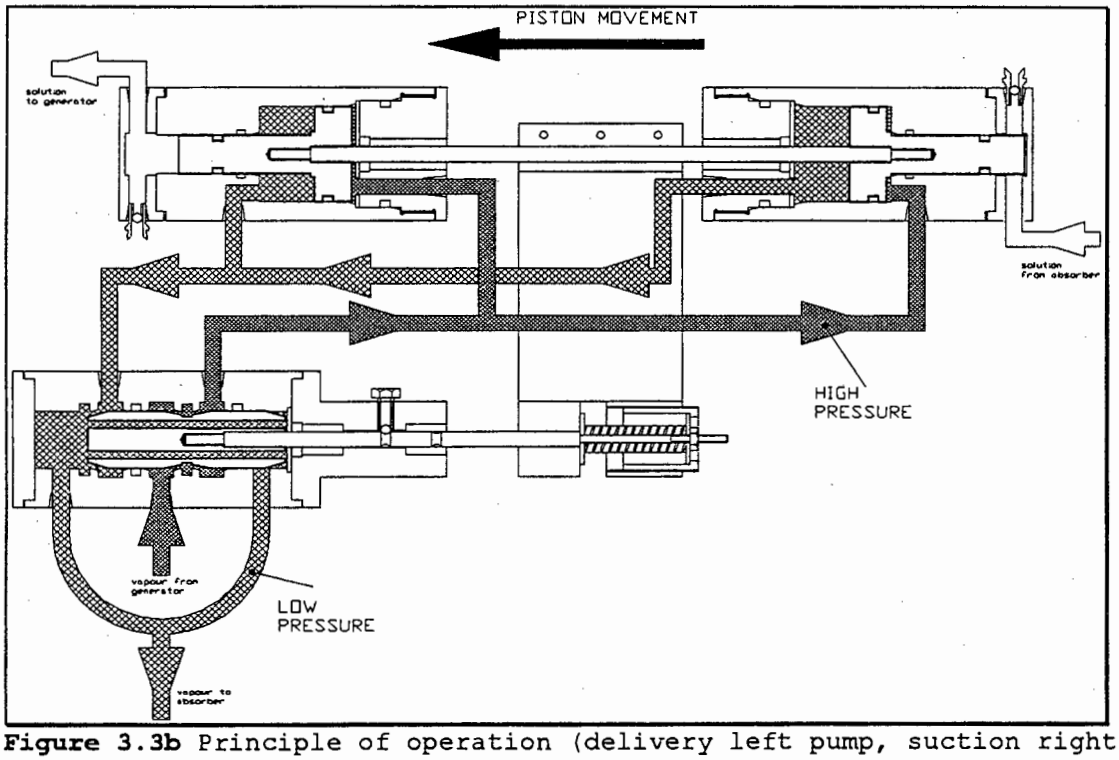


**Figure 3.3b** Principle of operation (delivery left pump, suction right pump)

over the high and low pressure ports, forcing the return movement of the pump pistons (figure 3.3b).

### 3.3 Energy balance of the pump

The pump draws its energy from the high pressure vapour coming from the generator. Energy is lost due to pipe friction and friction between the moving parts of the pump; then there are thermal losses which can be reduced by insulation of pipes and pump. The energy content of the low pressure vapour leaving the pump via stream 17 is a portion of the incoming energy (16) not converted into pump work. Figure 3.4 shows this in principle, but not to scale. The numerals refer to the position of the respective stream in the absorption cycle of figure 3.1.

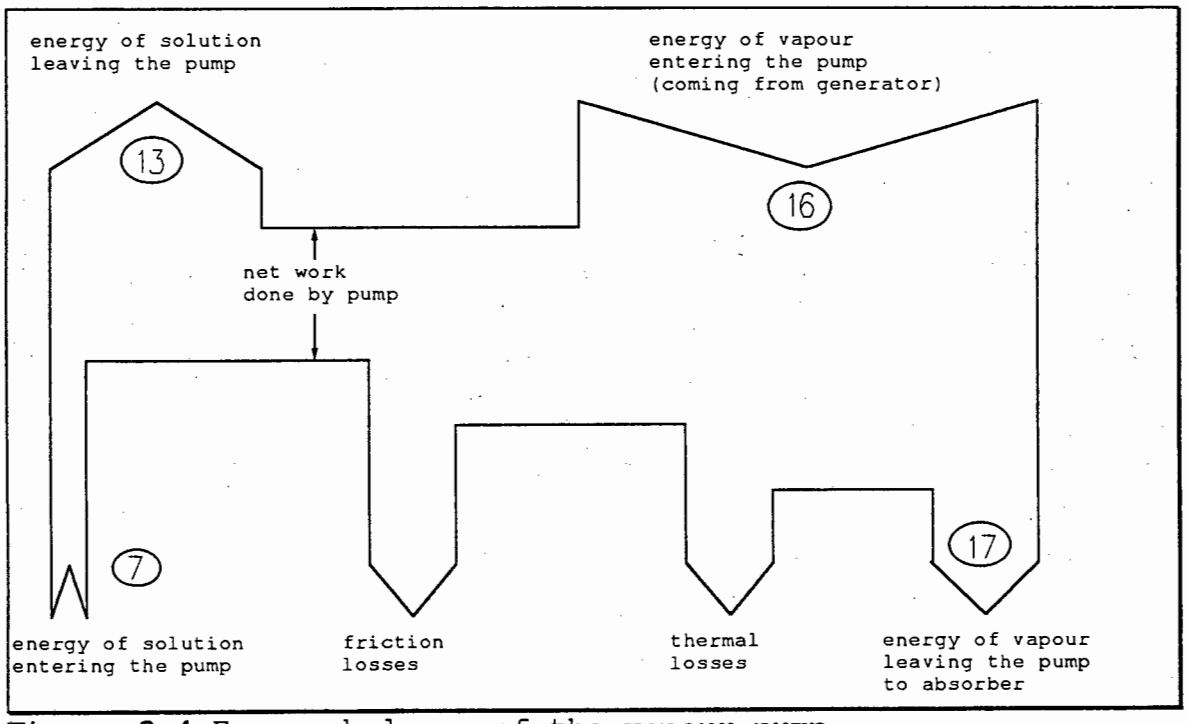


**Figure 3.4** Energy balance of the vapour pump

by conservation of mass

$$\dot{m}_{16} = \dot{m}_{17} = \dot{m}_v \quad \text{(vapour)}$$

$$\dot{m}_7 = \dot{m}_{13} = \dot{m}_s \quad \text{(solution)}$$

by conservation of energy

$$\dot{m}_v h_{16} + \dot{m}_s h_7 = \dot{m}_v h_{17} + \dot{m}_s h_{13} + Q_{fric} + Q_{thermal}$$

$$\dot{m}_v [h_{16} - h_{17}] = \dot{m}_s [h_{13} - h_7] + Q_{fric} + Q_{thermal}$$

$$\dot{m}_v [h_{16} - h_{17}] = W_{pump} + Q_{fric} + Q_{thermal}$$

The specific enthalpies h7, h13 and h16 can be evaluated since at those states two thermodynamic properties (pressure and temperature or temperature and concentration) are known. This is not the case with the exhaust vapour 17; here only the pressure can be assumed to be that of the absorber. The thermal and frictional losses are equally difficult to quantify.

### 3.4 Cycle analysis

Thermodynamic properties of the relevant streams around the vapour pump are summarised in table 3.1. The indices refer to those given in figure 3.1

| | |
|---|---|
| pressure | $P_{16} = P_h$<br>$P_{17} = P_l$ |
| temperature | $T_{16} = T_{11}$ |
| enthalpy | $h_{16} = h_{11}$ |
| mass flow rate | $m_{16} = m_{17}$<br>$m_7 = m_{13} = m_{10}$<br>$m_8 = m_9 = m_{14}$<br>$m_1 = m_6$ |
| concentration | $y_{16} = y_{11} = y_{17}$<br>$x_8 = x_9 = x_{14} = x_{we}$<br>$x_7 = x_{13} = x_{10} = x_{st}$ |

**Table 3.1** Cycle analysis around the vapour pump

'x' = liquid ammonia concentration $[m_{NH3}/m_{tot(liq)}]$
'y' = vapour ammonia concentration $[m_{NH3}/m_{tot(vap)}]$
'we' denotes weak solution
'st' denotes strong solution

mass balance at generator:

<u>total</u>: $m_{16} + m_{11} + m_8 = m_{12} + m_{10} = m_{12} + m_7$

and $m_{11} - m_{12} = m_1$

$\Rightarrow$ $m_{16} + m_1 + m_8 = m_7$ ----------(3.1)

<u>ammonia</u>: $y_{16}m_{16} + y_{11}m_{11} + x_8m_8 = x_{12}m_{12} + x_{10}m_{10}$

$y_{11}m_{16} + y_{11}m_{11} + x_{we}m_8 = x_{12}m_{12} + x_{st}m_7$

and $y_{11}m_{11} - x_{12}m_{12} = y_1m_1$

$$\Rightarrow \quad y_{11}m_{16} + y_1m_1 + x_{we}m_8 = x_{st}m_7$$

substituting (3.1) for $m_7$

$$y_{11}m_{16} + y_1m_1 + x_{we}m_8 = x_{st}(m_{16} + m_1 + m_8)$$

$$m_8(x_{we} - x_{st}) = m_1(x_{st} - y_1) + m_{16}(x_{st} - y_{11})$$

$$m_8 = \frac{m_1(x_{st} - y_1) + m_{16}(x_{st} - y_{11})}{(x_{we} - x_{st})} \quad \text{----------(3.2)}$$

mass balance at absorber:

<u>total</u>: $m_{17} + m_{14} + m_6 = m_7$

$$m_{16} + m_8 + m_1 = m_7$$

$$\Rightarrow \quad m_7 - m_{16} - m_1 = m_8 \quad \text{----------(3.3)}$$

<u>ammonia</u>: $y_{17}m_{17} + x_{14}m_{14} + y_6m_6 = x_7m_7$

$$y_{11}m_{16} + x_{we}m_8 + y_1m_1 = x_{st}m_7$$

substituting (3.3) for $m_8$

$$y_{11}m_{16} + x_{we}(m_7 - m_{16} - m_1) + y_1m_1 = x_{st}m_7$$

$$m_7(x_{st} - x_{we}) = m_1(y_1 - x_{we}) + m_{16}(y_{11} - x_{we})$$

$$m_7 = \frac{m_1(y_1 - x_{we}) + m_{16}(y_{11} - x_{we})}{(x_{st} - x_{we})} \quad \text{----(3.4)}$$

The coefficient of performance (COP) becomes

$$COP = \frac{Refrigeration\ Effect}{Heat\ Input} = \frac{RE}{Q_{gen}}$$

$$COP = \frac{RE}{(Q_1 + Q_8 + Q_{16} - Q_{10})}$$

$$COP = \frac{RE}{(m_1 h_1 + m_8 h_8 + m_{16} h_{16} - m_7 h_{10})} \quad \text{--------(3.5)}$$

The concentration of the strong solution is determined by the pressure and temperature of the absorber. The concentration of the weak solution is determined by the pressure and temperature of the generator. For a fixed set of pressure and temperature conditions, the solution concentrations remain unchanged, irrespective of the type of pump. Introducing an extra amount of refrigerant into the cycle means that a corresponding extra amount of solution has to be circulated between the absorber and generator. The solution flow rates are thus bigger when compared to a cycle with an electrical pump at the same pressures and temperatures.

# CHAPTER 4

## 4 Design of the vapour pump

The vapour pump was designed for experimentation in the Mechanical Engineering Department`s absorption refrigeration machine, which at time of the design operated with R22-E181 as working fluids.

### 4.1 The type of pump

The pump suggested is a double acting positive displacement piston pump. An alternative possible solution briefly considered is a centrifugal pump coupled to one or even two turbines. One turbine would be powered by a fraction of the high pressure vapour mixture, the second one by the flow of the weak solution streaming pressure driven from the generator to the absorber. Purely rotational motion has the added advantage that the driving flow has never to be reversed. However, the flow rates in refrigeration machines of around 1 kW, as the one used for the experiments, are of the order of 1 g/sec. It was felt that with such small flow rates a turbine could not practically be driven. In much larger industrial plants with greater flow rates and pipe sizes the idea might be worth considering. In the case of a positive displacement pump, the small flow rate is of no concern as the pistons are driven by the static pressure difference across them, rather than by the flow momentum. A piston pump with minimal clearance on the suction side, to minimise the likelihood of cavitation, seemed the best prospect for the 1 kW experimental refrigeration plant.

## 4.2 Force analysis

Consider figure 4.1. The forces acting to the right $F_r$

$$F_r = \tfrac{1}{4}\pi D_s^2 P_l + \tfrac{1}{4}\pi \left[D_v^2 - D_s^2\right] P_h + \tfrac{1}{4}\pi \left[D_v^2 - D_r^2\right] P_h$$

Forces acting to the left $F_l$

$$F_l = \tfrac{1}{4}\pi D_s^2 P_h + \tfrac{1}{4}\pi \left[D_v^2 - D_s^2\right] P_l + \tfrac{1}{4}\pi \left[D_v^2 - D_r^2\right] P_l + F_{sp}$$

Net force to the right $F_{net} = F_r - F_l$

$$F_{net} = \tfrac{1}{4}\pi \left[2 D_v^2 - 2 D_s^2 - D_r^2\right] \Delta P - F_{sp} \quad \text{---------(4.1)}$$

where Fsp = spring force
$\Delta P = P_h - P_l$

Alternatively, the driving force exerted by the vapour $F_{vap}$

$$F_{vap} = \tfrac{1}{4}\pi \left[ 2 D_v^2 - D_s^2 - D_r^2 \right] \Delta P \text{----------(4.2)}$$

the resistive force exerted by the liquid $F_{sol}$

$$F_{sol} = \tfrac{1}{4}\pi D_s^2 \Delta P \quad \text{----------(4.3)}$$

and the net force $F_{net} = F_{vap} - F_{sol} - F_{sp}$ yields the same result as (4.1)

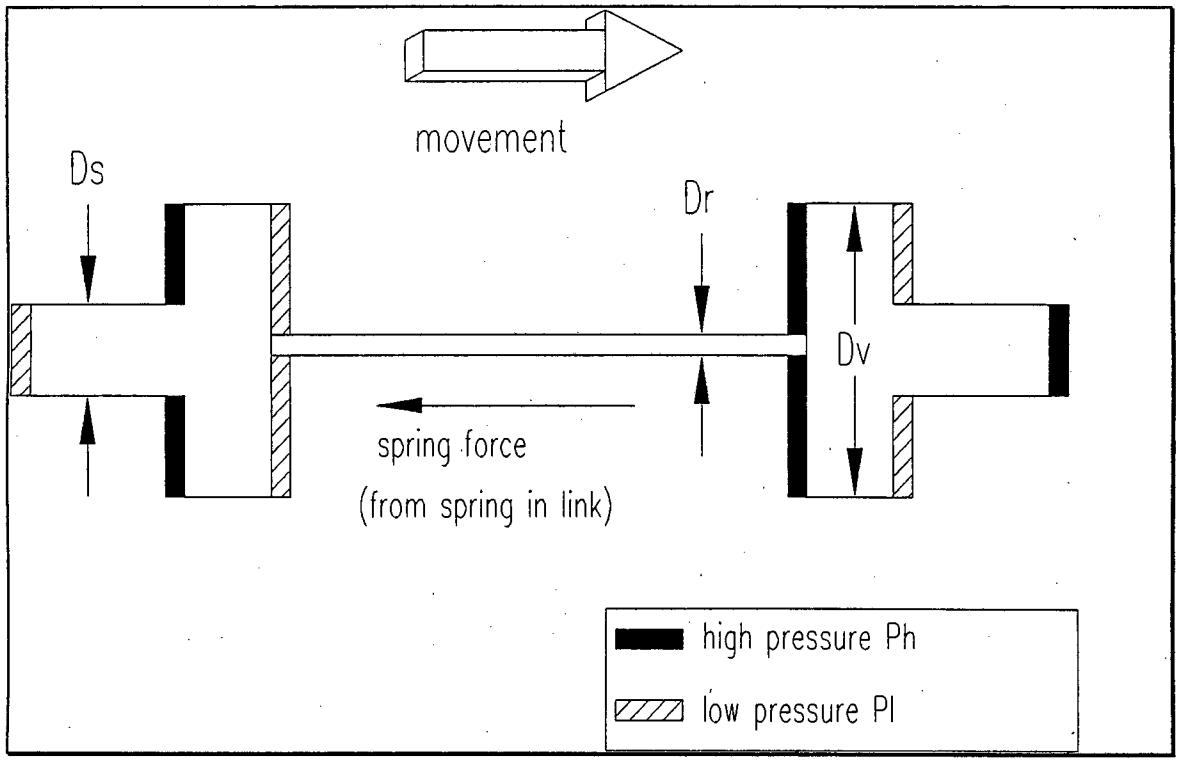


**Figure 4.1** Pressure forces acting on the pistons

### 4.3 The spring force and spring plunger

With reference to the description of the vapour pump in Chapter 3; 'spring plunger' is the spring-pressured ball mechanism to hold the control shaft in position for the duration of the stroke; 'spring' refers to the horizontal spring in the link mechanism. Information on spring plungers is given in appendix F. At the end of the pump stroke the spring must be compressed to such an extent that it exerts a force on the control shaft just big enough to release the spring plunger. Two grooves in the control shaft, separated by one stroke length, correspond to the two allowed rest positions of the shaft. Not only must the compressed spring release the spring plunger, but it must then push the control shaft into the other rest position, one stroke length away. It can be assumed that the spring plunger only resists motion when resting in the grooves.

Its friction on the smooth shaft surface between the two grooves is negligible. The stiffness of the spring has to be such that the spring force only manages to release the spring plunger when compressed by an amount equal or just less than the stroke length. The link mechanism includes an adjustable spring holder to enable fine tuning of the extent of precompression of the spring.

A M8 (WDS No 606-2708) spring plunger was selected. The spring plunger spring exerts a force of 30 N on the 5 mm diameter ball; the groove has a depth of 1.5 mm. The corresponding spring force required is calculated as follows. It is assumed that when the spring pulls the shaft, then the ball exerts a reaction to the top edge of the groove (see figure 4.2).

From figure 4.2

$$\sin \gamma = 1 / 2.5$$

$$\Rightarrow \quad \gamma = 23.578°$$

$$\tan \gamma = F_{lift} / F_{spring}$$

$$\Rightarrow \quad F_{spring} = F_{lift} / \tan \gamma$$

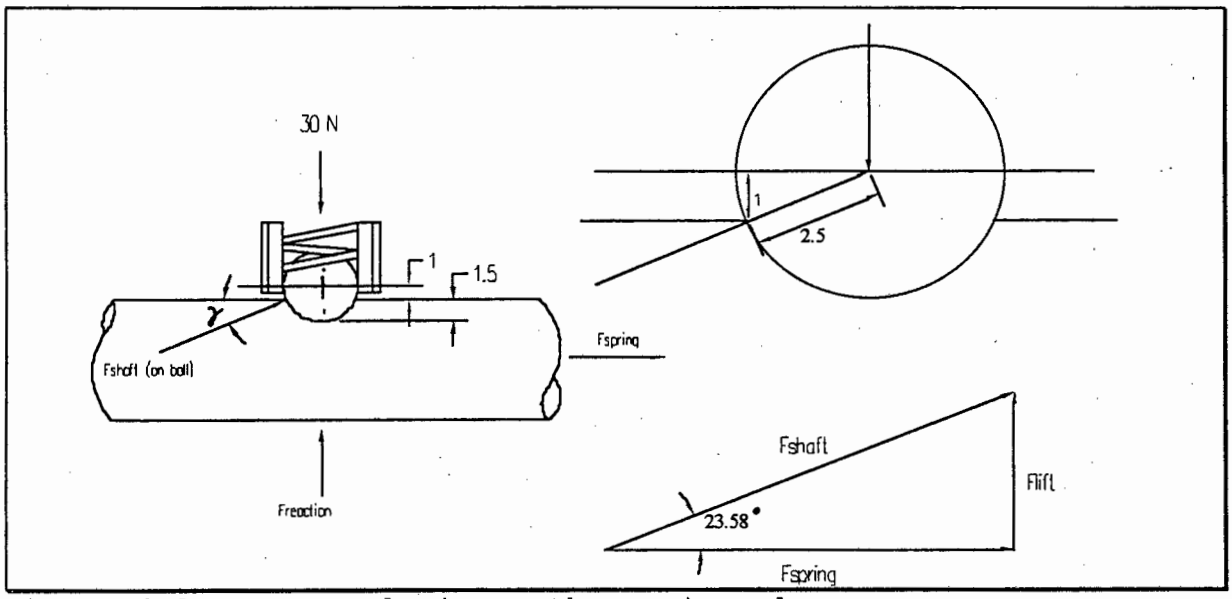


**Figure 4.2** Force analysis on the spring plunger

To release the spring plunger, the spring must induce a lift force bigger or equal to 30 N.

$$F_{spring} \geq 30 / \tan\gamma \quad [N]$$

$$\Rightarrow \quad F_o + kx \geq 30 / \tan(23.578)$$

$$\Rightarrow \quad F_o + kx \geq 68.7 \text{ N}$$

where $F_o$ = initial force if spring is precompressed
$k$ = spring stiffness [N/mm]
$x$ = displacement from rest position

for $F_o = 0$ and $x = L$ (stroke length) = 25mm

$$kL \geq 68.7$$

$$\Rightarrow \quad k \geq 68.7 / 25 \text{ [N/mm]}$$

$$\Rightarrow \quad k \geq 2.75 \text{ N/mm}$$

The required stiffness of the spring in the link mechanism can be reduced by precompressing the spring. A detailed spring design is presented in the following section.

### 4.3.1 Detailed spring design

The load profile for which the spring has to be designed is displayed in figure 4.3. It has previously been shown that an axial force of about 70 N is required to release the spring plunger. A minimum force of 5 N is chosen to ensure that the spring is in compression at all times. From the

space available, the corresponding lengths of the spring are specified to be 30 mm and 55 mm, the difference between them being the stroke length (25 mm).

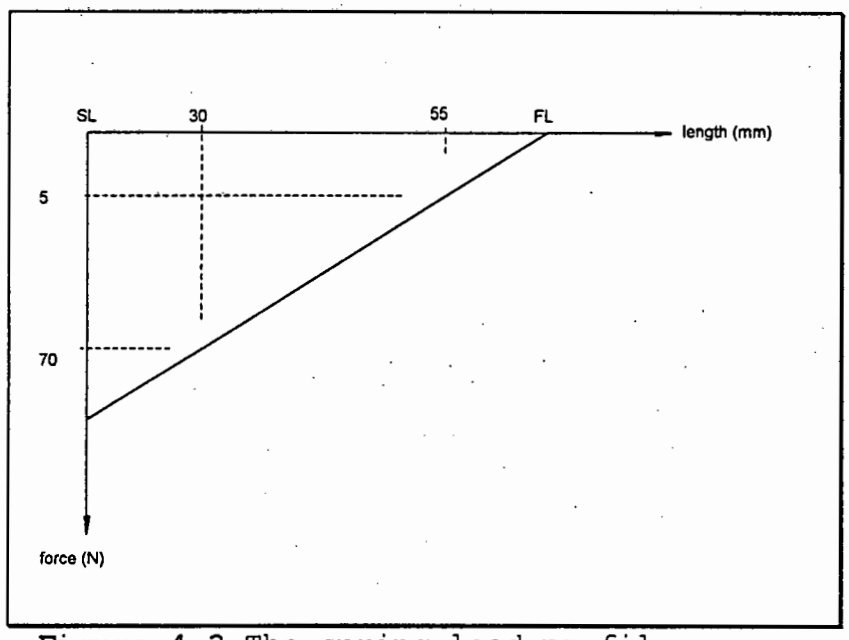


**Figure 4.3** The spring load profile

The design procedure is outlined by Shigley [19]. For helical coil compression springs the spring has to be designed against failure in shear and for fatigue. Therefor the maximum shear stress ($\tau_{max}$) has to be smaller than the yield shear stress ($S_{sy}$) and the alternating shear stress ($\tau_a$) has to be smaller than the endurance limit ($S_{se}$). Thus

$$\tau_{max} < S_{sy} \qquad \text{------(4.4)}$$

$$\tau_a < S_{se} \qquad \text{------(4.5)}$$

The shear stress is found by

$$\tau = \frac{8FCK}{\pi d^2} \qquad \text{----------(4.6)}$$

where

F is the axial force. From the load profile $F_{max}$ = 70 N and the alternating force $F_a = 0.5\ (F_{max} - F_{min})$ = 32.5 N

C is the spring index

$$C = \frac{D}{d} \qquad \text{----------(4.7)}$$

where D equals the mean outer diameter and d the wire diameter.

K is the Wahl stress correction factor found by

$$K = \frac{4C-1}{4C-4} + \frac{0.615}{C} \qquad \text{-------(4.8)}$$

Shigley gives the shear yield stress as a fraction of the tensile yield stress ($S_y$)

$$S_{sy} = 0.577\, S_y \qquad \text{--------(4.9)}$$

and

$$S_y = 0.75\, S_{ut} = 0.75 \frac{A}{d^m} \qquad \text{-----(4.10)}$$

where form Shigley [19] (table 10.2) A = 2160 MPa and exponent m = 0.145 for cold drawn BS 5216 grade 4 carbon steel.

The endurance limit (for infinite life) is given by Shigley as $S''_{se}$ = 310 MPa for unpeened springs. This result accounts for surface finish and size but needs to be corrected for reliability, temperature and stress concentration.

$$S_{se} = k_c\, k_d\, k_e\, S'_{se} \qquad \text{--------(4.11)}$$

and the reliability factor $k_c$ = 0.897 for 90% reliability (Shigley, table 7.7), the temperature factor $k_d$ = 1 for T < 350 °C and $k_e$ = 1 for no stress concentrations.

The spring rate or stiffness (k) is found from the load profile:

$$k = \frac{\Delta F}{\Delta y} = \frac{65}{25} = 2.6 \ \left\langle \mathrm{N/mm} \right\rangle \qquad \text{-----(4.12)}$$

Now the number of active coils can be found by

$$N = \frac{d\,G}{8\,C^3\,k} \qquad \text{----------(4.13)}$$

where G is the shear modulus of elasticity (79.3 GPa for steel) and k the spring rate.

For squared and ground ends the total number of coils equals $N_t$ = N + 2, and the solid length is given by SL = (N + 2)*d. The free length (FL) is easily calculated from the slope of the load profile. In this case FL = 56.92 mm. The outer diameter is calculated by OD = D + d and the inner diameter by ID = D - d.

Finally the spring must be checked for buckling stability and spring surge. For buckling stability the ratio of deflection to free length must not exceed a certain value which depends upon the ratio of free length to mean diameter. Spring surging occurs when the forced oscillation is to close to the natural frequency of the spring. The natural frequency is given by

$$f = \frac{\omega}{2\pi} = \frac{1}{4\pi}\sqrt{\frac{k}{m}} \qquad \text{----------(4.14)}$$

for a spring placed between two flat parallel plates. k is the spring rate and m the mass of the helical spring found by

$$m = Al\rho = \frac{\pi d^2}{4}(\pi d\, N)(\rho) = \frac{\pi^2 d^2 D N \rho}{4} \qquad \text{---(4.15)}$$

All of the above equations and information was stored in a spreadsheet. The procedure was the to vary the spring index (C) and the wire diameter (d) such that all conditions were satisfied. The results are tabulated below (table 4.1).

Material: BS 5216 grade 4, cold drawn carbon steel

| | | | |
|---|---|---|---|
| spring index C | 9 | $F_{max}$ [N] | 70 |
| mean D [mm] | 16.2 | $F_{min}$ [N] | 5 |
| d [mm] | 1.8 | shear yield stress [MPa] | 858 |
| rate k [N/mm] | 2.6 | max shear stress [MPa] | 575 safe |
| ends | squared ground | shear endurance [MPa] | 278 |
| active coils N | 9.41 | alt. shear stress [MPa] | 267 safe |
| total coils Nt | 11.41 | buckling: FL/D | 3.51 |
| ID [mm] | 14.4 | def/FL | 0.47 safe |
| OD [mm] | 18 | natural frequency [Hz] | 41.64 |
| solid length [mm] | 20.54 | forced frequency [Hz] | 0.2 safe |
| free length [mm] | 56.92 | | |

**Table 4.1** Spring design details

### 4.4 Volume being processed

The volume that is displaced per stroke of length L

$$V = \tfrac{1}{4}\pi D_s^2 L$$

then for a return stroke frequency of f the flow rate equals

$$Q = 2 f \tfrac{1}{4}\pi D_s^2 L$$

$$Q = \tfrac{1}{2} f\pi D_s^2 L \quad \text{----------(4.16)}$$

the corresponding mass flow rate

$$\dot{m} = \rho_{sol} Q \quad \text{----------(4.17)}$$

where $\rho_{sol}$ = density of the solution

## 4.5 Flow rate of vapour through the pump

Volume of vapour passing through pump per stroke L

$$V = \tfrac{1}{4}\left[\left[D_v^2 - D_r^2\right] + \left[D_v^2 - D_s^2\right]\right] L$$

the flow rate for pump frequency f

$$Q = \tfrac{1}{2} f \left[2D_v^2 - D_s^2 - D_r^2\right] L \quad \text{----------(4.18)}$$

the mass flow rate of vapour

$$\dot{m} = \rho_{vap}\, Q \quad \text{----------(4.19)}$$

The vapour passing through the pump is more than 95% ammonia (or more than 99% R22 if the R22- E181 combination is used). Vicatos [24] has developed a polynomial that evaluates the specific volume of superheated ammonia vapour as a function of pressure and temperature ($1/\rho = \upsilon = f(P,T)$). Details of this are given in appendix B.

## 4.6 Sizing the pump

The liquid piston side diameter was chosen as $D_s$ = 20 mm. The stroke length was selected to be L = 25 mm. With 25 mm stroke length of the control shaft there is sufficient space in the control mechanism to install the sealing rings (section 4.12). The vapour side piston diameter is calculated as follows. The main obstacle to overcome is the difficulty in quantifying the losses of the pump (refer to figure 3.4). The thermal heat loss, energy loss due to friction between stationary and moving parts and the energy

content of the exhaust vapour remain unknown and varying quantities. The heat loss can be reduced by insulation; friction depends upon the type of seals used and lubrication. The general approach is to group these unquantified losses together and account for them by introducing a safety factor (sf). The approach is based upon the principle that the vapour driving force exceeds the solution resisting force by that safety factor.

$$sf = 10$$

$$F_{vap} = sf\ F_{sol}$$

from equations (4.2) and (4.3)

$$\frac{\pi}{4}(2D_v^2 - D_s^2 - D_r^2)\Delta P = sf\ \frac{\pi}{4} D_s^2\ \Delta P$$

and solving for $D_v$ yields

$$D_v = \sqrt{\frac{(sf+1)D_s^2 + D_r^2}{2}} \quad \text{----------(4.20)}$$

where the diameter of the rod ($D_r$) was chosen to be 8mm.

$D_v$ = 47.2 mm

select $D_v$ = 50 mm

## 4.7 The pump frequency

'f' denotes the pump frequency and is defined as the number of return strokes per second. Using equation (4.16) and (4.17) and solving for the frequency yields:

$$f = \frac{2\ m\ \upsilon}{\pi\ L\ D_s^2} \qquad \text{----------(4.21)}$$

where $\nu = 1/\varphi$

## 4.8 The pump efficiency

The work that the pump delivers to the system equals

$$W_{out} = \Delta P\ \Delta V = \Delta P\ \frac{m_7}{\rho_7} \qquad \text{----------(4.22)}$$

and similarly the work going into the pump

$$W_i = \Delta P\ \Delta V = \Delta P \frac{m_{16}}{\rho_{16}} \qquad \text{----------(4.23)}$$

and the efficiency is then evaluated by

$$\eta = \frac{W_{out}}{W_i} = \frac{m_7 \rho_{16}}{m_{16} \rho_7} \qquad \text{----------(4.24)}$$

Alternatively, the efficiency can be found by

$$\eta = \frac{W_{out}}{Q_{16}} = \frac{\Delta P\ m_7}{\rho_7\ m_{16}\ h_{16}} \qquad \text{----------(4.25)}$$

Equation (4.25) yields a lower efficiency than equation (4.24). $W_i$ represents the net energy supplied to the pump while $Q_{16}$ is the total energy going to the pump via stream 16. Equation (4.24) thus accounts for thermal and friction losses, whereas equation (4.25) incorporates the energy loss associated with stream 17. Equation (4.25) gives the overall pump efficiency, equation (4.24) gives the efficiency of energy transfer inside the pump.

## 4.9 The control cylinder

The control mechanism serves the purpose of directing the incoming and exhaust vapour into the correct channels. The general principle of operation has already been discussed in section 3.2.

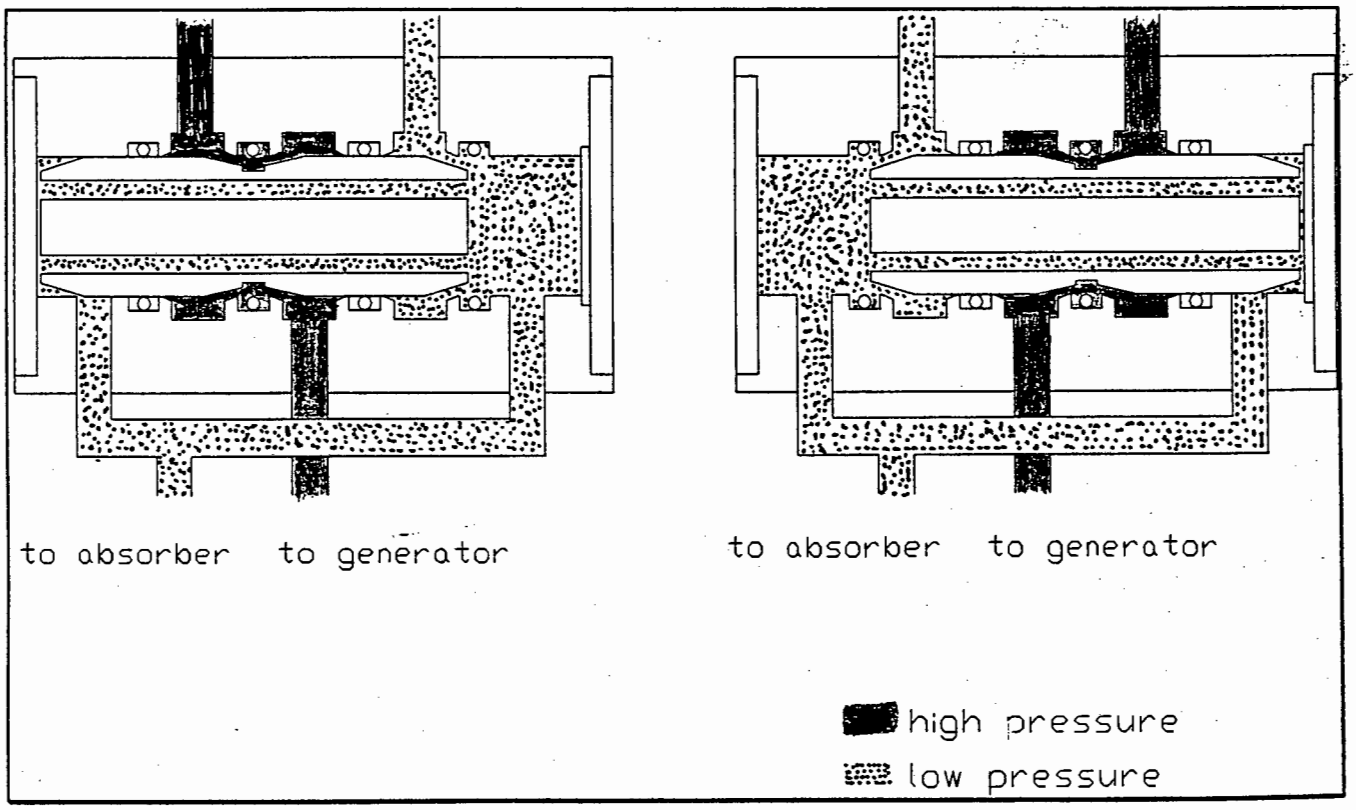


**Figure 4.4** Operation of the control mechanism

Assembly drawings are shown in figure 3.3a and 3.3b; appendix D gives detailed drawings. At the end of each stroke both the high pressure vapour and exhaust vapour has to be redirected. The is achieved by interchanging the high pressure and exhaust lines. Two lines are required between control cylinder and pump. Each line has one connection (port) to the control cylinder and one for each of the pump cylinders. The control cylinder has one incoming line from the generator and two outlet ports that lead to the absorber. The movement of the control shaft is provided by the movement of the pump shaft through the spring mounted coupling mechanism. Figure 4.4 depicts the operation of the control mechanism. The figure only shows how the profile of the cylinder core allows for the channelling of the high pressure and exhaust streams, and should be seen in conjunction with figure 3.3a/b. The O-ring seals cannot be placed onto the control core, because O-rings in dynamic applications cannot safely pass over a port. Instead the seals are housed in the control cylinder. The regions of either side of the core are connected to prevent resistance to the movement of the control core due to compression. This is done by passages through the core itself.

### 4.10 Material selection

The control cylinder -core and pump cylinder -piston pair, pump ends and pump caps are specified to be made from stainless steel. The reason for this is twofold:

- To prevent surface damage by impurities in the system.

- The cylinder-core and cylinder-piston pairs need to be of the same material to ensure that the clearance gaps remain unchanged during thermal expansion.

Mild steel is specified for most other parts, where tight tolerancing is not essential (link mechanism, control cap). The bushes for both shafts ~~are~~ were made from brass.

## 4.11 Strength calculations

*a) Cylinder wall thickness*

Thick-walled cylinder theory (Shigley [19]) yields the following:

$$\textit{tangential stress: } \sigma_t = \frac{a^2 p_i}{b^2 - a^2}\left(1 + \frac{b^2}{r^2}\right) \qquad \text{-------(4.26)}$$

$$\textit{radial stress: } \sigma_r = \frac{a^2 p_i}{b^2 - a^2}\left(1 - \frac{b^2}{r^2}\right) \qquad \text{---------(4.27)}$$

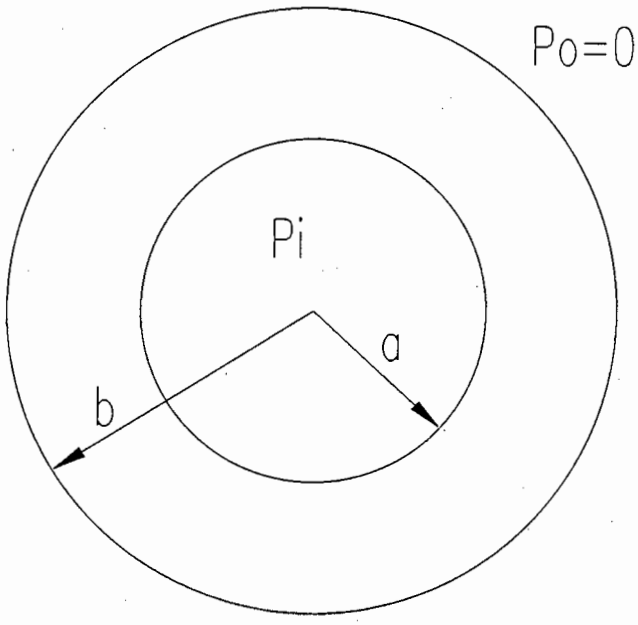


for zero external pressure. The maximum stresses occur at the inner surface, where r = a. Their magnitudes are obtained by substituting a for r in equations (4.26) and (4.27).

$$\sigma_{tmax} = p_i \frac{b^2+a^2}{b^2-a^2} \qquad \text{----------(4.28)}$$

$$\sigma_{rmax} = -p_i \qquad \text{----------(4.29)}$$

In case of the pump a = 25 mm, b = 35 mm and $p_i$ = 10 bar. Then $\sigma_{tmax}$ = 3.08 MPa and $\sigma_{rmax}$ = -1 Mpa. Stainless steel has an ultimate tensile strength of more than 500 MPa, therefor strength plays no role in specifying the cylinder wall thickness. The cylinder wall has to be of the oversized thickness to accommodate the threaded piping connections.

*b) Bolt stresses in end pieces*

Pump cap bolts:

Maximum force acting on bolts: F = P A

$$F = 10*10^5 * \pi/4\ 0.022^2\ [N]$$

$$F = 380.13\ N$$

the stress in each of the six 4 mm bolts:

$$\sigma = (F/6)\ /\ A$$

$$\sigma = 63.36/(\pi/4\ 0.004^2)\ [Pa]$$

$$\sigma = 5.04\ MPa \Rightarrow \textit{safe}$$

Cylinder lid bolts:

Maximum force acting on bolts: F = P A

$$F = 3*10^5 * \pi/4\ 0.064^2\ [N]$$

$$F = 965.10\ N$$

the stress in each of the six 4 mm bolts:

$$\sigma = (F/6)\ /\ A$$

$$\sigma = 160.8/(\pi/4\ 0.004^2)\ [Pa]$$

$$\sigma = 12.8\ MPa \Rightarrow \textit{safe}$$

*c) Strength of pump shaft*

For a yield stress of 300 N/mm² the maximum axial force that can safely be transmitted through the 8mm shaft equals

$$F = \sigma_y\ A = 300\ \pi/4\ 8^2 = 15079.6\ N \Rightarrow \textit{safe}$$

The forces involved are significantly smaller than this (see the simulation results in appendix G). Buckling is very unlikely to occur because the shaft is guided in bushes and supported by the clamping mechanism. Buckling would be most likely to occur between the two pumping cylinders. Ignoring the clamping, the force at which buckling occurs is given by:

$$\textit{Euler buckling}\quad F = \frac{\pi^2 E I}{l_k^2}$$

For the end conditions in this case $l_k$ = ½ l (Dubbel [8]).

length l = 125 mm
modulus of elasticity E = 200 GPa
moment of inertia I = $\pi$ $d^4/64$

Substituting in above equation yields:

F = 101601 N at which buckling begins $\Rightarrow$ *safe*

**4.12 Sealing of the pump**

The sealing of the pump and control mechanism is complicated by the fact that the working fluids involved attack normal nitrile rubber seals. In static applications deterioration might not be severe or occur rapidly, but in dynamic uses, such as the pumping pistons, nitrile rubber seals can not be used. It is especially the tetraethylene glycol dimethyl ether (E181) that from past experiments [24] is known to be harmful to standard rubber seals. Initially it was intended to use teflon seals, teflon being a material that is safe to use with R22 and E181. Experts

in the field, however, warn that teflon is too static a seal to effectively seal the volatile R22. Teflon has a low resistance to permanent deformation and any dent or other slight misfit in shape becomes a permanent problem which leads to leakage. Rubber seals have an excellent resistance to permanent deformation. Nitrile and neoprene seals have caused problems before. Viton is resistant to R22 and E181 but is not suitable for dynamic uses. Ethylene propylene (EPDM) seals on the other hand can be operated in the -40 to 160 °C temperature range, have excellent resistance to permanent deformation and can be used with ozone, atmospheric agents, ketones and diluted acids. A piece of EPDM has been soaked in E181 for days and shows no sign of any adverse effects. It was decided to use EPDM seals in the pump. For the double acting pistons either quad- or O-rings have to be used (the quad-ring is similar to a back to back lipseal). For the relatively low pressures involved (<10 bar), the use of O-rings is suggested. The oily nature of the E181 provides lubrication of the O-rings. Seal specifications are given in appendix E.

### 4.9 Simulation of the vapour pump

Vicatos [24] has developed a computer program that simulates and optimises the conventional absorption refrigeration cycle, operating with ammonia and water. It requires the evaporator and sink temperatures as input, then determines all relevant thermodynamic properties (such as temperature, pressure, concentration, enthalpy) of the working fluids at every stage of the cycle. A complete simulation is produced by a similar program in which the heat effects of the components, the refrigeration effect and the coefficient of performance is evaluated for varying generator temperature. In other words, for a certain set

of temperature conditions (evaporator & sink), the program predicts the coefficient of performance as a function of the generator temperature.

A routine is incorporated into the original model simulation to include the vapour pump. Its main function is to calculate the pump's stroke frequency and the mass flow rates of the vapour (16) and solution (7) stream. From this the work input and output and efficiency can be determined. The flow chart in figure 4.5 shows how the subroutine functions. The simulation model evaluates all pressures and temperatures and the solution flow rate for the electrical pump as a first estimate. Then the vapour pump subroutine is called to evaluate the amount of vapour (m16) required to deliver the solution flow rate (m7). An extra amount of absorbent is required to absorb the vapour, that is driving the pump. Hence the solution flow rate m7 has to be re-evaluated. The value predicted for the vapour flow rate m16 is fed to equation (3.4) to obtain a corrected value of the solution flow rate m7. These calculations are iterated within a loop until convergence of the solution flow rate m7 occurs. Then the work input, work output and pump efficiency is calculated using equations (4.22) to (4.25). The forces on the pistons are determined by equations (4.1) to (4.3). Finally, the COP is evaluated by equation (3.5).
The complete program, amended to accommodate the vapour pump, is listed in appendix A.

The pump subroutine goes through the following steps:

a) The density of the solution (7) is evaluated. The ammonia and water specific volumes are determined by polynomials; then the mixture specific volume is found by knowing its concentration.

b) The pump frequency is evaluated using equation (4.21).

c) The density of the high pressure hot vapour (16) is evaluated as a function of pressure and temperature.

d) The mass flow rate $m_{16}$ is now calculated. Using equation (4.18) in (4.19) yields:

$$m_{16} = \tfrac{1}{2}\rho_{vap}\, f \left[ 2D_v^2 - D_s^2 - D_r^2 \right] L \qquad \text{--------(4.30)}$$

e) The corrected flow rate $m_7$ is determined by equation (3.4) within an iterative loop.

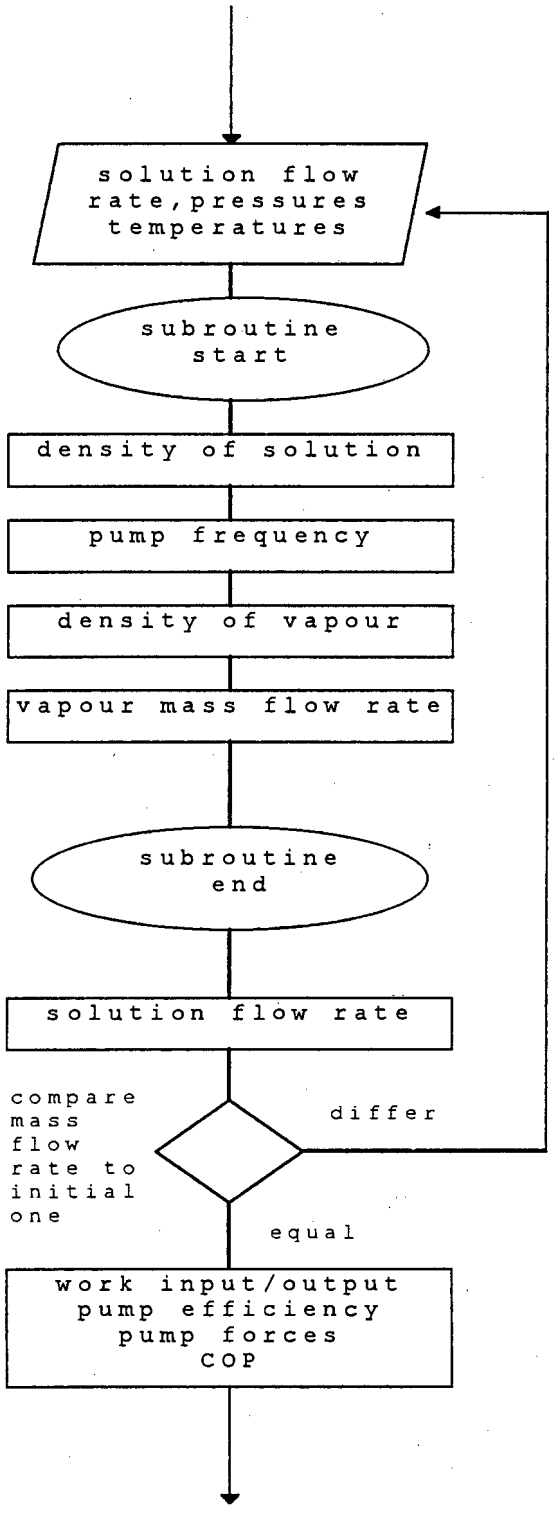


**Figure 4.5**
Vapour pump subroutine

# CHAPTER 5

## 5 Pump behaviour as predicted by computer simulation

The simulation was run with varying operating conditions to investigate how they affect pump operation and cycle performance. Operating conditions refer to the generator, evaporator and sink (absorber and condenser) temperatures. The working conditions of the unit were adjusted such that the evaporator would receive a refrigerant flow rate to produce 1kW of cooling capacity in each case. The trends that emerged are shown in the following.

### 5.1 Varying generator temperature with constant evaporator and sink temperatures for cycle with an electric pump and for cycle with a vapour pump:

Figure 5.1 shows that the coefficient of performance changes with the generator (operating) temperature. For both the electrical and the vapour pump there is a minimum operating temperature $T_{Gmin}$ for which COP becomes zero; then with increasing generator temperature the COP increases until it reaches a maximum; thereafter the ~~cop~~ COP drops off with increasing temperature.

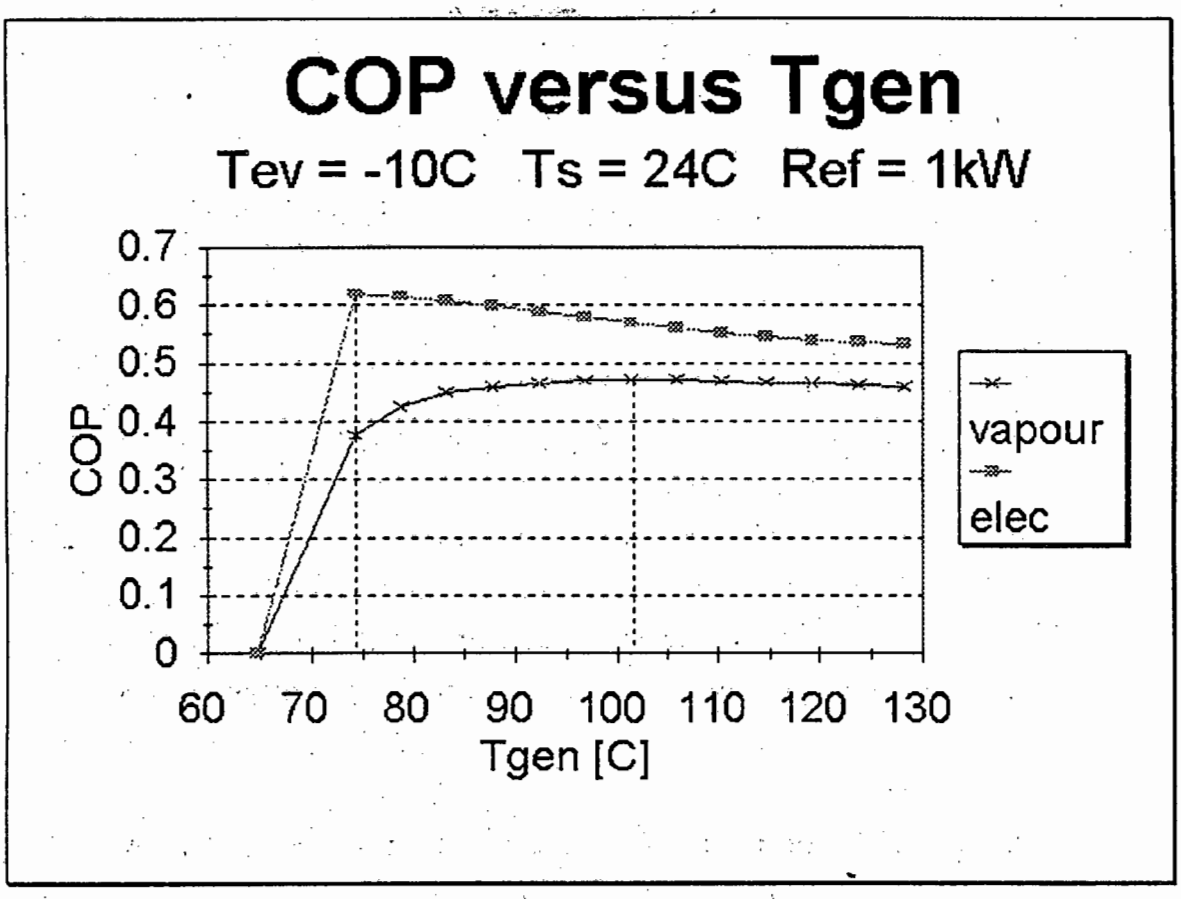


**Figure 5.1**

For generator temperatures ($T_{gen}$) less or equal to $T_{Gmin}$ no vapour will be liberated from the solution and thus no refrigeration takes place. The minimum generator temperature ($T_{Gmin}$) is the saturation temperature of the strong solution at the high (generator) pressure. For $T_{gen}$ equal to $T_{Gmin}$ the weak solution leaving the generator has the same temperature and concentration as the strong solution entering the generator. Hence, heat is solely transferred from the generator to the absorber with zero flow rate through the evaporator. With increasing $T_{gen}$ more vapour boils off the solution, increasing the refrigeration effect. The maximum COP is reached at the optimum operating temperature ($T_{gopt}$). The COP drops with further increasing $T_{gen}$. Vicatos [24] names various reasons for this reduction of COP:

- The irreversibility of the processes increases with temperature.

- Increasing amounts of absorbent are liberated in the generator, which have to be removed in the distillation column.

- At solution temperatures close to the water boiling point inert gasses (nitrogen) form by dissociation of ammonia. The presence of inert gasses in the evaporator decreases the refrigeration effect. This effect becomes especially significant in the water-ammonia system at temperature in the region of 170 C.

There are two distinct differences between the electrical pump case and the vapour pump case. Generally, for the vapour pump the coefficient of performance is less and the maximum COP occurs at a higher generator temperature. Both these trends were expected, as is explained in the following.

For the same refrigeration effect more heat energy has to be supplied to the system in the case of the vapour pump, thus reducing the COP. To understand why the optimum operating temperature is higher for the vapour pump the flow rates m7, m8 and m16 have to be considered. With the generator temperature increasing the weak solution concentration decreases. And according to equations (3.2) and (3.4) this decreases the solution flow rates as the difference between strong and weak solution concentration increases. This trend is confirmed by the figures 5.2 and 5.3. The flow rates m7 and m16 decrease exponentially with increasing generator temperature.

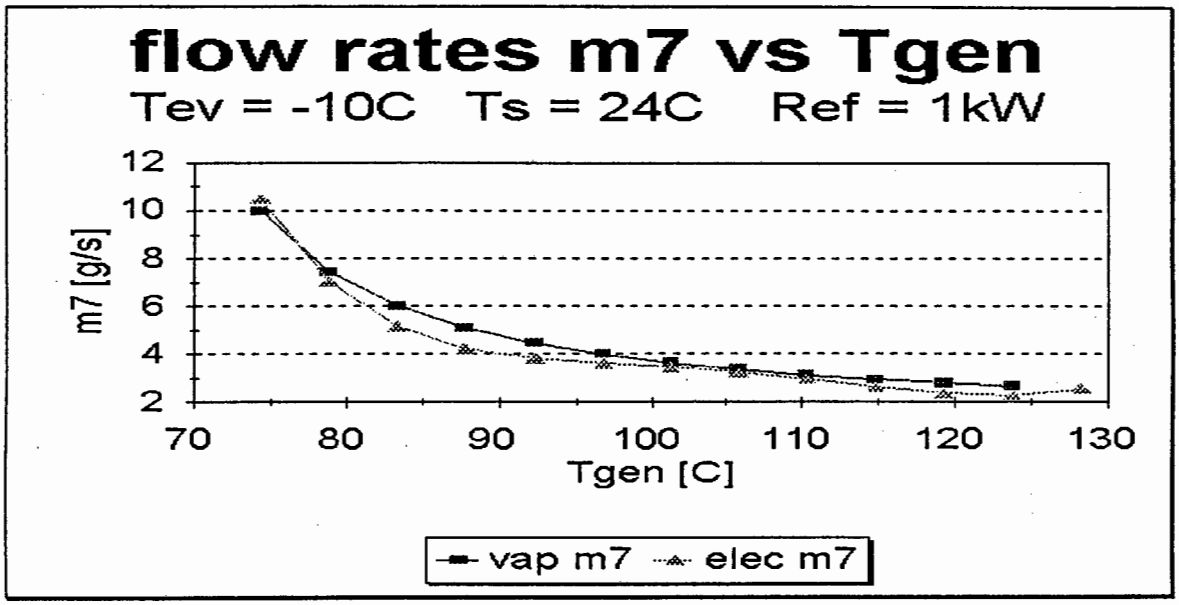


Figure 5.2

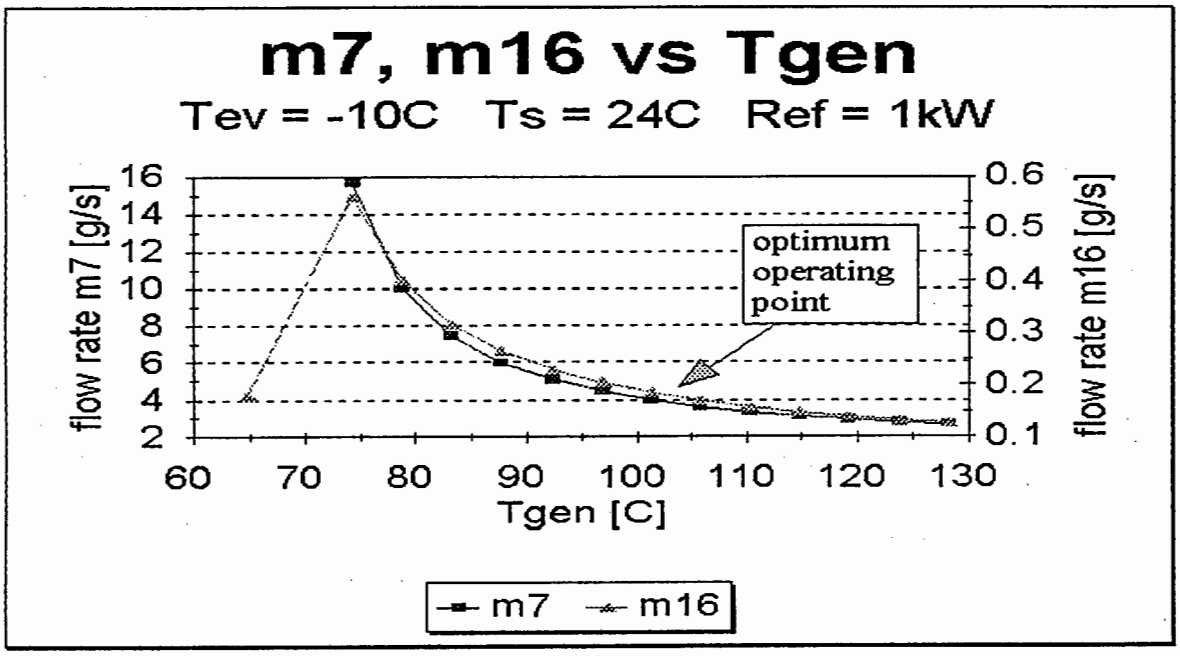


Figure 5.3

Decreased flow rates (m8, m7, m16) mean that less energy has to be supplied to the generator and vapour pump. Therefor the COP increases.

To summarise: Increasing the generator temperature means a decrease in flow rates of weak solution m8, strong

solution m7 and of the vapour m16 to drive the pump and this, in turn, results in lower heat input to the generator. The COP increases with generator temperature until the adverse effects (irreversibility etc.) become dominant. For the vapour pump the flow rates m7 and m8 are higher when compared to the electrical pump because of the additional flow rate of the vapour stream m16 (equation (3.1)) (figure 5.2). And with increased flow rates it pays more to reduce them by increasing the generator temperature. For this reason the optimum generator temperature is higher for the vapour pump when compared to the electric pump (figure 5.1). This concludes the argument.

The stroke frequency follows closely the m7 and m16 mass flow trends as is reflected in figure 5.4. Changing the generator temperature has no influence on the driving force of the vapour pump since the difference between high and low cycle pressure remains constant.

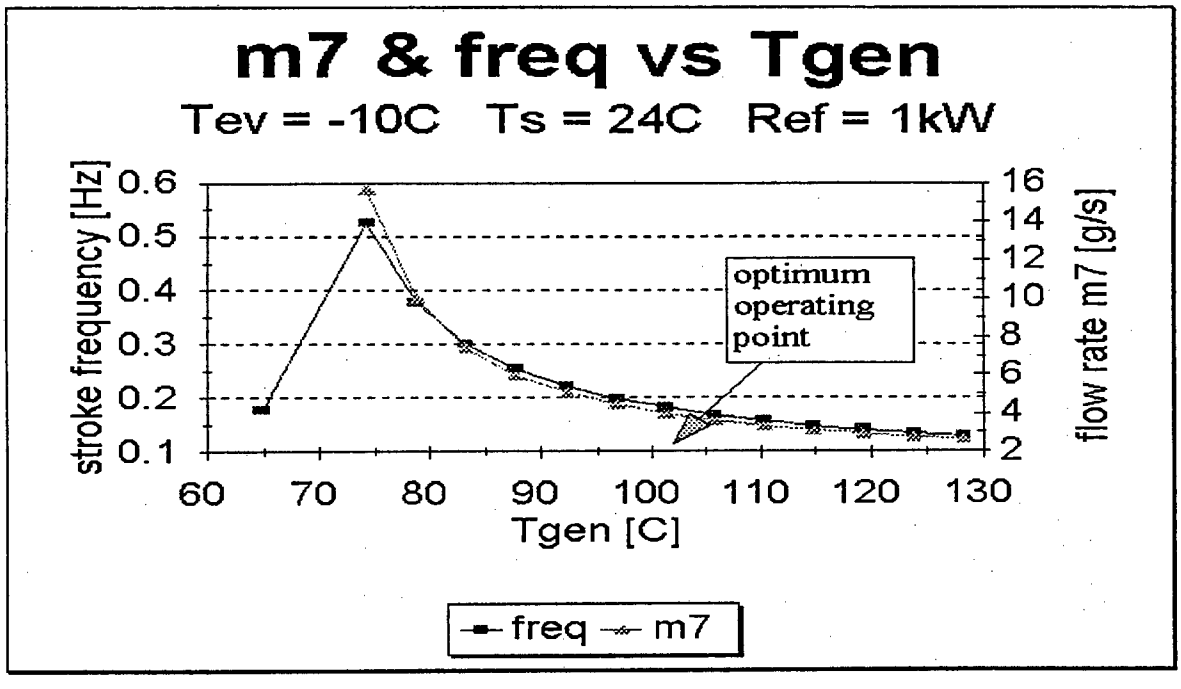


**Figure 5.4**

5.2 Varying the evaporator temperature while keeping the sink temperature constant and optimising generator temperature in each case

The evaporator temperature dictates the low pressure of the cycle. For a greater pressure difference between generator and absorber, more energy needs to be supplied to the system to achieve the same refrigeration effect. The coefficient of performance therefor decreases with decreasing evaporator temperature, as displayed in figure 5.5.

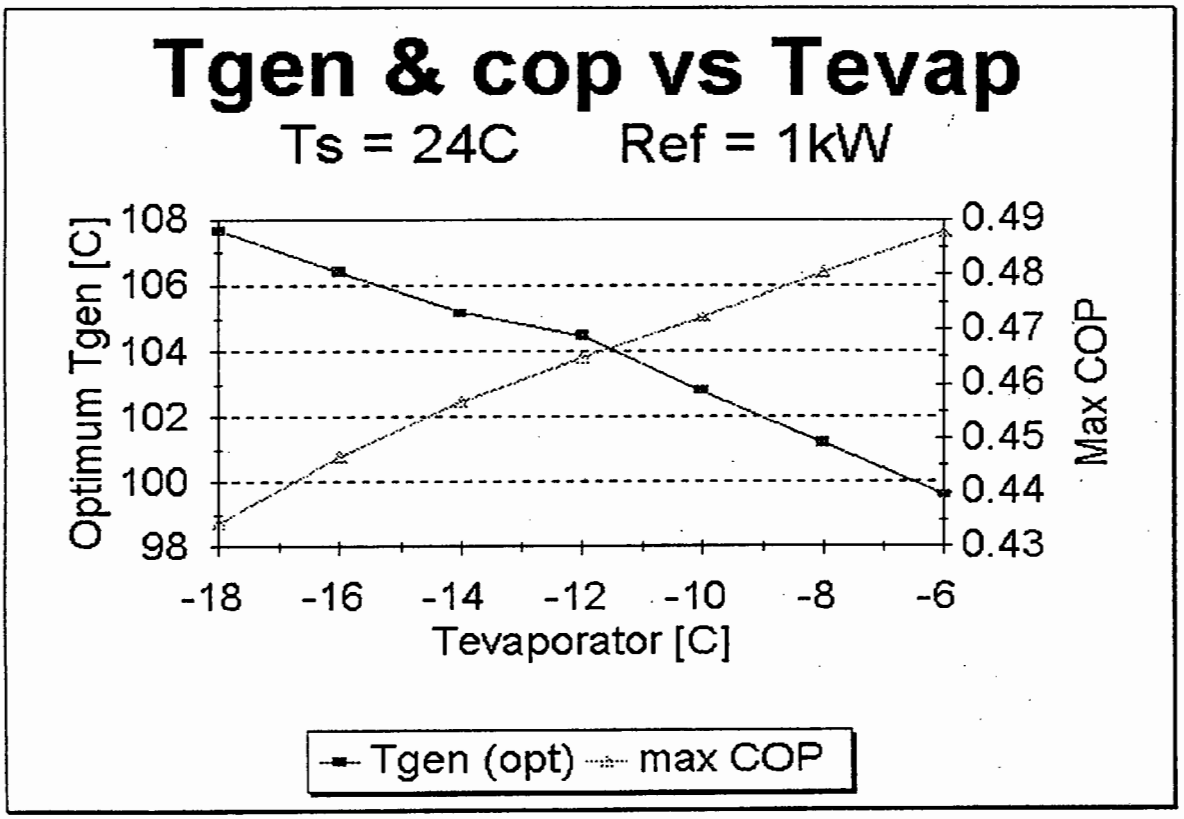


**Figure 5.5**

The mass flow rates (m8, m7 & m16) for optimum operating conditions increase with decreasing evaporator temperature. The reason is that at lower pressure in the

absorber (i.e. lower evaporator temperature) the absorption capability of the absorbent decreases. Therefor the difference in concentration between weak and strong solution decreases which leads to an increased mass flow rate of m7, m8 and m16 according to equations (3.4) and (3.2). This is shown graphically in figures 5.6.

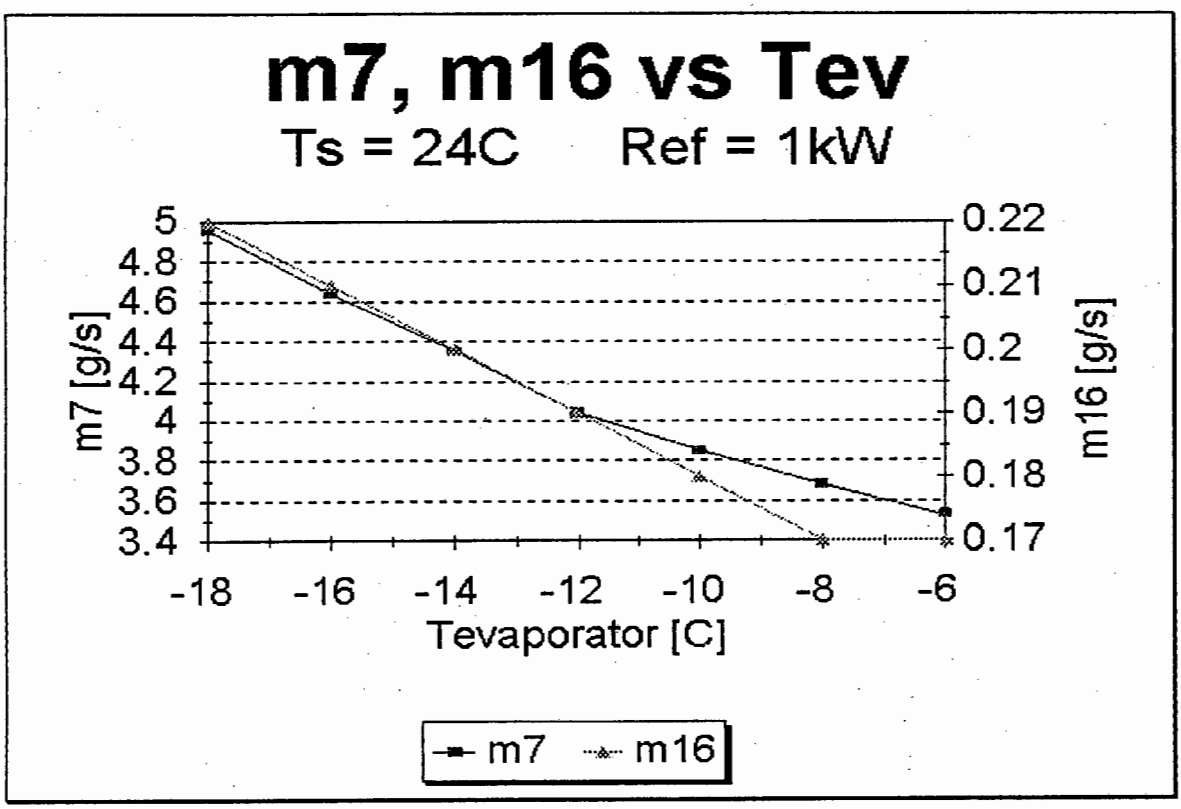


**Figure 5.6**

The optimum generator temperature (figure 5.5) increases with decreasing evaporator temperature. This is because, at the greater flow rates for lower evaporator temperatures, more input energy is saved by increasing the generator temperature.

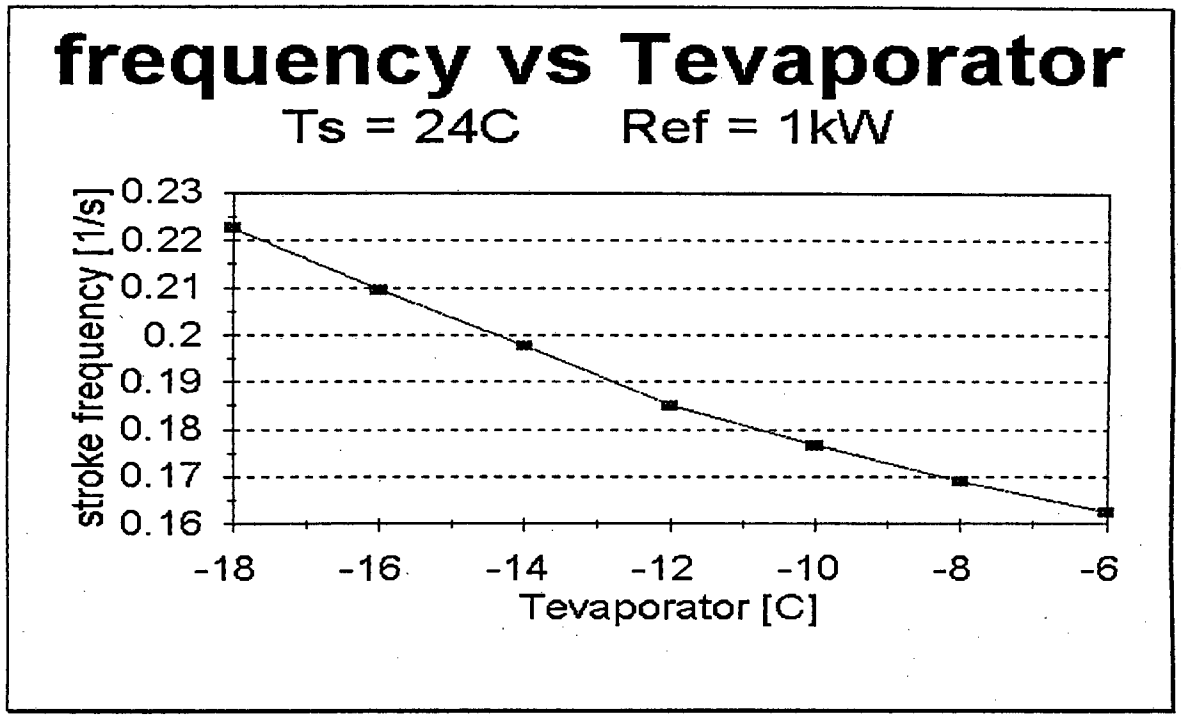


Figure 5.7

The stroke frequency follows the m16/m7 mass flow trend as shown by figure 5.7.

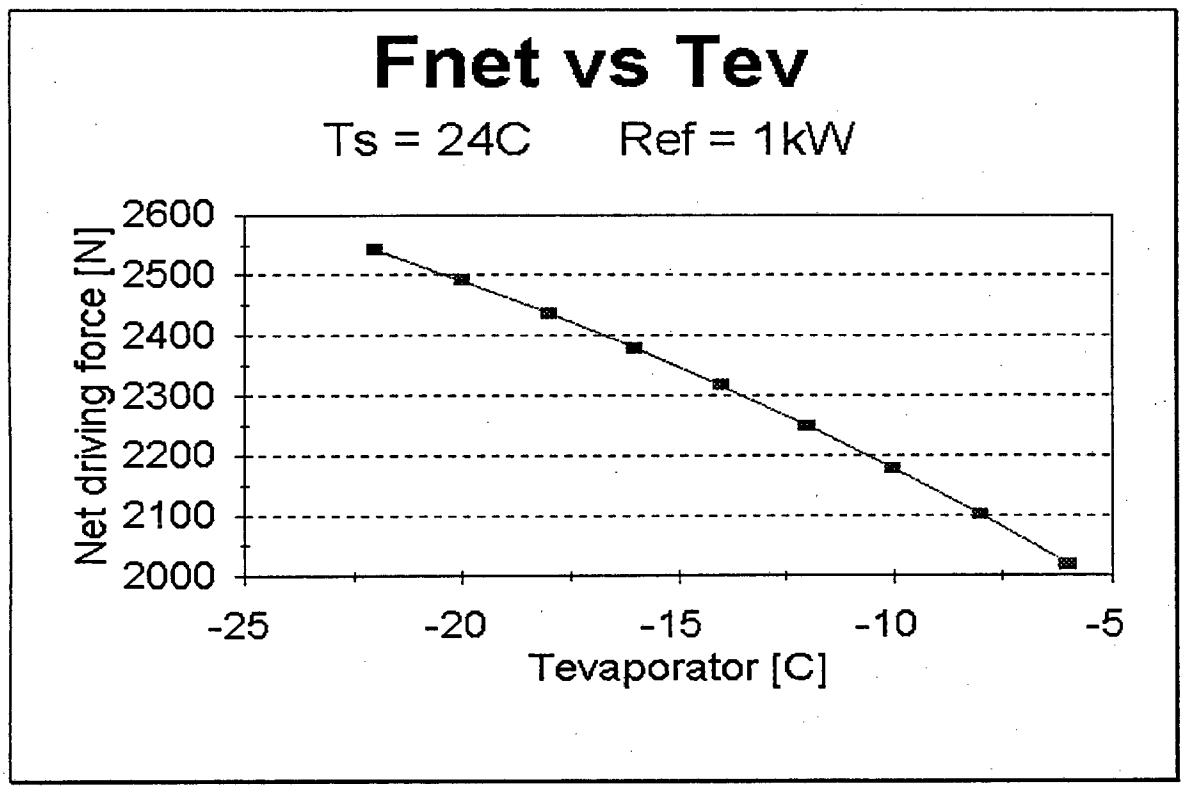


Figure 5.8

The net driving force of the vapour pump increases with decreasing evaporator temperature due to the greater pressure difference across the pistons of the pump.

## 5.3 Varying the sink temperature while keeping the evaporator temperature constant and optimising the generator temperature in each case

To understand the trends displayed when changing the sink temperature ($T_s$), it must be remembered that the condenser temperature and the absorber temperature are both set to $T_s$. Both are water cooled with water off the same source. The condenser temperature dictates the high pressure of the cycle. An increase in condenser temperature means an increase in the high pressure of the cycle.

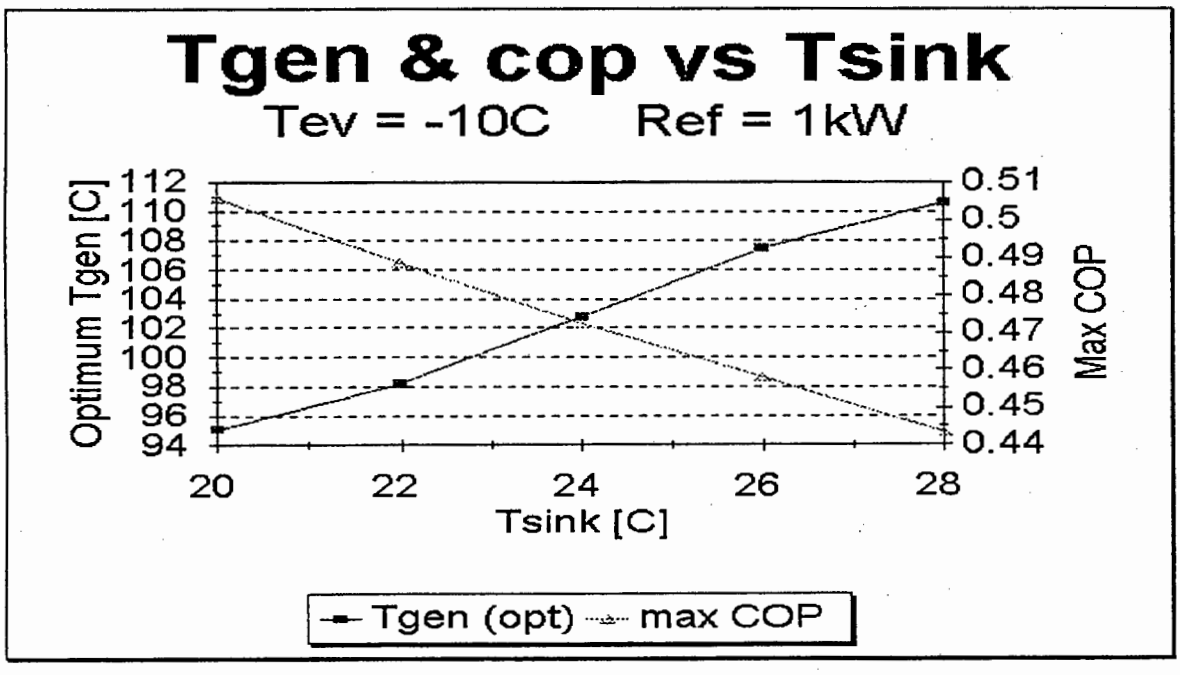


**Figure 5.9**

The generator pressure increases with condenser temperature and it follows that a greater energy input is needed to liberate the refrigerant vapour. This lets us expect that the maximum coefficient of performance drops with increasing sink temperature and this trend is reflected in figure 5.9.

Figure 5.10 shows that the mass flow rates (m7, m16 and so m8) increase with increasing sink temperatures for optimum generator temperature. During the absorption process gas absorption occurs more readily when the absorber temperature is low. The strong solution concentration increases with decreasing absorber temperature. The difference between strong and weak solution concentration increases and this decreases the flow rates m8 and m7 in accordance with equations (3.2) and (3.4).

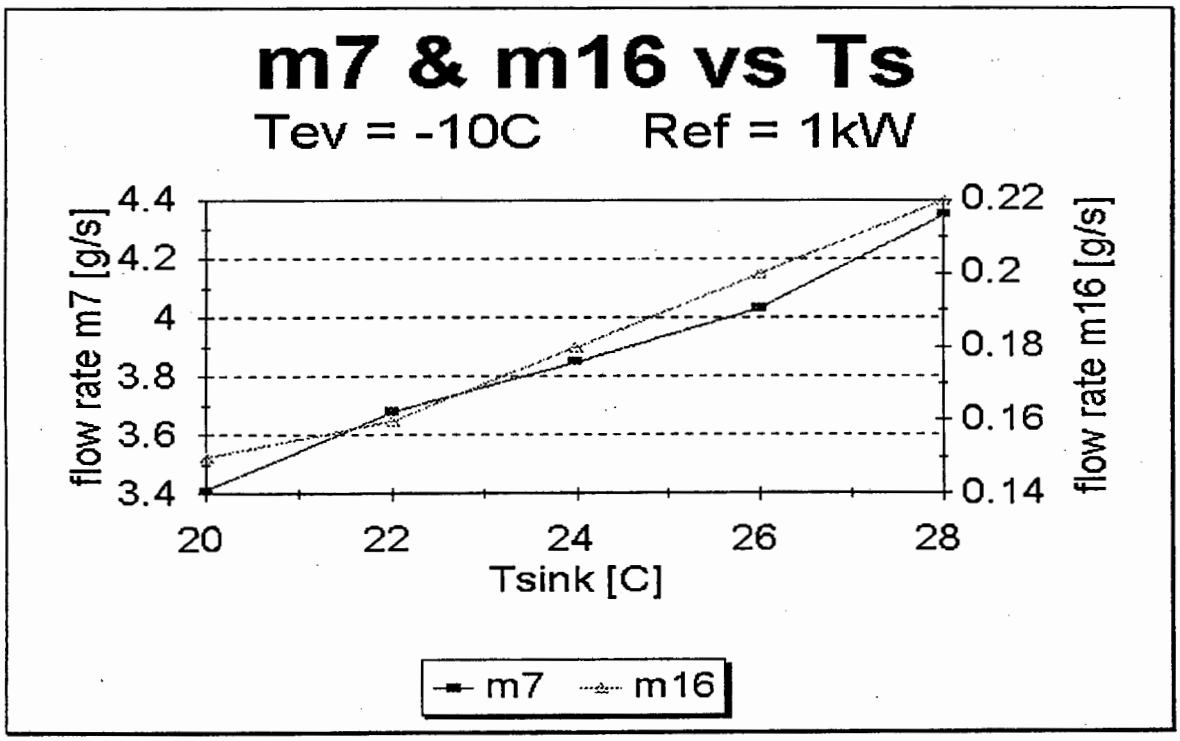


**Figure 5.10**

And, as before, an increase in mass flow rate m7 is associated with higher optimum generator temperatures (because it pays more in heat input reduction by increasing $T_{gen}$); therefor the optimum $T_{gen}$ increases with absorber temperature (figure 5.9).

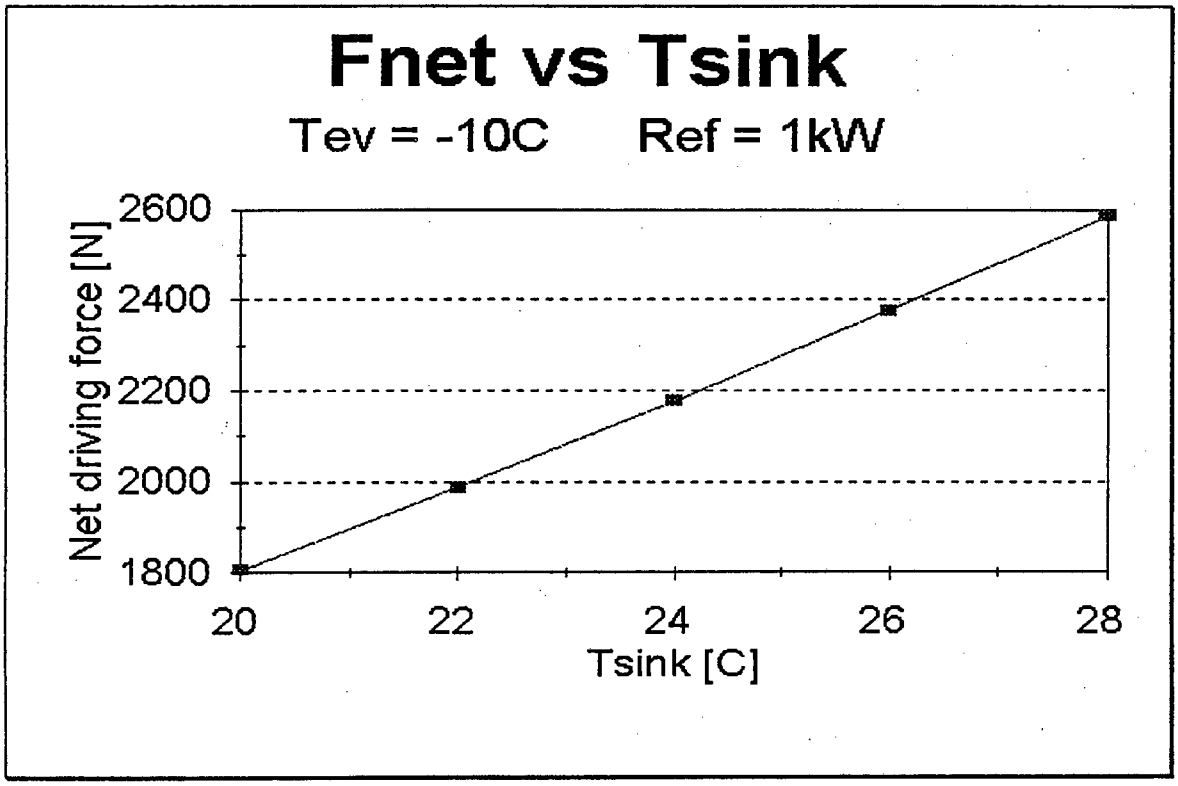


**Figure 5.11**

Figure 5.11 shows that an increases in sink temperature brings about an increase in net driving force of the vapour pump, due to the increased pressure difference across the pistons of the pump.

Since the mass flow rates m7 and m16 increase with increasing sink temperatures the vapour pump stroke frequency has to increase accordingly (figure 5.12)

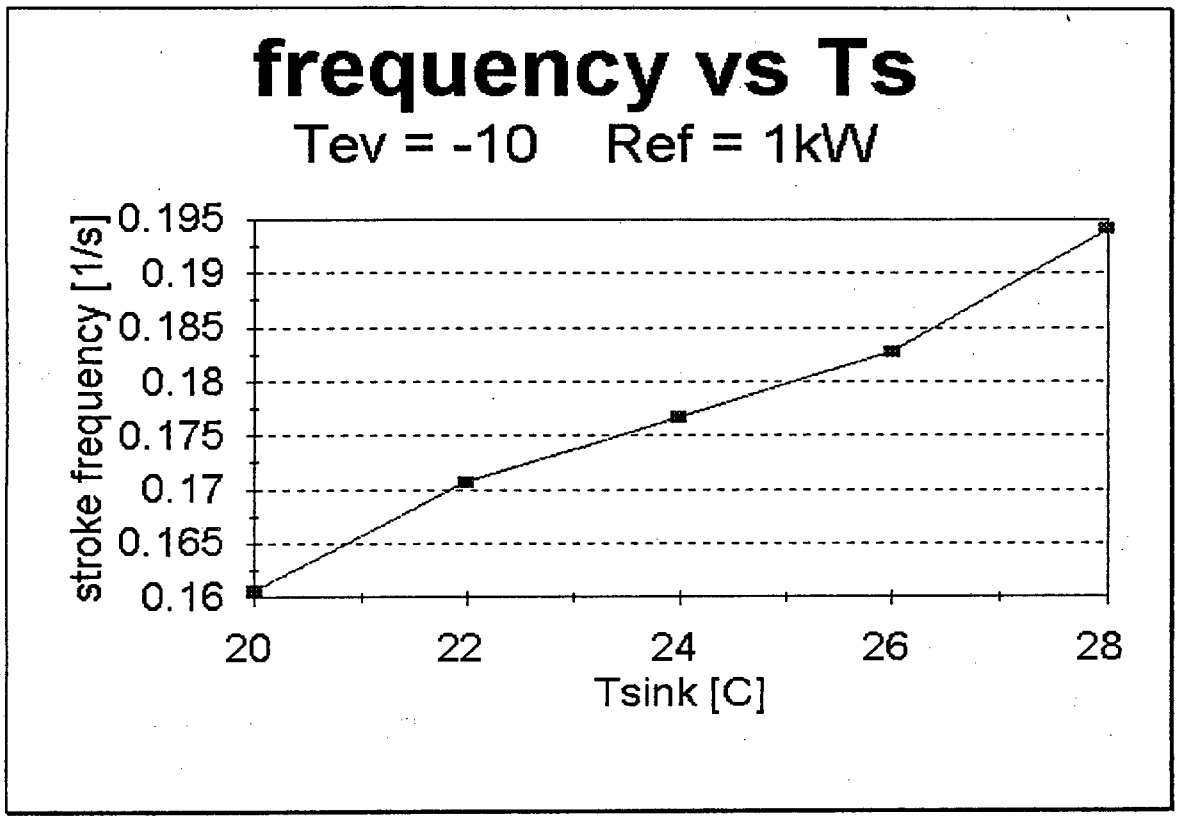


Figure 5.12

# CHAPTER 6

## 6 Experimentation

### 6.1 Bench test of the vapour pump

The vapour pump was tested prior to installation into the refrigeration rig.

#### 6.1.1 Apparatus

The experimental set up for the bench test is shown schematically in figure 6.1

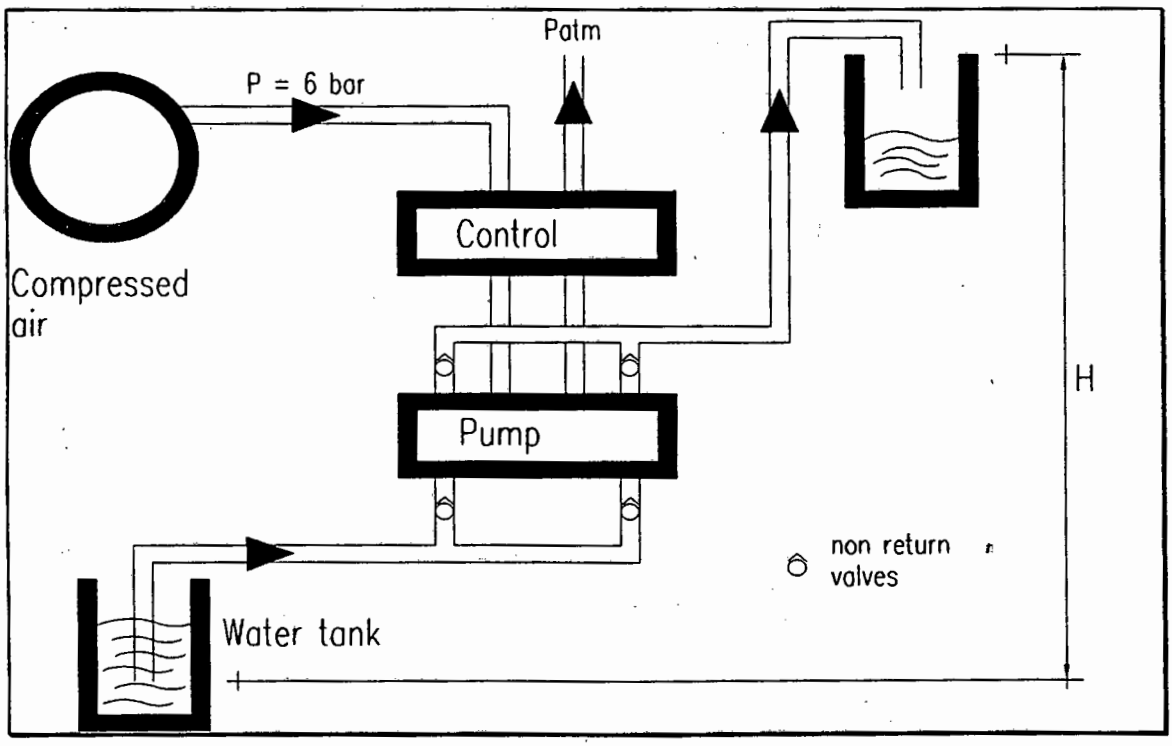


**Figure 6.1** The bench test experimental set up

Compressed air of approximately six bar gauge pressure is used to drive the pump. The exhaust air was exposed to atmospheric conditions. This pressure difference corresponds to the one encountered between generator and absorber in the refrigeration machine. The non-return valves were custom made and consist of a steel ball and male connector fitting as shown in figure 6.2.

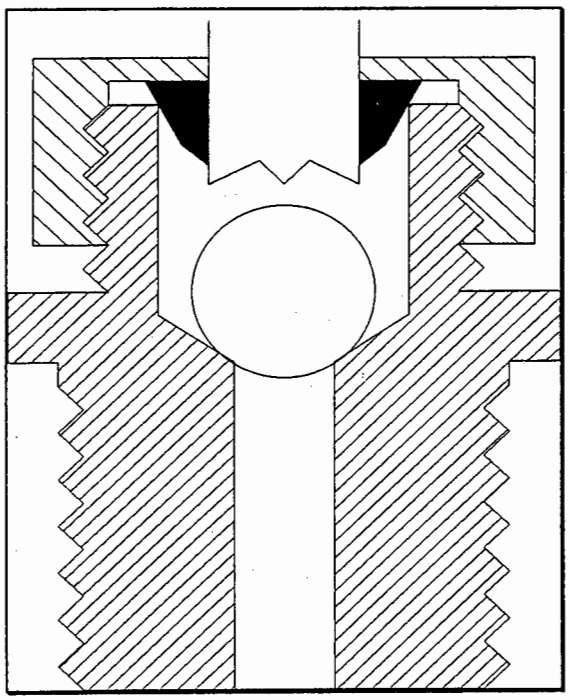

**Figure 6.2**
The non- return valve

The steel ball blocks flow in one direction by sealing on the smooth seat as shown in figure 6.2. The pipe connected at the top of the valve has an uneven end to prevent the steel ball from sealing the flow in both directions. In upright position, as in figure 6.2, gravity holds the valve closed. A light spring (not shown figure 6.2) to force the ball upon its sealing seat was also used.

### 6.1.2 Troubles encountered with the design of the pump

Initially, the running of the pump was troublesome. The following immediate problems were encountered.

1. Both pump pistons seized repeatedly. This was due to a very fine clearance fit between piston and cylinder and was corrected by increasing the clearance to approximately 150μm.

2. High pressure air from the vapour side leaked through to the liquid side. As the retracting piston tries to create a vacuum, air penetrates the space on the liquid side of the piston and prevents liquid from being drawn in. This type of failure is shown in figure 6.3.

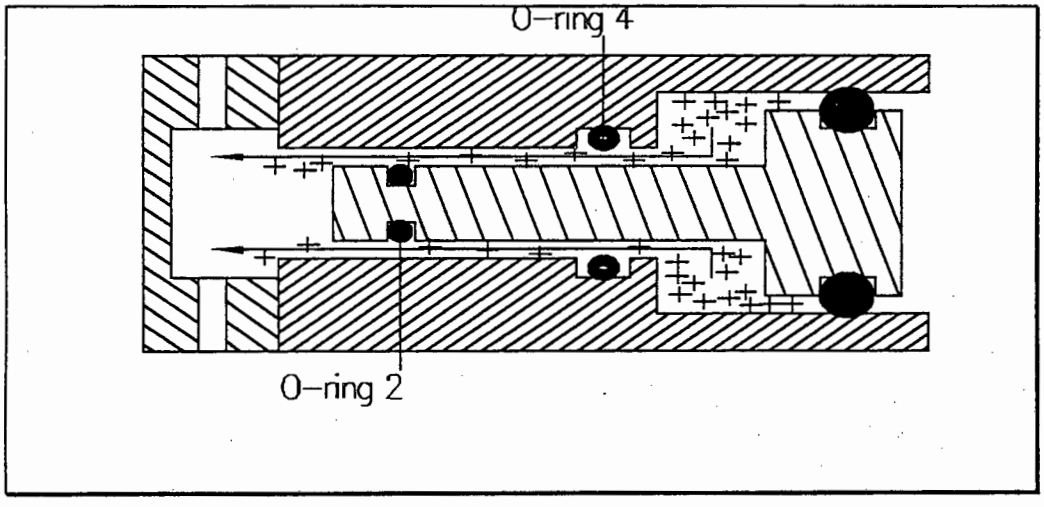


**Figure 6.3** Vapour leak to liquid side

The leaks of this kind were observed with O-ring 4 (figure 6.3 or figure E.1) not being used. O-ring 4 was initially thought superfluous and as such unnecessarily increasing friction. With the installation of O-ring 4 no further leakage was observed.

3. The spring in the link mechanism failed to provide motion to the control shaft in a reliable way. Typically, the spring would return the control shaft once and then get stuck in-between the end positions. No spring to satisfy the marginal spring design specifications could be obtained for experimentation. Various springs with characteristics close to those calculated malfunctioned. A detailed analysis of the causes of failure of the spring mechanism is presented in appendix K. As a result of the failure of the spring mechanism a pneumatic system was used to reciprocate the control shaft.

### 6.1.3 The pneumatic system to simulate the link mechanism

A double acting cylinder with stroke length 25 mm, mounted onto the base plate and coupled to the control shaft, replaces the link mechanism to provide motion to the control mechanism. Thermodynamically, this does not defeat the purpose of the study. Only about 3% of the energy going into the pump is consumed by compressing the spring in the link mechanism. And the pump draws only 1% of the energy supplied to the generator. Overall, the energy associated with the spring action can be considered negligible. The double acting cylinder is connected to the pneumatic cycle. Two time delay control valves in the pneumatic cycle enable the duration between strokes to be adjusted. The frequency of the pump pistons can easily be controlled by changing the time delay control valve settings. Details about the pneumatic system are given in appendix H.

### 6.1.4 Results and analysis

The graph in figure 6.4 shows how the pump frequency changes with the time delay control valve setting of the pneumatic cycle.

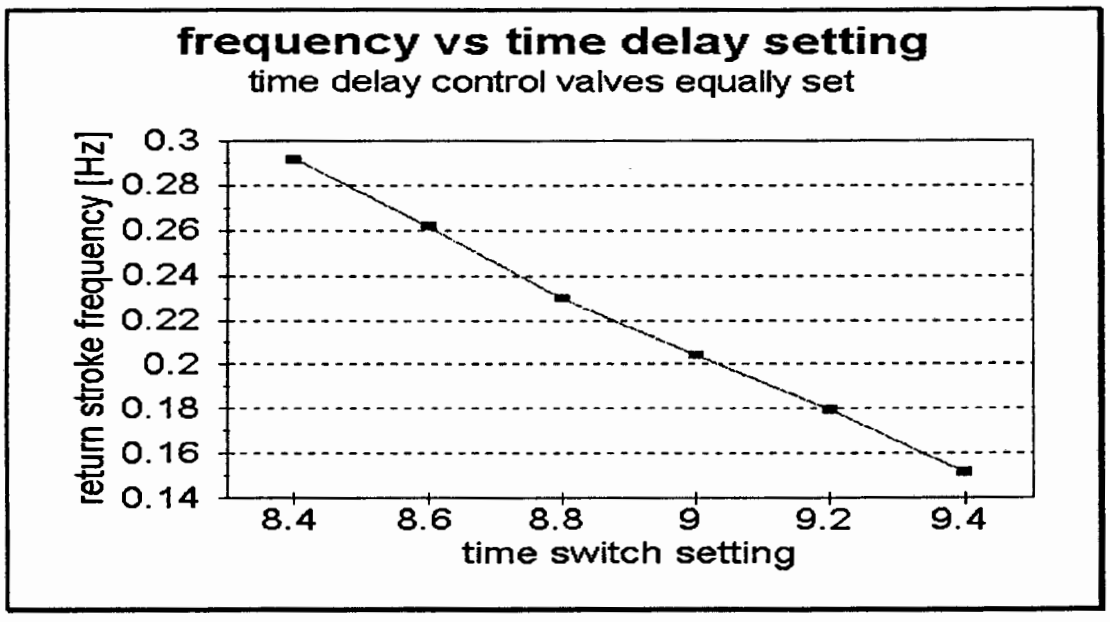


**Figure 6.4**

The pump was run for a minute for various time switch settings and height differences between inlet and outlet of the water line. The flow rates obtained are recorded in tables 6.1 & 6.2.

| Switch setting | frequency [Hz] | H [m] | volume pumped [ml/min] | volume pumped [ml/s] | calc. flow rate [ml/s] | flow rate η [%] |
|---|---|---|---|---|---|---|
| 8.40 | 0.292 | 0 | 541 | 9.017 | 4.587 | 196.6 |
| 8.40 | 0.292 | 1.8 | 581 | 9.683 | 4.587 | 211.1 |
| 8.80 | 0.230 | 0 | 407 | 6.783 | 3.613 | 187.7 |
| 8.80 | 0.230 | 1.8 | 420 | 7.000 | 3.613 | 193.7 |
| 9.00 | 0.204 | 0 | 414 | 6.900 | 3.204 | 215.4 |
| 9.00 | 0.204 | 1.8 | 404 | 6.733 | 3.204 | 210.2 |
| 9.20 | 0.180 | 0 | 390 | 6.500 | 2.827 | 229.9 |
| 9.20 | 0.180 | 1.8 | 327 | 5.450 | 2.827 | 192.8 |
| one | pump | only | | | | |
| 8.80 | 0.230 | 0 | 267 | 4.450 | 1.806 | 246.3 |

**Table 6.1** Pumping rates (no springs in non-return valves)

| Switch setting | frequency [Hz] | H [m] | volume pumped [ml/min] | volume pumped [ml/s] | calc. flow rate [ml/s] | flow rate η [%] |
|---|---|---|---|---|---|---|
| 8.40 | 0.292 | 0 | 251 | 4.183 | 4.587 | 91.2 |
| 8.40 | 0.292 | 1.8 | 264 | 4.400 | 4.587 | 95.9 |
| 8.80 | 0.230 | 0 | 223 | 3.717 | 3.613 | 102.9 |
| 8.80 | 0.230 | 1.8 | 202 | 3.367 | 3.613 | 93.2 |
| 9.00 | 0.204 | 0 | 181 | 3.017 | 3.204 | 94.2 |
| 9.00 | 0.204 | 1.8 | 195 | 3.250 | 3.204 | 101.4 |
| 9.20 | 0.180 | 0 | 166 | 2.767 | 2.827 | 97.7 |
| 9.20 | 0.180 | 1.8 | 166 | 2.767 | 2.827 | 97.7 |

**Table 6.2** Pumping rates (with springs in non-return valves)

The experimentally obtained flow rate was compared to the theoretical one as calculated using equation 4.16. The

calculated flow rate is based upon the volume displaced by the pump pistons. It came as a surprise to observe that, with no springs in the non-return valves, the actual flow rate is about twice the theoretical one. An explanation for this observation is found when considering the dynamic effects of the fluid flow. The speed by which the fluid is drawn in to the pump is such that its momentum pushes fluid through to the delivery line. This was confirmed when operating the double pump with only one pump in action. It was observed that water was supplied to the outlet tank during the suction stroke. The results displayed in table 6.2 show that by installing springs into the valves the observed discrepancy in flow rates was eliminated.

The above observations might be relevant during start up of the cycle when there is no significant pressure difference between the solution inlet and outlet of the pump.

## 6.2 Cycle test

### 6.2.1 Experimental apparatus

Experiments were conducted on the 1 kW absorption refrigeration plant. Vicatos [24] originally designed the rig for experimentation with ammonia and water as the working fluids. Subsequent experiments were done using Freon R22 and tetraethelene glycol dimethyl ether (E181). A schematic diagram of the experimental apparatus is shown in figure 6.5. All components except for the evaporator, precooler and vapour pump were part of the old rig. A brief description of each component is given in the following:

**a) the generator**

The gas fired generator was designed to supply up to 3 kW power to the solution. It consists of a shell and seven U-tubes. Hot gasses of about 700 C, simulating the exhaust gas of an IC engine, are passed through the tubes to heat up the mixture contained inside the shell. An external fan forces air into the exhaust stream to increase the gas flow through the tubes. The generator shell has three outlets: one at the top to carry the liberated vapour to the condenser, one at the bottom for the weak solution and one (at bottom) for draining purposes. The strong solution inlet is situated at the top. The generator is also equipped with a level indicator and a pressure gauge.

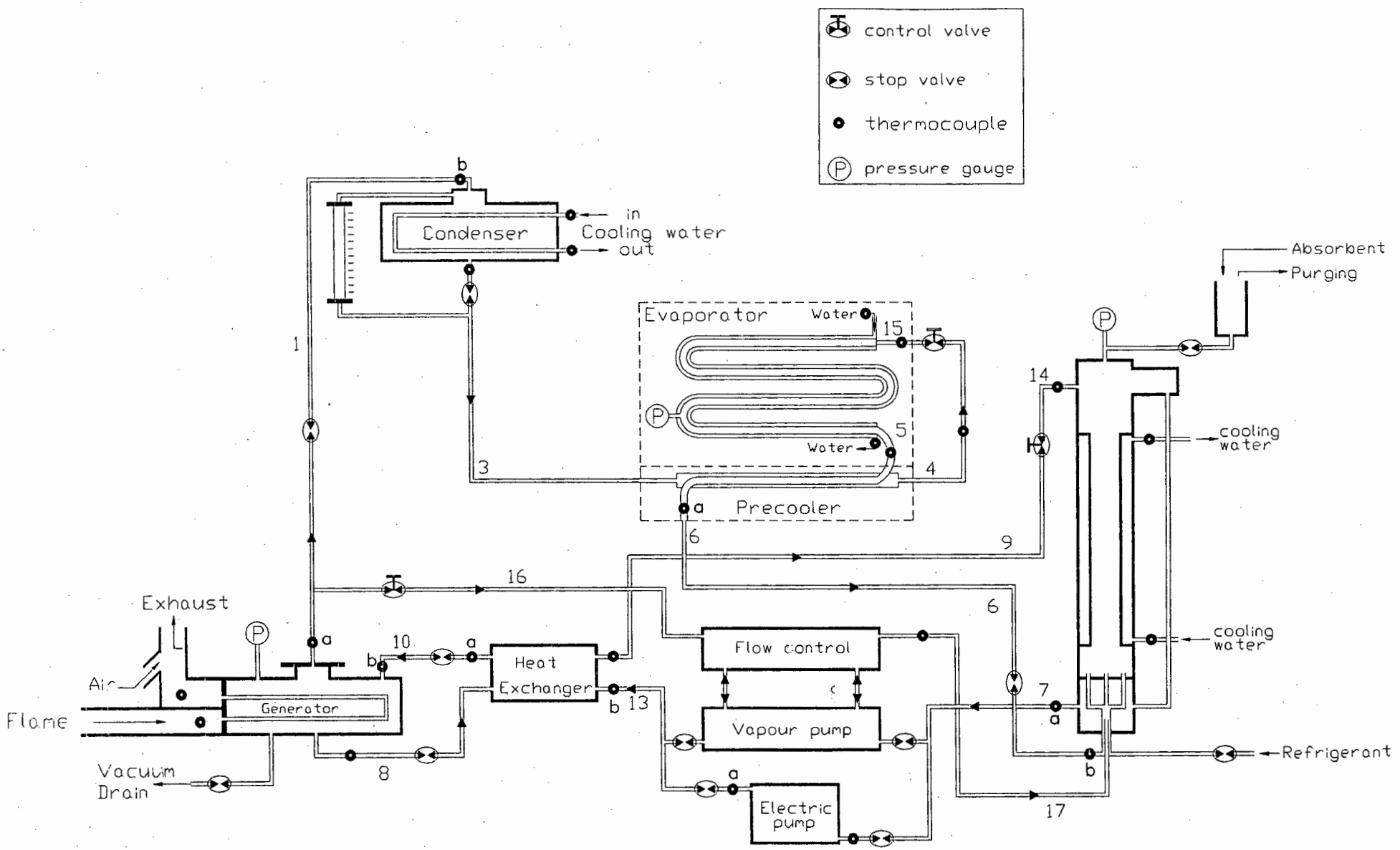


Figure 6.5 Schematic diagram of the experimental apparatus

**b) the condenser**

The condenser is of the shell and tube type and has been designed for a capacity of 1.5 kW. Cooling water, passing through tubes inside a shell, removes heat from the refrigerant inside the shell and the condensate leaves the condenser shell at the bottom. A glass tube bypass serves as level indicator and for mass flow measurement.

**c) the precooler**

The precooler consists of two 50 cm long concentric tubes. Liquid from the condenser flows in the outer tube towards the expansion valve. Vapour refrigerant from the evaporator flows in the opposite direction through the inner tube.

**d) the evaporator**

The evaporator consists of two meter long concentric copper tubes. Water, that supplies energy to the evaporating refrigerant, is passed through the outside tube. The refrigerant flows through the inner tube. For a cooling capacity of 1 kW the water flow rate is calculated as follows.

$$RE = m \bullet c_p \bullet \Delta T$$

where RE = refrigeration effect
m = water mass flow rate
$c_p$ = specific heat = 4.2 kJ/kg
$\Delta T$ = difference in water temperature

The water should not freeze up and block the passage. The flow rate must therefor be sufficiently high. For a minimum inlet temperature of 20 C the $\Delta T$ should not exceed 15 C. So

$$[kW] = m\ [kg/s] \cdot 4.2\ [kJ/kg/C] \cdot 15\ [C]$$

$$m = 0.01587\ [kg/s] = 57.14\ [l/h] \quad \text{---(min)}$$

| type | double tube |
|---|---|
| capacity | 1 kW |
| heating medium | water |
| total length | 2 meter |
| inner tube OD | 22 mm |
| outer tube OD | 28 mm |

**Table 6.3** Evaporator details

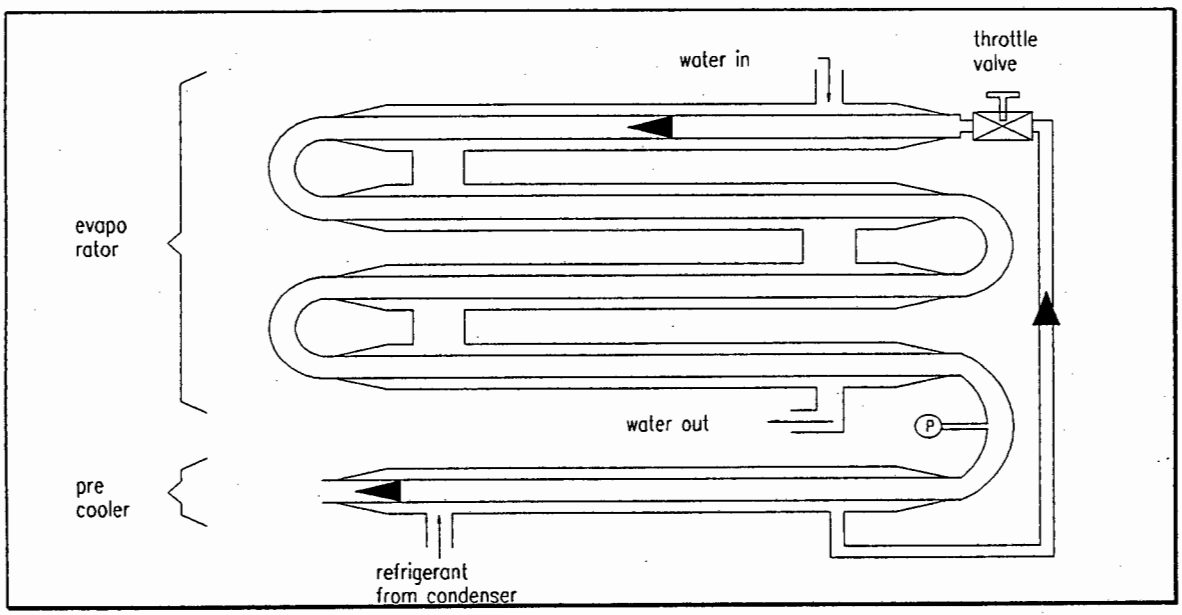


**Figure 6.6** Diagram of the evaporator-precooler combination

**e) the absorber**

The absorber is of the tubular type. Weak solution coming in at the top absorbs vapour refrigerant coming in from the bottom end. The liquid mixture accumulates at the bottom, from where it is pumped back to the generator. The heat of mixing, together with the heat carried by the weak solution, is removed by cooling water that flows in the outer jacket. Detailed information is tabulated below (table 6.4). The absorber is also equipped with a level indicator, pressure gauge and an inlet/outlet for draining and refrigerant charging purposes.

| | |
|---|---|
| type | tubular |
| heat rejected | 3 kW |
| coolant | water |
| tube inside diameter | 17 mm |
| tube thickness | 1.5 mm |
| overall tube height | 70 cm |

**Table 6.4** Absorber details

**f) the pump**

The electric and vapour pumps are connected in parallel. Either of the pumps can be isolated by stop valves. The electric pump is a double acting piston pump, driven by an electric motor through a reduction gear. The stroke length is 25 mm, the piston diameter 30 mm. It is not possible to control the delivery flow rate as the pump operates at one constant speed. Its frequency is 0.52 cycles per second. This corresponds to a nominal flow rate of 18.38 ml per second.

**g) the heat exchanger**

The heat exchanger consists of a double coil. Weak solution flows through the inside coil (6mm OD). The strong solution flows countercurrent through the outer tube (10mm OD).

## 6.2.2 Experimental procedure

Experimental data is collected from the absorption machine shown schematically in figure 6.5, being operated in two pumping modes: 1) with the electric pump 2) with the vapour pump. The start-up procedure is as follows:

i. Burner, sink cooling water and electric pump are switched on.

ii. Once liquid R22 is present in the condenser, the evaporator load water is turned on.

iii. For vapour pump operation the electric pump is switched off, and the vapour pump switched on.

iv. The evaporator valve, pressure reducing valve (weak solution line) and vapour pump frequency (when using the vapour pump) are adjusted to achieve equilibrium.

The various control valves affect the cycle behaviour as set out in the following:

a) The *burner gas valve* regulates partly the input power and temperature of the gasses heating the generator.

b) The *evaporator throttle valve* controls the mass flow rate of refrigerant through the evaporator.

c) The *pump frequency* can only be altered when using the vapour pump. This is done by changing the setting of the time delay control valves of the pneumatic system as set out in section 6.1.3. The pump frequency controls the flow rate of the strong solution to the generator. A small flow rate implies a high generator solution temperature. This in turn causes more R22 to be liberated; the weak solution is of lower refrigerant concentration.

d) The *pressure reducing valve* controls the flow rate of the weak solution from the generator to the absorber. The valve is adjusted to keep the liquid level in the absorber constant.

### 6.2.3 Experimental measurements

Measurement of the following variables and properties are taken:

a) The fuel *consumption* of the burner is measured by a volumetric flow meter.

b) The *sink (absorber and condenser) cooling water flow rate* is measured using a calibrated flow meter.

c) The *evaporator load water flow rate* is measured manually.

d) The *pressure* is measured by pressure gauges as indicated in figure 6.5.

e) K-type thermocouples measure the *temperature* at positions as indicated in figure 6.5.

### 6.2.4 Results and analysis

The running of the absorption machine was very problematic. It was difficult to achieve stability, mainly because the evaporator throttle valve occasionally blocked up, either because of impurities in the stream or because of moisture freezing up the valve. Nitrogen was used for pressure testing before running the cycle; air, however, got into the system during repair work, that had to done on the electric pump (leaks and non-return valves). On the other hand, opening the throttle valve further resulted in increasing the absorber pressure, as not all of the refrigerant could be absorbed. Initially it was observed that high pressure R22 in the control mechanism leaked through to the absorber line, without going through the pump pistons. When the control mechanism was opened, it was found that two of the EPDM sealing rings had been damaged by extrusion. The others were enlarged and softened. Teflon rings were successfully installed instead.

The results are presented in tables 6.5 and 6.6. Although readings were taken at all points indicated in figure 6.6, only those required to evaluate the coefficient of

performance are given. To obtain the COP, the following variables have to be calculated:

a) the *refrigeration capacity:* There are two ways to calculate the refrigeration capacity:

i) measuring the refrigerant flow rate through the evaporator and determining the enthalpies at entry and exit of the evaporator from the pressures and temperatures at those points. Then the cooling capacity equals $Q_{ref} = m \Delta h$.

ii) measuring the water flow rate through the outer tube of the evaporator and the temperature difference between inlet and outlet of the water. Then the refrigeration capacity is given by $Q_{ref} = m_{H2O} c_p \Delta T$.

It was decided to use method (ii) since the evaporator water flow rate could be measured more accurately than the refrigerant flow rate.

b) the *heat input:* Ideally the heat input is calculated by measuring the flow rates of the strong solution (10), weak solution (8), refrigerant going to the condenser (1) and the corresponding specific enthalpies. However, due to the lack of thermodynamic data for the R22-E181 combination, the enthalpies could not be determined. Kriebel et al [12] have published data giving the enthalpy as a function of the concentration and pressure (or temperature) for saturated liquid for the temperature range -90C to 70C. The temperatures measured in the experiments range from 58C to 111C for the strong solution and from 107C to 197C for the weak solution.

Alternatively, the heat input calculation is based on the calorific value (heat of combustion) of the gas used in the burner. Capegas, that supplies the gas (town-gas), gives the calorific value as 16.76 $MJ/m^3$. A breakdown of the composition of the gas is given in appendix I. Since only a fraction of the heat energy of the gas is transferred to the boiler, a conversion factor ($\eta$) is introduced (appendix J). The heat input is then calculated by:

$$Q_{gen}\ [kW] = \eta\ 16.76\ \dot{V}_{gas}\ [l/\text{sec}] \qquad \text{------(6.1)}$$

A third method evaluating the heat input is to make use of the energy balance for the cycle:

$$Q_{gen} = Q_{abs} + Q_{con} - Q_{evap} + Q_{losses}$$

$Q_{abs}$ is difficult to evaluate as the absorber cooling water flow rate is not known. The flow meter in the rig measures the combined flow rate of the absorber and condenser cooling water. Also, the thermal losses cannot be quantified. It was therefor decided to proceed using equation 6.1.

| Burner | | Pressure | | Evaporator | | | | | | |
|---|---|---|---|---|---|---|---|---|---|---|
| *gas flow rate* | *solution temp.* | *high* | *low* | *entry temp.* | *water flow rate* | *water inlet temp.* | *water outlet temp.* | *ref capacity* | *heat input* | *COP* |
| *l/sec* | *C* | *bar* | *bar* | *C* | *l/sec* | *C* | *C* | *kW* | *kW* | |
| 0.38 | 136 | 11.7 | 4.6 | -3.0 | 0.020 | 29.0 | 24.0 | 0.42 | 1.40 | 0.30 |
| 0.49 | 128 | 11.6 | 4.6 | -3.9 | 0.025 | 27.1 | 23.6 | 0.37 | 1.72 | 0.21 |
| 0.38 | 107 | 11.6 | 5.0 | 0.0 | 0.034 | 25.4 | 22.6 | 0.40 | 1.50 | 0.27 |
| 0.53 | 158 | 12.2 | 5.0 | 0.2 | 0.068 | 26.8 | 23.9 | 0.83 | 1.70 | 0.49 |
| 0.52 | 197 | 12.8 | 5.2 | 1.4 | 0.034 | 28.3 | 24.2 | 0.59 | 1.52 | 0.39 |
| 0.49 | 168 | 12.0 | 5.0 | 0.2 | 0.021 | 27.1 | 23.4 | 0.33 | 1.56 | 0.21 |
| 0.51 | 111 | 10.2 | 4.4 | -4.1 | 0.029 | 27.7 | 24.1 | 0.44 | 1.86 | 0.24 |

**Table 6.5** Cycle performance using electric pump

Figure 6.7 and 6.8 depict how the COP's and refrigeration capacities compare for cycles with electric and vapour pump.

| Burner | | Pressure | | Evaporator | | | | | | | |
|---|---|---|---|---|---|---|---|---|---|---|---|
| *gas flow rate* | *solution temp.* | *high* | *low* | *entry temp.* | *water flow rate* | *water inlet temp.* | *water outlet temp.* | *pump freq* | *ref capacity* | *heat input* | *COP* |
| *l/sec* | *C* | *bar* | *bar* | *C* | *l/sec* | *C* | *C* | *Hz* | *kW* | *kW* | |
| 0.46 | 115 | 9.6 | 6.o | 5.2 | 0.013 | 27.6 | 24.0 | 0.290 | 0.19 | 1.70 | 0.11 |
| 0.46 | 126 | 9.6 | 6.o | 5.2 | 0.013 | 27.7 | 23.6 | 0.290 | 0.22 | 1.65 | 0.13 |
| 0.46 | 115 | 9.6 | 6.o | 5.2 | 0.013 | 27.7 | 23.8 | 0.290 | 0.21 | 1.70 | 0.12 |
| 0.51 | 136 | 9.4 | 5.8 | 4.0 | 0.020 | 28.1 | 24.7 | 0.204 | 0.26 | 1.74 | 0.16 |
| 0.53 | 130 | 9.4 | 5.8 | 4.2 | 0.019 | 28.0 | 24.6 | 0.204 | 0.27 | 1.82 | 0.15 |
| 0.42 | 129 | 9.4 | 6.2 | 5.0 | 0.014 | 27.7 | 23.4 | 0.204 | 0.25 | 1.53 | 0.17 |
| 0.45 | 156 | 9.4 | 6.2 | 5.3 | 0.020 | 26.9 | 24.1 | 0.180 | 0.24 | 1.51 | 0.16 |
| 0.54 | 167 | 9.4 | 5.9 | 4.9 | 0.019 | 27.8 | 24.3 | 0.180 | 0.28 | 1.68 | 0.17 |

**Table 6.6** Cycle performance using vapour pump

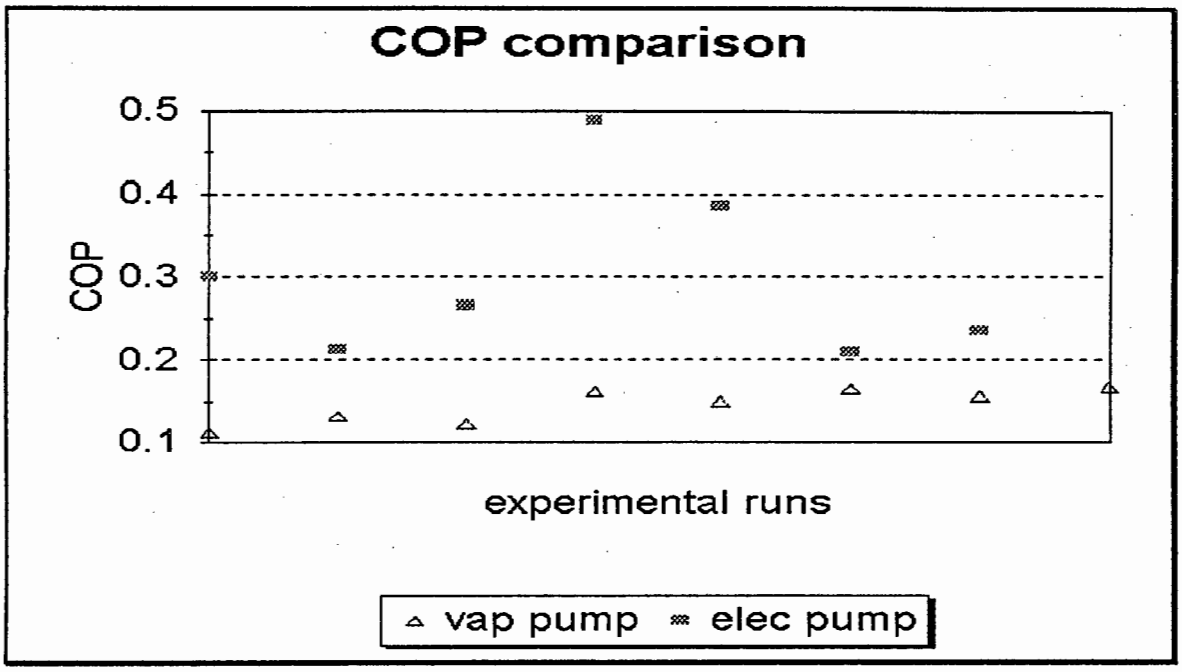


Figure 6.7

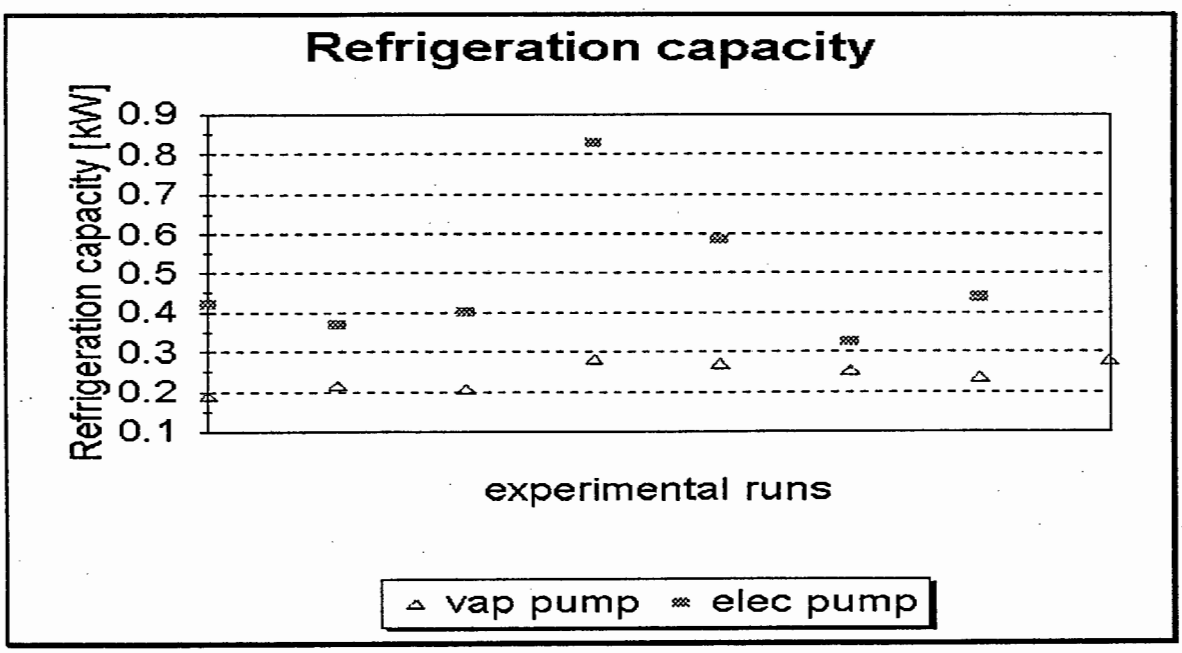


Figure 6.8

### 6.2.5 Discussion

The results show that the vapour pump works in principle. The COP's for the vapour pump (≈ 0.15) are approximately half that of the COP's for the electric pump (≈ 0.30). The COP's in Vicatos experiments [24] were around 0.4. One reason for this decrease could be that during the frequent repairs on the cycle air has come into the system, reducing the refrigeration capacity. Also, in Vicatos` experiments the cooling water was 21.5 C compared to the ≈23 C in these experiments. As discussed in section 5.3, an increase in sink temperature leads to a decrease in COP.

Data was not collected at complete stability since it took excessively long (2-2.5 hrs) for the cycle to settle to thermodynamic equilibrium. Although the results for the vapour pump must be considered more of a qualitative nature, the readings clearly show a decrease in COP when using the vapour pump. Performance would increase when insulating the pump and piping.

**CHAPTER 7**

## 7.1 Conclusions

Based upon the results of experimentation and the simulation of the cycle with vapour pump, the following conclusions were drawn:

*on the absorption cycle with vapour pump:*

- The vapour pump system works in principle. The simulation of the cycle shows that it is thermodynamically possible to return the strong solution in the absorption cycle by means of a vapour pump. This is confirmed by the experiments.

- The cycle simulation predicts that, when using the vapour pump,:

  a) the maximum COP decreases by approximately 20% from around 0.60 for the electric pump to 0.47 and occurs at a higher generator temperature.
  b) the maximum COP increases, while the corresponding optimum generator temperature decreases, with increasing evaporator temperature.
  c) the maximum COP decreases, while the corresponding optimum generator temperature increases, with increasing sink temperature.

- In the experiments the COP dropped by 50% from around 0.30 to 0.15. The experimentally obtained performance

can be increased by reducing radiation losses by insulting vapour pump and piping.

- Complete thermodynamic equilibrium (stability) could not be confirmed when running the cycle with the vapour pump. The cycle behaviour for changing operating conditions as predicted by the simulation (chapter 5) could, for this reason, not be verified by the experiments.

*on the design of the vapour pump:*

- The vapour pump has been overdesigned. The friction forces are less than estimated. The vapour side piston diameter could be reduced. This would allow more refrigerant passing through the evaporator, resulting in an increased COP.

- The spring mechanism to provide motion to the control shaft does not function reliably. The operation of the spring mechanism relies upon very fine tolerancing and adjustment, which practically was not achieved.

- The EPDM sealing rings do not function flawlessly. Some have been damaged by extrusion, other have been enlarged as closer inspection showed. It is not clear whether the enlargement is due to the E181 or the lubrication oil that was used when initially installing the rings. The teflon rings that were subsequently installed into the control mechanism worked satisfactorily.

## 7.2 Recommendations

The vapour pump system was shown to work in principle. More experimental work is required to:

- accurately determine the performance of the absorption cycle with vapour pump
- confirm the trends predicted by the simulation when changing the operating conditions
- operate the vapour pump without the pneumatic system, that was used to provide motion to the control mechanism

For future experimentation the following recommendations are made:

- The refrigeration machine should be completely cleaned. Especially the absorber contains a lot of rust particles, that originate from the time when the system was run with ammonia and water. Ideally, all moisture should be removed from the system. This would solve the throttle valve blocking up problem

- The spring mechanism to provide motion to the control shaft should be replaced with a more reliable system. One possible solution would be a cam shaft type system. The pump shaft could drive a cam shaft. The cam would supply motion to the control shaft in one direction. The return movement could be by spring action.

- All dynamic seals should be replaced with teflon seals.

- Once the absorption-vapour pump system works stably and reliably, work should be carried out to automate the control of the system in an effort to make it more user friendly.

# BIBLIOGRAPHY


1. American Society of Refrigerating Engineers
   Air Conditioning, Refrigerating, Data Book
   ASRE, New York, 10th edition, 1957

2. Althouse AD and Turnquist CH
   Modern Electric and Gas Refrigeration
   The Goodheart- Wilcox Co, INC, USA, 1943

3. Althouse AD, Turnquist CH and Bracciano AF
   Modern Refrigeration and Air Conditioning
   The Goodheart- Wilcox Co, INC, South Holland, Illinois, 1979

4. Beasley D and Hester JCH
   Short Communications. Analysis of a Pressure Driven Absorption Refrigeration Cycle
   International Journal of Energy Research, Vol 12, 1988, pp 175-184

5. Çengel YA and Boles MA
   Thermodynamics
   Mc-Graw Hill Book Co.,Singapore, 1989

6. Cerepnalkovski I
   Modern Refrigerating Machines
   Elsevier Science Publishers, Amsterdam, 1991

7. Dossat RJ
   Principles of Refrigeration
   John Wiley and Sons, USA, 2nd edition, 1960

8. Dubbel
   Taschenbuch für den Maschinenbau
   Springer Verlag, Berlin, 14th edition, 1981

9. Howell JR and Buckius RO
   Fundamentals of Engineering Thermodynamics
   McGraw-Hill Book Co., Singapore, 1987

10 Hull HB
   Household Refrigeration
   Nickerson & Collins Co., Chicago, 4th edition, 1933

11. Plank R and Kuprianoff J
    Die Kleinkältemaschine
    Springer Verlag, Berlin, 2nd edition, 1960

12. Kriebel M and Löffler HJ
Thermodynamische Eigenschaften des Binären Systems Difluormonochlormethan (R22) - Tetraäthylenglykol-dimethyläther (E181)
Mitteilung aus dem Institut für Thermodynamik und Kältetechnik der Technischen Universität Berlin, Heft 9, 1965

13. Macintire HJ
Handbook of Mechanical Refrigeration
John Wiley and Sons, New York, 1st edition, 1928

14. Mastrangelo SVR
Solubility of some Chlorofluorohydrocarbons in tetraethylene glycol dimethyl ether
ASHRAE-Journal, Vol 1, No 10, pp 64/68, 1959

15. Parker Catalogue
Medien Beständigkeitstabelle
Parker-Prädifa GmbH, Pleidelsheim, January 1994

16. Pearson SF
An Engineering View of Refrigerants
Class Notes, Mechanical Enginnering, UCT

17. Pita EG
Refrigeration, Principles and Systems
John Wiley & Sons, New York, 1984

18. Sharpe N
Refrigerating Principles and Practices
McGraw-Hill, New York, 1949

19. Shigley JE
Mechanical Engineering Design
McGraw-Hill Kogakusha Ltd., Tokyo, 3rd edition, 1977

20. Sparks NR and Dillio CC
Mechanical Refrigeration
McGraw-Hill, New York, 1959

21. Spauschus HO
Emerging Issues for Refrigeration: Energy, Environment and Economics
Georgia Tech Research Institute, Atlanta

22. Szücs L
New Pumping Method in Absorption Refrigeration
Proceedings of the XI$^{th}$ International Congress of Refrigeration. Refrigeration Science and Technology, Vol 1

23. Tribus M
Thermostatics and Thermodynamics
D. van Nostrand Co., New Jersey, 1961

24. Vicatos G
Absorption Refrigeration Using Waste Heat
National Energy Council, CSIR Pretoria, 1989

25. Vicatos G and Gryzagoridis J
A Graphical Evaluation of the Heat Effects of the Single Stage Absorption Refrigeration Cycle
S.A. Refrigeration and Air-conditioning, July 1994, Vol 10 No4, pp 47-57

26. Zellhoefer GF, Copley MJ and Marvel CS
R22-E181
J A.m. Chem. Soc.,1937

# Appendix A

## The cycle simulation

**'PROGRAM "AMMONIA"**

**'PREDICTED OPTIMUM CYCLE**

**amended to include vapour pump**

**Thermodynamic and Performance calculations**
**of Water-Ammonia**
**Absorption Refrigeration Machines**

```
DIM HV(8), X(15), Y(17), COP(150), CPT(150), T15(20), M(8), MS(8)
DIM f(51) AS DOUBLE, Psat(11) AS DOUBLE
DIM K(50, 50)  AS DOUBLE, PL(210) AS DOUBLE
DIM PV1(100)  AS DOUBLE, PV2(210) AS DOUBLE, Bt(95), SUM(95)
DIM HDE1(8), HDE2(8), P2NEW(8), PDE1(8), PDE2(8), XS(8)
DIM mf(10000)
DIM O(20)

 CLS
 OPEN "C:\AMMO3\DAT.AMM" FOR INPUT AS #1 '     BLOCK DATA
 FOR I = 1 TO 10: INPUT #1, Psat(I): NEXT I    'I=1 to 5  -ammonia ,I=6 to 10 - water
 FOR I = 0 TO 49: INPUT #1, f(I): NEXT I       'P-T-x relation data
 FOR I = 0 TO 4: INPUT #1, C(I): NEXT I
 FOR I = 1 TO 100: INPUT #1, PL(I): NEXT I     'H-x (P=const) data for FOURIER equations
 FOR I = 1 TO 50: INPUT #1, PV1(I): NEXT I     'H-y (P=const) data for FOURIER equations (y=0.90 to 0.90)
 FOR I = 1 TO 100: INPUT #1, PV2(I): NEXT I    'H-y (P=const) data for FOURIER equations (y=0.90 to 1.00)
 FOR I = 0 TO 9
 FOR J = 0 TO 42: INPUT #1, K(J, I)            'T-x-y relation data
 NEXT J
 NEXT I
 FOR I = 0 TO 15: INPUT #1, O(I): NEXT I       'Optimum generator temp
 FOR I = 1 TO 10: INPUT #1, DNH(I): NEXT I     'DENSITY OF NH3 SUPERHEAT
 CLOSE #1

50
 INPUT "DO YOU HAVE A DATA FILE ? (Y/N) "; FIL$
 IF FIL$ = "Y" OR FIL$ = "y" THEN GOTO 55 ELSE CLS : RUN "C:\AMMO3\DAMMO3F"
55
 INPUT "ENTER THE DATA SHEET No TO BE PROCESSED"; TH$
 FILEN$ = "C:\AMMO3\AMMON" + TH$
 OPEN FILEN$ FOR INPUT AS #3

 INPUT #3, NUMEV
 FOR IEV = 1 TO NUMEV
 INPUT #3, T15(IEV)
 NEXT IEV
 INPUT #3, NUMAB
 FOR IAB = 1 TO NUMAB
 INPUT #3, TWA(IAB)
 NEXT IAB
 INPUT #3, ITN
 CLOSE #3


 'CLS
```

```
'INPUT "ENTER THE CONCENTRATION OF THE REFRIGERANT (0.990 is recomended) "; X(15)
X(15) = .99
'CLS
'INPUT "ENTER THE % INCREASE IN EVAPORATOR'S TEMPERATURE (20% is recommended)"; Dt
Dt = 20
CLS
PRINT
PRINT "TYPE  ' 0 ' FOR PEAK C.O.P. VALUES "
PRINT
INPUT "TYPE  ' 1 ' FOR MASS/HEAT BALANCE AND C.O.P. CURVES "; IABS
CLS
PRINT
PRINT "TYPE  ' 0 ' FOR ELECTRICAL PUMP"
PRINT
INPUT "TYPE  ' 1 ' FOR VAPOUR PUMP"; PM$

TIME$ = "00:00:00"
CLS
NOM = 91

MAIN PROGRAM STARTS HERE

   TKEL = 273.15
   PI = 3.141529
   QIN = 100000
   REF = 0
   X(3) = X(15)
   Dt = Dt / 100

   GOSUB 8210
   LOCATE 4, 40: PRINT "AMMO3"
   LOCATE 6, 30: PRINT "PREDICTED OPTIMUM CYCLE"
   LOCATE 8, 21: PRINT "Thermodynamic and Performance calculations"
   LOCATE 9, 17: PRINT "of Water-Ammonia Absorption Refrigeration Machines"

   LOCATE 14, 30: PRINT "THE PROGRAM WILL EXECUTE"
   LOCATE 15, 30: PRINT USING "####"; ITN * NUMEV * NUMAB;
   PRINT "-CYCLES";
   INPUT " OK ?  (Y/N)"; OK$
   IF OK$ = "Y" OR OK$ = "y" THEN GOTO 60 ELSE CLS : GOTO 50

60    FOR IAB = 1 TO NUMAB
      FOR IEV = 1 TO NUMEV
      ICY = 1
      CLS

I = 15
          LOCATE 23, 2: PRINT "Point "; I; " Evaporator  "
          GOSUB 2000
          T0 = T15(IEV) + TKEL
          T(I) = T0
          P0 = EXP(Fa + Fb * T0 + Fc / T0 + Fd * T0 ^ 2 + Fe * LOG(T0))
          P2 = P0       'Low Pressure
          GOSUB 4000
          Hx15 = ENTHL
          GOSUB 3000
          Y(15) = X(I) * ALPHA / (1 + X(I) * (ALPHA - 1))
          GOSUB 5000
          Hy15 = ENTHV
          T(5) = T(15) + Dt * ABS(T15(IEV))

          X(I) = X(15)
          Dx = .005
          IFLIP = 1
```

```
57 I = 5
        LOCATE 7, 15: PRINT "Adjusting Refrigerant Concentration X(3) =";
        LOCATE 7, 58: PRINT USING "#.#####"; X(3)
        LOCATE 13, 34: PRINT "PLEASE WAIT"
        X(I) = X(3)
        T0 = T(5)
        GOSUB 2000
        P0 = EXP(Fa + Fb * T0 + Fc / T0 + Fd * T0 ^ 2 + Fe * LOG(T0))
        GOSUB 4000
        HA = ENTHL

I = 3
   LOCATE 23, 2: PRINT "Point "; I; " Condenser   "
   T(I) = TWA(IAB) + TKEL
   T0 = T(I)
   GOSUB 2000
   P0 = EXP(Fa + Fb * T0 + Fc / T0 + Fd * T0 ^ 2 + Fe * LOG(T0))
   P1 = P0       'High Pressure
   GOSUB 4000    'Enthalpy of the liquid mixture
   H3 = ENTHL
   QprMAX = H3 - HA
   QPR = .7 * QprMAX
   H4T = H3 - QPR
   X3 = (Y(15) - X(15)) * (H4T - Hx15) / (Hy15 - Hx15) + X(15)

        IF ABS(X(3) - X3) < .00001 THEN GOTO 65
        IF IFLIP = -1 THEN GOTO 133
        IF X(3) > X3 THEN IFLIP = -1: Dx = IFLIP * Dx / 2
        IF IFLIP = 1 THEN GOTO 134
133   IF X(3) < X3 THEN IFLIP = 1: Dx = -IFLIP * Dx / 2
134   X(3) = X(3) + Dx
        GOTO 57

65    I = 4
        H4 = H4T
        P0 = P2
        Dp = 1
        IFLIP = 1
        X(I) = X(3)
67    GOSUB 4000
        H4T = ENTHL
        IF ABS(H4T - H4) < .01 THEN GOTO 66
        IF IFLIP = -1 THEN GOTO 167
        IF H4T > H4 THEN IFLIP = -1: Dp = IFLIP * Dp / 2
        IF IFLIP = 1 THEN GOTO 168
167   IF H4T < H4 THEN IFLIP = 1: Dp = -IFLIP * Dp / 2
168   P0 = P0 + Dp
        GOTO 67

66    X = X(I)
        GOSUB 2300
        T(I) = T0
        H15 = H4
        CLS

I = 1
   Y(I) = X(3)
   LOCATE 13, 34: PRINT "PLEASE WAIT"
   LOCATE 23, 2: PRINT "Point "; I; " Condenser   "
   T(I) = TWA(IAB) + TKEL
   T0 = T(I): P0 = P1
   X(I) = .525
   XSTEP = .05
```

```
   LOCATE 7, 18: PRINT "Y(1) = "; : PRINT USING "#.#####"; Y(I);
   PRINT " ..... Hunting for X(1) = ";
   IFLIP = 1
9  LogA = 0
   LOCATE 7, 58: PRINT USING "#.#####"; X(I)

   GOSUB 3000    'T-X-alpha relation

   T(I) = T0
   YTEST = X(I) * ALPHA / (1 + X(I) * (ALPHA - 1))
   IF ABS(Y(I) - YTEST) < .000005 THEN GOTO 131
   IF IFLIP = -1 THEN GOTO 11
   IF YTEST > Y(I) THEN IFLIP = -1: XSTEP = IFLIP * XSTEP / 2
   IF IFLIP = 1 THEN GOTO 15
11 IF YTEST < Y(I) THEN IFLIP = 1: XSTEP = -IFLIP * XSTEP / 2
15 X(I) = X(I) + XSTEP
   GOTO 9

131
   GOSUB 5000    'Enthalpy of the vapour
   H1 = ENTHV

   m3 = 1 / 1202
   m5 = m3
   M6 = m3
   M4 = m3


FOR I = 5 TO 6
   LOCATE 23, 2: PRINT "Point "; I; " Evaporator   "
   P0 = P2
   IF I = 6 THEN X(I) = X(3): GOSUB 400: GOTO 132

  T0 = T(I)
   GOSUB 2500

   GOSUB 3000    'T-X-alpha relation
   Y(I) = X(I) * ALPHA / (1 + X(I) * (ALPHA - 1))

   MS(I) = m5 * (Y(I) - Y(1)) / (Y(I) - X(I))
   IF MS(I) < 0 THEN GOTO 3300
132   M(I) = m5 - MS(I)
   GOSUB 5000    'Enthalpy of the vapour
   HV(I) = ENTHV
   GOSUB 4000    'Enthalpy of the liquid mixture
   HS(I) = ENTHL
   HDE(I) = (MS(I) * HS(I) + M(I) * HV(I)) / m5
   GOTO 3495

3300 GOSUB 3000
        XS(I) = Y(1) / (ALPHA - Y(1) * (ALPHA - 1))
        X = XS(I)
        GOSUB 2300
        GOSUB 1000
        P2NEW(I) = P2SAT * 14.5
        PDE2(I) = (17 * P2NEW(I) * (17 - .8 * XS(I)) * (1 - XS(I)) / (17 + XS(I)) ^ 2) / 14.5
        PDE1(I) = P0 - PDE2(I)
        Y(I) = 1
        P0 = PDE1(I)
        GOSUB 5000                    'Enthalpy of ammonia vapour
        HDE1(I) = ENTHV
        Y(I) = 0
        P0 = PDE2(I)
        GOSUB 5000          'Enthalpy of water vapour
```

```
        HDE2(I) = ENTHV
        HDE(I) = HDE1(I) * X(I) + HDE2(I) * (1 - X(I))

3495 NEXT I
        H5 = HDE(5)
        REF = H5 - H4
        Qref = REF * m3
I = 7
   P0 = P2
   LOCATE 23, 2: PRINT "Point "; I; " Absorber   "
   X(I) = .3
   T(I) = TWA(IAB) + TKEL
   T0 = T(I)

   GOSUB 2500
   XST = X(I)    'Maximum concentration

   GOSUB 4000    'Enthalpy of the liquid mixture
   H7 = ENTHL

I = 10
   LOCATE 23, 2: PRINT "Point "; I; " H. Exchanger"
   X = XST
   X(I) = XST
   P0 = P1

   GOSUB 2300
   T(I) = T0

   GOSUB 4000    'Enthalpy of the liquid mixture
   H10 = ENTHL

   T0 = 100 + TKEL
   P0 = P1
   X = 0
   GOSUB 2300
   TGEN = T0 - TKEL'Generator's maximum temperature

I = 8
   LOCATE 23, 2: PRINT "Point "; I; " Generator   "
   X = XST
   X(I) = XST
   P0 = P1

   GOSUB 2300
   T(I) = T0

   TG = T(I) - TKEL'Generator's minimum temperature
   TINCR = (TGEN - TG) / ITN
   IF IABS = 0 THEN TINCR = .5: ITN = INT((TGEN - TG) / TINCR)


   CLS
   GOSUB 8210

190    IF PM$ = "1" THEN GOTO 635

'-------------------------------------------ELECTRICAL PUMP
I = 8
   LOCATE 23, 2: PRINT "Point "; I; " Generator   "
   T8 = T(8) - TKEL
   T0 = T(8)
   P0 = P1
```

```
    GOSUB 2500
    XWE = X(I)    'Weak solution concentration

    IF (XST - XWE) < .0001 THEN LOCATE 12, 17: CLS : GOSUB 8210: GOSUB 111: LOCATE 12, 25:
PRINT "ZERO PERFORMANCE": GOTO 1300

    M8 = m3 * (Y(1) - XST) / (XST - XWE)
    M7 = m3 + M8
    M13 = M7
    M9 = M8
    X(I) = XWE

    GOSUB 4000    'Enthalpy of the liquid mixture
    H8 = ENTHL

    Q8 = M8 * H8

I = 12
    LOCATE 23, 2: PRINT "Point "; I; " Generator   "
    XB = (XST + XWE) / 2'Generator's bulk solution concentration
    X(I) = XB
    X = XB
    P0 = P1
    GOSUB 2300
    T(I) = T0

    GOSUB 4000    'Enthalpy of the liquid mixture
    H12 = ENTHL

I = 11
    LOCATE 23, 2: PRINT "Point "; I; " Generator   "
    T(I) = T(12)
    T0 = T(I): P0 = P1
    X(I) = X(12)

    GOSUB 3000    'T-X-alpha relation
    Y(I) = ALPHA * X(I) / (1 + (ALPHA - 1) * X(I))

    GOSUB 5000    'Enthalpy of the vapour
    H11 = ENTHV

    Q3 = H3 * m3
    Q5 = H5 * m5
    Q7 = H7 * M7
    Q6 = H6 * M6
    Q4 = H4 * M4
    GOSUB 4500    'REFLUX

    Q1 = H1 * M1
    Q12 = H12 * M12
    Q11 = H11 * M11
    QR = H3 * MR

630  'ELECTRICAL PUMP
    T0 = T(7): P0 = P2
    M7 = (1 + (XST - Y(1)) / (XWE - XST)) * M6
    GOSUB 6910
    QW = WIN * M7    'Work done at pump
    H13 = H7 + WOUT
    Q13 = M7 * H13

    QEXopt = H10 * M7 - Q13
    Q10 = Q13 + QEXopt
```

```
408
   QIN = Q8 + Q11 - Q12 - Q10

   COP(ICY) = Qref / (QIN + QW)'(COP)
   CPT(ICY) = T(5) * (T(8) - T(3)) / (T(8) * (T(3) - T(5)))'CARNOT (COP)
   IF IABS = 0 AND COP(ICY) < COP(ICY - 1) THEN CM = COP(ICY): TM = T(8) - TKEL: QM = QIN:
GOSUB 500


   LOCATE 12, 17: PRINT SPACE$(32)
   GOSUB 111
   GOTO 1200

'-------------------------------------------------VAPOUR PUMP

635

I = 8
   LOCATE 23, 2: PRINT "Point "; I; " Generator   "
   T8 = T(8) - TKEL
   T0 = T(8)
   P0 = P1

   GOSUB 2500
   XWE = X(I)    'Weak solution concentration

   IF (XST - XWE) < .0001 THEN LOCATE 12, 17: CLS : GOSUB 8210: GOSUB 111: LOCATE 12, 25:
PRINT "ZERO PERFORMANCE": GOTO 1300

   X(I) = XWE

   GOSUB 4000    'Enthalpy of the liquid mixture
   H8 = ENTHL


I = 12
   LOCATE 23, 2: PRINT "Point "; I; " Generator   "
   XB = (XST + XWE) / 2'Generator's bulk solution concentration
   X(I) = XB
   X = XB
   P0 = P1
   GOSUB 2300
   T(I) = T0

   GOSUB 4000    'Enthalpy of the liquid mixture
   H12 = ENTHL

I = 11
   LOCATE 23, 2: PRINT "Point "; I; " Generator   "
   T(I) = T(12)
   T0 = T(I): P0 = P1
   X(I) = X(12)

   GOSUB 3000    'T-X-alpha relation
   Y(I) = ALPHA * X(I) / (1 + (ALPHA - 1) * X(I))

   GOSUB 5000    'Enthalpy of the vapour
   H11 = ENTHV

   Q3 = H3 * m3
   Q5 = H5 * m5
   Q6 = H6 * M6
   Q4 = H4 * M4
   GOSUB 4500    'REFLUX
```

```
    Q1 = H1 * M1
    Q12 = H12 * M12
    Q11 = H11 * M11
    QR = H3 * MR


    'V-PUMP
    T0 = T(7): P0 = P2
    z = 1
    mf(z) = (1 + (XST - Y(1)) / (XWE - XST)) * M6

636  GOSUB 6915
    z = z + 1
    mf(z) = ((Y(6) - XWE) * M6 + M16 * (Y(11) - XWE)) / (XST - XWE)
    IF mf(z) - mf(z - 1) > .02 THEN GOTO 636
    M7 = mf(z)
    Q16 = H11 * M16

   Win=101.3793*(P1-P2)*m16/DENS
   Wout= 101.3793*(P1-P2)*VFX*m7
    TVPEFF = WOUT * M7 / Q16
    VPEFF = WOUT * M7 / (WIN * M16)
     H13 = H7 + WOUT
    Q13 = M7 * H13

    Fright =100000*3.14159/4*(P2*DS^2+1*(DV^2 - DS^2) + P1 * (DV ^ 2 - DR ^ 2))
    Fleft =100000*3.14159/4*(P1*DS^2+P2*(DV ^ 2 - DS ^ 2) + P2 * (DV ^ 2 - DR ^ 2))
    Fvap = (P1 - P2) * 100000 * 3.14159 / 4 * (2 * DV ^ 2 - DS ^ 2 - DR ^ 2)
    Fsol = (P1 - P2) * 100000 * 3.14159 / 4 * DS ^ 2

    QEXopt = H10 * M7 - Q13
    Q10 = Q13 + QEXopt

    M8 = (m3 * (Y(1) - XST) + M16 * (Y(11) - XST)) / (XST - XWE)
    M7 = m3 + M8 + M16
    M13 = M7
    M9 = M8
    Q8 = M8 * H8
    Q7 = H7 * M7

638
    QIN = Q8 + Q11 - Q12 - Q10 + Q16

    COP(ICY) = Qref / QIN'(COP)
    CPT(ICY) = T(5) * (T(8) - T(3)) / (T(8) * (T(3) - T(5)))'CARNOT (COP)
    IF IABS = 0 AND COP(ICY) < COP(ICY - 1) THEN CM = COP(ICY): TM = T(8) - TKEL: QM = QIN:
GOSUB 500


    LOCATE 12, 17: PRINT SPACE$(32)
    GOSUB 111

1200
    T10 = T(10) - TKEL
    T13 = T(13) - TKEL

1300
    IF IABS = 0 THEN GOTO 1400

    FILR$ = "C:\AMMO3\COPF" + TH$ + PM$ + ".prn"
    OPEN FILR$ FOR APPEND AS #2
    PRINT #2, TWA(IAB), T15(IEV), T(8) - TKEL, COP(ICY), QIN
    PRINT #2, P1, P2, M7, H7, H13
```

```
    PRINT #2, H11, H12, H1, H17
    PRINT #2, REF, Qref, VFX, Q16, QIN
    PRINT #2, Q8, Q11, Q12, Q10, QW
    PRINT #2, XWE, XST, mf(z), z, M16
    PRINT #2, DV, DS, M6, M9, DENS
    PRINT #2, Y(6), Y(11), Y(1), VPEFF, TVPEFF
    PRINT #2, Fright, Fleft, Fvap, Fsol, fr
    CLOSE #2

1400
    T(8) = T(8) + TINCR
    IF IABS = O AND COP(ICY) < COP(ICY - 1) THEN GOTO 1500
    IF ICY = ITN THEN GOTO 1500
    IF T(8) > 130 + TKEL THEN GOTO 1500
    NOM = NOM + 1
    ICY = ICY + 1
    IF IABS = 0 AND PM$ = "1" AND ICY = 2 THEN T(8) = T(8) + 10
    IF IABS = 1 AND PM$ = "1" AND ICY = 2 THEN T(8) = T(8) + 5

    GOTO 190

1500

    NEXT IEV
    NEXT IAB


    CLS
    LOCATE 12, 23: PRINT "TOTAL TIME FOR DATA:  "; FILEN$; " = "; TIME$
    LOCATE 20, 20: INPUT "DO YOU WISH TO PROCESS ANOTHER DATA FILE ?  Y/N  "; PROCESS$
    IF PROCESS$ = "N" OR PROCESS$ = "n" THEN GOTO 1800
    IF PROCESS$ = "Y" OR PROCESS$ = "y" THEN GOTO 50

1800 CLS : END


'   E N D   O F   P R O G R A M
    LOCATE 8, 15: PRINT "(Bars A)"
    LOCATE 8, 24: PRINT "L PRESSURE  H PRESSURE      CAPACITY (KW)"
    LOCATE 9, 26: PRINT USING "##.###"; P2
    LOCATE 9, 39: PRINT SPACE$(5)
    LOCATE 9, 39: PRINT USING "##.###"; P1
    LOCATE 9, 53: PRINT SPACE$(8)
    LOCATE 9, 53: PRINT USING "####.###"; Qref
    LOCATE 12, 53: PRINT "Time"
    LOCATE 12, 58: PRINT TIME$
    LOCATE 12, 17: PRINT SPACE$(32)
    LOCATE 14, 61: PRINT SPACE$(5)
    LOCATE 14, 16: PRINT "MAXIMUM SOLUTION CONCENTRATION....."
    LOCATE 14, 61: PRINT USING "#.###"; XST
    LOCATE 15, 16: PRINT "MINIMUM GENERATOR TEMPERATURE. ....."
    LOCATE 15, 59: PRINT USING "###.###"; TG
    LOCATE 20, 16: PRINT "REFRIGERANT MASS FLOW RATE...(g/sec)..."
    LOCATE 20, 58: PRINT USING "####.###"; m3 * 1000
    LOCATE 19, 16: PRINT "TEMPERATURE INCREMENT.....(Deg.C)..."
    LOCATE 19, 59: PRINT USING "###.###"; TINCR
    LOCATE 18, 16: PRINT "HEAT SUPPLY.....(kW)....."
    LOCATE 18, 55: PRINT USING "#######.###"; QIN
    LOCATE 16, 16: PRINT "GENERATOR'S TEMPERATURE.....(Deg.C)..."
    LOCATE 16, 59: PRINT USING "###.###"; T(8) - TKEL
    'IF (XST0 - XWE) < .0001 THEN GOTO 112
    LOCATE 12, 17: PRINT "C.O.P. OF (";
    PRINT USING "## "; ICY; IEV; IAB;
```

```
    PRINT ") = ";
    PRINT USING "#.###"; COP(ICY)
112  RETURN


400 '  Precooler evaluation
    H6 = H3 + HDE(5) - H4
    T0 = T(5)
    X(I) = X(5)
    XSTEP = .05
    IFLIP = 1

409  X = X(I)
    P0 = P2
    GOSUB 4000
    Hx = ENTHL
    GOSUB 2300
    GOSUB 3000
    Y(I) = X * ALPHA / (1 + X * (ALPHA - 1))
    GOSUB 5000
    Hy = ENTHV
    MX = ((Y(I) - X3) / (X3 - X(I))) / (1 + (Y(I) - X3) / (X3 - X(I)))
    H6T = Hy * (1 - MX) + Hx * MX
    IF ABS(H6 - H6T) < .05 THEN GOTO 420
    IF IFLIP = -1 THEN GOTO 411
    IF H6 - H6T > 0 THEN IFLIP = -1: XSTEP = IFLIP * XSTEP / 2
    IF IFLIP = 1 THEN GOTO 415
411  IF H6 - H6T < 0 THEN IFLIP = 1: XSTEP = -IFLIP * XSTEP / 2
415  X(I) = X(I) + XSTEP
    T(6) = T0
    GOTO 409
420  RETURN


500
    FILEN$ = "C:\AMMO3\OPTF-" + TH$ + PM$ + ".prn"
    LOCATE 23, 52: PRINT "STORING INFORMATION"
    OPEN FILEN$ FOR APPEND AS #2
    PRINT #2, USING " ######.##### "; T15(IEV); TWA(IAB); TM; CM; DV; DS; M6; M7; M8; M16; REF;
Qref; QIN; Fright; Fleft; Fvap; Fsol; VPEFF; TVPEFF; VFX; DENS; P1; P2; H7; H13; H11; H12; H1; Q16; Q8;
Q11; Q12; Q10; XWE; XST; mf(z); z; Y(6); Y(11); Y(1); WOUT; WIN; fr; mf(z)
    CLOSE #2
    LOCATE 23, 52: PRINT SPACE$(23)
    RETURN


1000 'Saturation pressures
    P1SAT = EXP(Psat(1) + Psat(2) * T0 + Psat(3) / T0 + Psat(4) * T0 ^ 2 + Psat(5) * LOG(T0))
    P2SAT = EXP(Psat(6) + Psat(7) * T0 + Psat(8) / T0 + Psat(9) * T0 ^ 2 + Psat(10) * LOG(T0))
    RETURN


2000 'Pressure coefficients
    X = X(I)
    IF X < .0001 THEN GOSUB 1000: P0 = P2SAT: GOTO 2100
    IF X > .9999 THEN GOSUB 1000: P0 = P1SAT: GOTO 2100
2010
    Fa = f(0) + f(1) * X + f(2) * X ^ 2 + f(3) * X ^ 3 + f(4) * X ^ 4 + f(5) * X ^ 5 + f(6) * X ^ 6 + f(7) * X ^ 7 +
f(8) * X ^ 8 + f(9) * X ^ 9
    Fb = f(10) + f(11) * X + f(12) * X ^ 2 + f(13) * X ^ 3 + f(14) * X ^ 4 + f(15) * X ^ 5 + f(16) * X ^ 6 + f(17)
* X ^ 7 + f(18) * X ^ 8 + f(19) * X ^ 9
    Fc = f(20) + f(21) * X + f(22) * X ^ 2 + f(23) * X ^ 3 + f(24) * X ^ 4 + f(25) * X ^ 5 + f(26) * X ^ 6 + f(27)
* X ^ 7 + f(28) * X ^ 8 + f(29) * X ^ 9
```

```
   Fd = f(30) + f(31) * X + f(32) * X ^ 2 + f(33) * X ^ 3 + f(34) * X ^ 4 + f(35) * X ^ 5 + f(36) * X ^ 6 + f(37)
* X ^ 7 + f(38) * X ^ 8 + f(39) * X ^ 9
   Fe = f(40) + f(41) * X + f(42) * X ^ 2 + f(43) * X ^ 3 + f(44) * X ^ 4 + f(45) * X ^ 5 + f(46) * X ^ 6 + f(47)
* X ^ 7 + f(48) * X ^ 8 + f(49) * X ^ 9
2100    RETURN


2300 'Simpson's rule (X-P0 known)
   GOSUB 2010
2310 UL = LOG(P0) - (Fa + Fb * T0 + Fc / T0 + Fd * T0 ^ 2 + Fe * LOG(T0))
   UL1 = -(Fb - Fc / T0 ^ 2 + 2 * Fd * T0 + Fe / T0)
   T1 = T0 - UL / UL1
   IF ABS(T1 - T0) < .001 THEN GOTO 2320
   T0 = T1
   GOTO 2310
2320 RETURN



2500 'Simpson's rule (T-P known)
  X = .3
2510 GOSUB 2010
  Fa1 = f(1) + 2 * f(2) * X + 3 * f(3) * X ^ 2 + 4 * f(4) * X ^ 3 + 5 * f(5) * X ^ 4 + 6 * f(6) * X ^ 5 + 7 * f(7) *
X ^ 6 + 8 * f(8) * X ^ 7 + 9 * f(9) * X ^ 8
  Fb1 = f(11) + 2 * f(12) * X + 3 * f(13) * X ^ 2 + 4 * f(14) * X ^ 3 + 5 * f(15) * X ^ 4 + 6 * f(16) * X ^ 5 + 7
* f(17) * X ^ 6 + 8 * f(18) * X ^ 7 + 9 * f(19) * X ^ 8
  Fc1 = f(21) + 2 * f(22) * X + 3 * f(23) * X ^ 2 + 4 * f(24) * X ^ 3 + 5 * f(25) * X ^ 4 + 6 * f(26) * X ^ 5 + 7
* f(27) * X ^ 6 + 8 * f(28) * X ^ 7 + 9 * f(29) * X ^ 8
  Fd1 = f(31) + 2 * f(32) * X + 3 * f(33) * X ^ 2 + 4 * f(34) * X ^ 3 + 5 * f(35) * X ^ 4 + 6 * f(36) * X ^ 5 + 7
* f(37) * X ^ 6 + 8 * f(38) * X ^ 7 + 9 * f(39) * X ^ 8
  Fe1 = f(41) + 2 * f(42) * X + 3 * f(43) * X ^ 2 + 4 * f(44) * X ^ 3 + 5 * f(45) * X ^ 4 + 6 * f(46) * X ^ 5 + 7
* f(47) * X ^ 6 + 8 * f(48) * X ^ 7 + 9 * f(49) * X ^ 8
  UL = LOG(P0) - (Fa + Fb * T0 + Fc / T0 + Fd * T0 ^ 2 + Fe * LOG(T0))
  UL1 = -(Fa1 + Fb1 * T0 + Fc1 / T0 + Fd1 * T0 ^ 2 + Fe1 * LOG(T0))
  X1 = X - UL / UL1
  IF ABS(X1 - X) < .00005 THEN GOTO 2540
  X = X1
  GOTO 2510
2540 X(I) = X
  RETURN



3000 'Ammonia concentration in the vapour - the T-x-y relation
    X = X(I)
  IF I > 1 THEN GOTO 3100
  GOSUB 2300
3100 ALPHA = 0
   LogA = 0
   Xk = X(I) * 10
   Tk = (((T0 - TKEL) * 9 / 5 + 32) + 60) / 10
    FOR M = 0 TO 42
          SUM(M) = 0
    FOR N = 1 TO 9
          Ax = K(M, N) * COS(2 * PI * N * Xk / 20)
          SUM(M) = SUM(M) + Ax
    NEXT N
          Bt(M) = (K(M, 0) + 2 * SUM(M)) / 20
          BB = Bt(M) * COS(2 * PI * M * Tk / 86)
  IF M = 0 THEN GOTO 3500
  LogA = LogA + BB
3500    NEXT M

LogA = (Bt(0) + 2 * LogA) / 86
```

```
ALPHA = EXP(LogA)
RETURN



4000 'Enthalpy of the liquid mixture
ENTHL = 0
 Xk = X(I) * 20
 A(0) = PL(1) + PL(2) * P0 + PL(3) / P0 + PL(4) / P0 ^ 2 + PL(5) * LOG(P0)

    FOR N = 1 TO 19
          A(N) = PL(5 * N + 1) + PL(5 * N + 2) * P0 + PL(5 * N + 3) / P0 + PL(5 * N + 4) / P0 ^ 2 + PL(5 * N
+ 5) * LOG(P0)
          B = A(N) * COS(2 * PI * N * Xk / 40)
          ENTHL = ENTHL + B
     NEXT N
 ENTHL = (A(0) + 2 * ENTHL) / 40
 RETURN



4500 'DIST. REFLUX
    QD = ((Y(1) - X(12)) * (H11 - H12) / (Y(11) - X(12)) - (H1 - H12)) * m3
    REFLUX = (QD / m3) / (H1 - H3)'Reflux Ratio
    MR = REFLUX * m3
    M1 = m3 + MR
    M12 = m3 * (Y(1) - Y(11)) / (Y(11) - X(12))
    M11 = m3 * (Y(1) - X(12)) / (Y(11) - X(12))
    RETURN


5000 'Enthalpy of vapour at "y" between 0.000 and 0.900
 ENTHV = 0
 IF Y(I) > .9 THEN GOTO 6000
 Yk = Y(I) * 10
 A(0) = PV1(1) + PV1(2) * P0 + PV1(3) / P0 + PV1(4) / P0 ^ 2 + PV1(5) * LOG(P0)

    FOR N = 1 TO 9
          A(N) = PV1(5 * N + 1) + PV1(5 * N + 2) * P0 + PV1(5 * N + 3) / P0 + PV1(5 * N + 4) / P0 ^ 2 +
PV1(5 * N + 5) * LOG(P0)
          B = A(N) * COS(2 * PI * N * Yk / 18)
          ENTHV = ENTHV + B
    NEXT N
 ENTHV = (A(0) + 2 * ENTHV) * .874972   '(100/6.34941/18)
 GOTO 6050
6000              'Enthalpy of vapour at "y" between 0.900and 1.000
 Yk = 100 * Y(I) - 90
 A(0) = PV2(1) + PV2(2) * P0 + PV2(3) / P0 + PV2(4) / P0 ^ 2 + PV2(5) * LOG(P0)

    FOR N = 1 TO 19
          A(N) = PV2(5 * N + 1) + PV2(5 * N + 2) * P0 + PV2(5 * N + 3) / P0 + PV2(5 * N + 4) / P0 ^ 2 +
PV2(5 * N + 5) * LOG(P0)
          B = A(N) * COS(2 * PI * N * Yk / 40)
          ENTHV = ENTHV + B
     NEXT N
 ENTHV = (A(0) + 2 * ENTHV) / 40
6050 RETURN

6910 'Subroutine  "ELECRTICAL PUMP"
    T = T0 - TKEL
    VOLA = C(4) * T0 ^ 4 + C(3) * T0 ^ 3 + C(2) * T0 ^ 2 + C(1) * T0 + C(0)
    VOLW = (3.086 - .899017 * (374.1 - T) ^ .147166 - .4 * (P0 - 218.5) * (385 - T) ^ -1.6) * 10 ^ -3
    VFX = (1 - XST) * VOLW + .85 * XST * VOLA
```

```
    EPEFF = .7
    WOUT = (101.37931# * (P1 - P2) * M7 * VFX) / (M7)
    WIN = (101.37931# * (P1 - P2) * VFX) / (EPEFF)
    RETURN

6915 'Subroutine  "VAPOUR PUMP"
    T = T0 - TKEL
    VOLA = C(4) * T0 ^ 4 + C(3) * T0 ^ 3 + C(2) * T0 ^ 2 + C(1) * T0 + C(0)
    VOLW = (3.086 - .899017 * (374.1 - T) ^ .147166 - .4 * (P0 - 218.5) * (385 - T) ^ -1.6) * 10 ^ -3
    VFX = (1 - XST) * VOLW + .85 * XST * VOLA
    Dr = .008:
    L = .025
    DS = .02
    fr = (mf(z) * VFX * 2) / (3.14159 * L * DS ^ 2)
    DV = .05
    DENS = 1 / (DNH(1) + DNH(2) * T(11) + DNH(3) * T(11) * P1 + DNH(4) * T(11) * P1 ^ 2 + DNH(5)
           T(11)* P1 ^ 3 + DNH(6) * T(11) / P1 + DNH(7) / T(11) ^ 3 + DNH(8) * P1 / T(11) ^ 11 + DNH(9) /
           T(11)^ 11 +  DNH(10) * P1 ^ 3 / T(11) ^ 10)
    M16 = DENS * fr * L * 3.14159 / 2 * (2 * DV ^ 2 - DR ^ 2 - DS ^ 2)
    RETURN


8210
    ZAZ$ = SPACE$(10)
    PRINT ZAZ$; "+"; STRING$(16, 205); "-"; STRING$(26, 205); "-"; STRING$(16, 205); "+"
    PRINT ZAZ$; "Ý +"; STRING$(14, 205); "Ý";
    PRINT " ABSORPTION REFRIGERATION "; "Ý"; STRING$(14, 205); "+ Ý"
    PRINT ZAZ$; "Ý Ý"; SPACE$(14); "+"; STRING$(26, 205); "+"; SPACE$(14); "Ý Ý"
    PRINT ZAZ$; "Ý Ý"; SPACE$(56); "Ý Ý"
    PRINT ZAZ$; "Ý Ý"; SPACE$(56); "Ý Ý"
    PRINT ZAZ$; "Ý Ý"; SPACE$(56); "Ý Ý"
    PRINT ZAZ$; "Ý Ý"; SPACE$(56); "Ý Ý"
    PRINT ZAZ$; "Ý Ý"; SPACE$(56); "Ý Ý"
    PRINT ZAZ$; "Ý Ý"; SPACE$(56); "Ý Ý"
    PRINT ZAZ$; "Ý Ý"; SPACE$(56); "Ý Ý"
    PRINT ZAZ$; "Ý +—"; STRING$(32, 205); "-"; STRING$(17, 205); "—+ Ý"
    PRINT ZAZ$; "Ý——Ý"; SPACE$(32); "Ý"; SPACE$(17); "Ý——Ý"
    PRINT ZAZ$; "Ý +—"; STRING$(32, 205); "-"; STRING$(17, 205); "—+ Ý"
    PRINT ZAZ$; "Ý Ý"; SPACE$(56); "Ý Ý"
    PRINT ZAZ$; "Ý Ý"; SPACE$(56); "Ý Ý"
    PRINT ZAZ$; "Ý Ý"; SPACE$(56); "Ý Ý"
    PRINT ZAZ$; "Ý Ý"; STRING$(56, 205); "Ý Ý"
    PRINT ZAZ$; "Ý Ý"; SPACE$(56); "Ý Ý"
    PRINT ZAZ$; "Ý Ý"; SPACE$(56); "Ý Ý"
    PRINT ZAZ$; "Ý Ý"; SPACE$(56); "Ý Ý"
    PRINT ZAZ$; "Ý +"; STRING$(22, 205); "-"; STRING$(10, 205); "-"; STRING$(22, 205); "+ Ý"
    PRINT ZAZ$; "+"; STRING$(24, 205); "Ý"; SPACE$(10); "Ý"; STRING$(24, 205); "+"
    PRINT ZAZ$; SPACE$(25); "+"; STRING$(10, 205); "+"
    LOCATE 22, 38: PRINT "DEC 1993"
    RETURN
```

# Appendix B

## Specific volume of superheated ammonia

(reproduced from Vicatos)

"$\upsilon$" superheated ammonia vapour

for pressures form 0.1 to 24 bars
from saturation temperature to 480 K

P in [bars]
T in [K]
$\upsilon$ in [$m^3/kg$]

$$\upsilon = a + bT + cTP + dTP^2 + eTP^3 + fT/P + g/T^3 + hP/T^{11} + i/T^{11} + jP^2/T^{10}$$

a = 1.972067E-03
b = -5.178901E-06
c = -5.265812E-08
d = 1.217014E-09
e = 3.802621E-11
f = 4.881826E-03
g = -4.106189E+05
h = -2.164457E+23
i = -1.222804E+23
j = -1.769827E+18

| | | |
|---|---|---|
| accuracy | -2.6390% | max |
| | -0.6957% | min |
| | -0.0824% | average |

Enthalpy–Concentration ( Mass fraction ) —— *Enthalpie–Concentration massique*

Ammonia–Water —— *Ammoniac–Eau*

*( According to the equation of Ziegler —— D'après l'équation de Ziegler )*

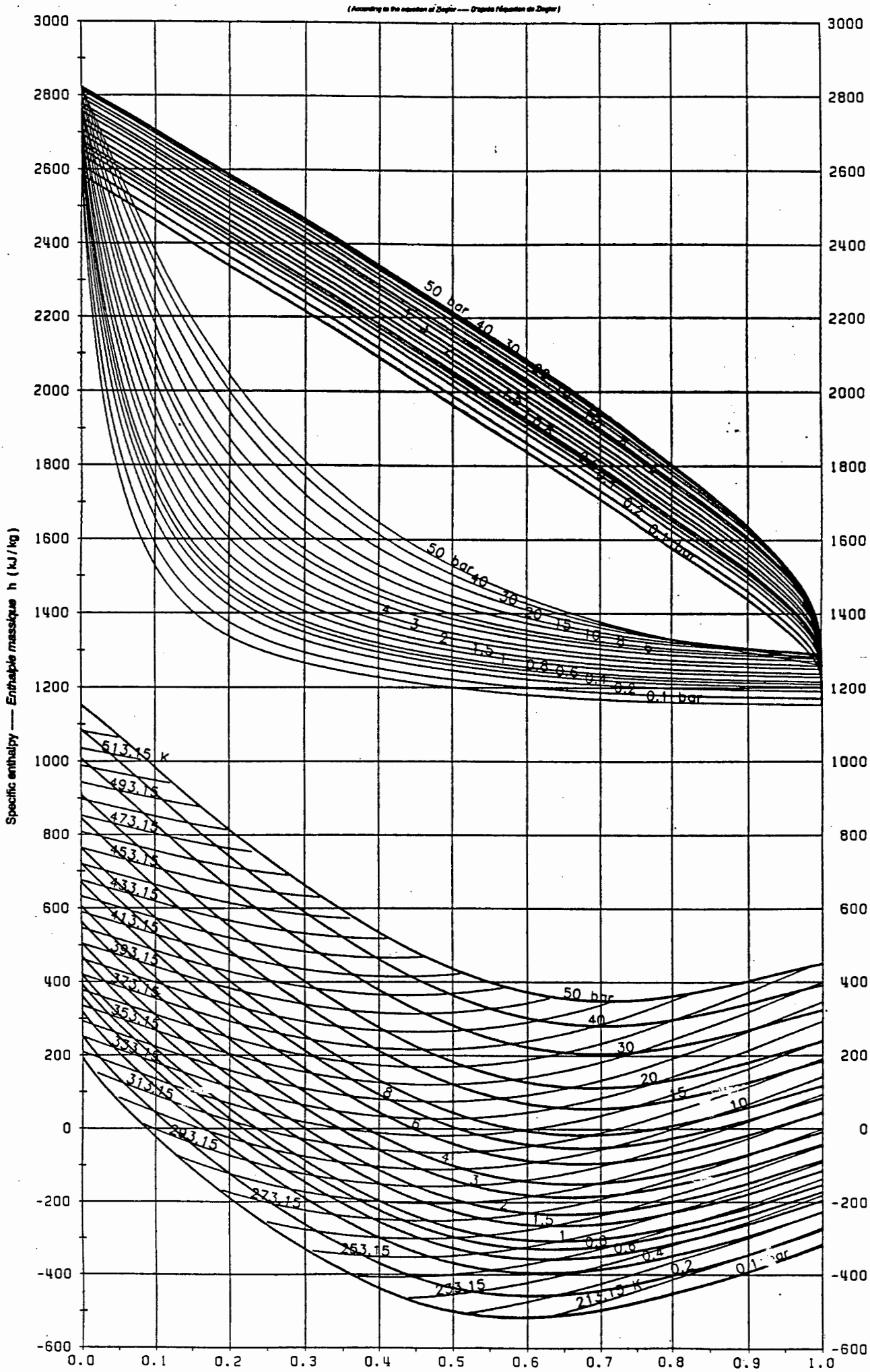


B-2

# Appendix C

## Tetraglyme (E181)

Tetraethylene Glycol Dimethyl Ether
$CH_3-O-CH_2-CH_2-O-CH_2-CH_2-O-CH_2-CH_2-O-CH_2-CH_2-O-CH_3$

Specifications

| | | |
|---|---|---|
| Purity (by G.C.), wt% | 98.0 min | typically 99.0 |
| Acidity (as acetic acid), ppm | 150 max | typically 25 |
| Water content, ppm | 500 max | typically 100 |
| Peroxide content, ppm | 15 max | typically 5 |
| Suspended Matter | nil | |
| Appearance | clear, colourless | |
| Odor | very mild, non-residual | |

Properties

| | |
|---|---|
| Molecular weight | 222.28 |
| Specific Gravity, 20/20°C | 1.0132 |
| Pounds per Gallon, 20°C | 8.45 |
| Boiling Point, °C, 760mm Hg | 275 |
| Freezing Point, °C | -29.7 |
| Vapour Pressure,mm Hg at 20°C | <0.01 |
| Volatility (n-butyl acetate = 100) | <0.1 |
| Azeotrope with water | none |
| Heat of Vapourization, Kcal/mole, 760mm Hg | 18.7 |
| Refractive Index, 20°C | 1.4330 |
| Viscosity, centipoise, 20°C | 4.1 |
| Solubility in water | complete |
| Solubility, water in | complete |
| Flash point, closed cup | 141°C (286°F) |

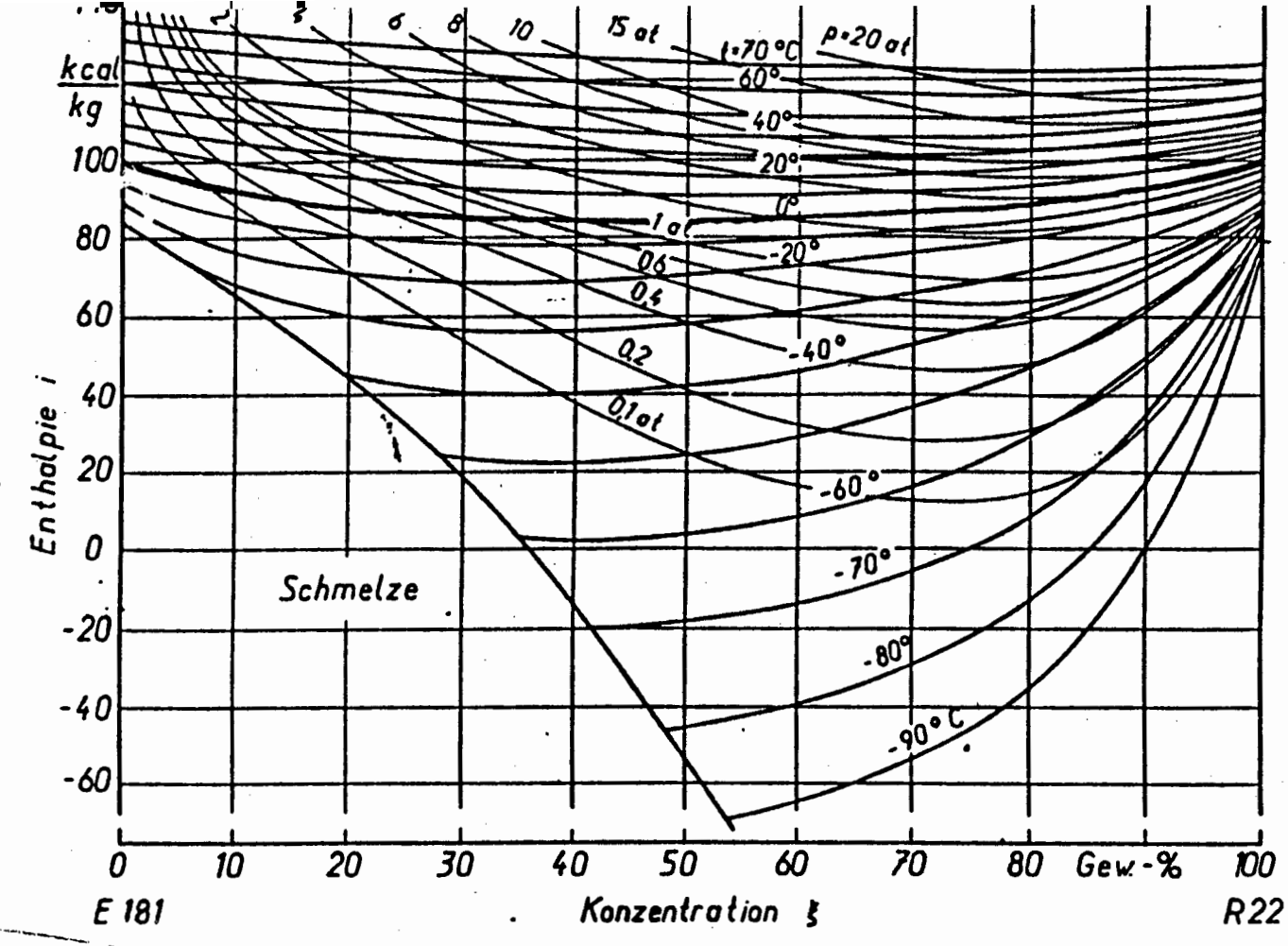


Enthalpy - concentration diagram

Source: Kreibel et al [12]

Anh. M 1 Tabelle 5. Bevorzugte Kältemittel in Klimakälteanlagen nach Frigen-Fibel, Hoechst AG

| Bezeichnung | Chemische Formel | Internationale Kennziffer | Molmasse | Siedepunkt bei 1,013 bar | Erstarrungspunkt | Kritische Temperatur | Kritischer Druck | Verdampfungswärme (Siedepunkt) | Spezifische Wärme der Flüssigkeit (Siedepunkt) | Dichte der Flüssigkeit bei 20 °C | Exponent der Adiabaten 30°; 1,013 bar |
|---|---|---|---|---|---|---|---|---|---|---|---|
| Trichlorfluormethan | $CCl_3F$ | R 11 | 137,38 | 23,8 | −111 | 198,0 | 44,0 | 182,2 | 0,871 | 1,49 | 1,13 |
| Dichlordifluormethan | $CCl_2F_2$ | R 12 | 120,92 | −29,8 | −158 | 112,0 | 41,6 | 166,0 | 0,854 | 1,328 | 1,139 |
| Bromtrifluormethan | $CBrF_3$ | R 13 B1 | 148,93 | −57,8 | −168 | 67,0 | 39,8 | 118,2 | 0,682 | 1,574 | 1,143 |
| Chlordifluormethan | $CHClF_2$ | R 22 | 86,48 | −40,8 | −160 | 96,2 | 49,9 | 234,7 | 1,089 | 1,213 | 1,178 |
| 1,1,2-Trichlortrifluoräthan | $CClF_2$-$CCl_2F$ | R 113 | 187,39 | 47,6 | − 35 | 214,1 | 34,1 | 144,7 | 0,946 | 1,582 | 1,082 |
| 1,2-Dichlortetrafluoräthan | $CClF_2$-$CClF_2$ | R 114 | 170,93 | 3,6 | − 94 | 145,7 | 32,6 | 136,8 | 0,971 | 1,473 | 1,084 |
| Azeotrop aus: Difluoräthan/ Dichlordifluormethan | $CH_3$-$CHF_2$/ $CCl_2F_2$ | R 500 | 99,29 | −33,5 | −159 | 105,5 | 44,3 | 201,3 | 1,214 | 1,173 | 1,14 |
| Azeotrop aus: Chlordifluormethan/ Chlorpentafluoräthan | $CHClF_2$/ $CClF_2$-$CF_3$ | R 502 | 111,6 | −45,6 | −160 | 82,2 | 40,8 | 172,6 | 1,277 | 1,240 | 1,135 |

Anh. M 1 Tabelle 7. Dampftafel für Kältemittel R 22 (Frigen 22). Naßdampfgebiet (Hoechst AG)

| Temperatur $t$ °C | Druck $p$ bar | Spezifisches Volumen der Flüssigkeit $v'$ l/kg | Spezifisches Volumen des Dampfes $v''$ l/kg | Enthalpie der Flüssigkeit $h'$ kJ/kg | Enthalpie des Dampfes $h''$ kJ/kg | Entropie der Flüssigkeit $s'$ kJ/kg·K | Entropie des Dampfes $s''$ kJ/kg·K |
|---|---|---|---|---|---|---|---|
| −100 | 0,021 | 0,639 | 7906,83 | 95,95 | 357,78 | 0,5339 | 2,0461 |
| −95 | 0,033 | 0,644 | 5235,42 | 100,24 | 360,26 | 0,5584 | 2,0179 |
| −90 | 0,049 | 0,649 | 3556,81 | 104,61 | 362,77 | 0,5825 | 1,9921 |
| −85 | 0,073 | 0,654 | 2473,79 | 109,08 | 365,31 | 0,6065 | 1,9684 |
| −80 | 0,105 | 0,659 | 1757,88 | 113,62 | 367,85 | 0,6304 | 1,9466 |
| −75 | 0,149 | 0,665 | 1273,99 | 118,27 | 370,41 | 0,6541 | 1,9266 |
| −70 | 0,206 | 0,671 | 940,11 | 123,02 | 372,97 | 0,6778 | 1,9081 |
| −65 | 0,281 | 0,677 | 705,32 | 127,88 | 375,53 | 0,7013 | 1,8911 |
| −60 | 0,376 | 0,683 | 537,29 | 132,84 | 378,07 | 0,7249 | 1,8754 |
| −55 | 0,497 | 0,689 | 415,07 | 137,92 | 380,60 | 0,7483 | 1,8608 |
| −50 | 0,646 | 0,695 | 324,82 | 143,10 | 383,09 | 0,7718 | 1,8473 |
| −45 | 0,830 | 0,702 | 257,23 | 148,40 | 385,55 | 0,7952 | 1,8347 |
| −40 | 1,053 | 0,709 | 205,95 | 153,80 | 387,97 | 0,8186 | 1,8229 |
| −35 | 1,321 | 0,717 | 166,57 | 159,30 | 390,34 | 0,8418 | 1,8119 |
| −30 | 1,640 | 0,724 | 135,98 | 164,89 | 392,65 | 0,8649 | 1,8016 |
| −25 | 2,016 | 0,732 | 111,97 | 170,58 | 394,90 | 0,8880 | 1,7919 |
| −20 | 2,455 | 0,740 | 92,93 | 176,33 | 397,07 | 0,9108 | 1,7827 |
| −15 | 2,964 | 0,749 | 77,70 | 182,17 | 399,17 | 0,9335 | 1,7740 |
| −10 | 3,550 | 0,758 | 65,40 | 188,06 | 401,18 | 0,9559 | 1,7658 |
| −5 | 4,219 | 0,768 | 55,39 | 194,00 | 403,10 | 0,9781 | 1,7579 |
| 0 | 4,980 | 0,778 | 47,18 | 200,00 | 404,93 | 1,0000 | 1,7502 |
| 5 | 5,839 | 0,788 | 40,40 | 206,03 | 406,65 | 1,0216 | 1,7429 |
| 10 | 6,803 | 0,799 | 34,75 | 212,10 | 408,27 | 1,0430 | 1,7358 |
| 15 | 7,882 | 0,811 | 30,03 | 218,21 | 409,77 | 1,0641 | 1,7289 |
| 20 | 9,081 | 0,824 | 26,04 | 224,34 | 411,15 | 1,0848 | 1,7220 |
| 25 | 10,411 | 0,837 | 22,66 | 230,50 | 412,39 | 1,1053 | 1,7153 |
| 30 | 11,880 | 0,852 | 19,78 | 236,70 | 413,49 | 1,1255 | 1,7086 |
| 35 | 13,496 | 0,867 | 17,31 | 242,93 | 414,43 | 1,1454 | 1,7019 |
| 40 | 15,269 | 0,884 | 15,17 | 249,21 | 415,19 | 1,1651 | 1,6952 |
| 45 | 17,209 | 0,902 | 13,32 | 255,57 | 415,76 | 1,1847 | 1,6882 |
| 50 | 19,327 | 0,923 | 11,70 | 262,03 | 416,11 | 1,2043 | 1,6811 |
| 55 | 21,635 | 0,945 | 10,29 | 268,62 | 416,20 | 1,2238 | 1,6736 |
| 60 | 24,146 | 0,970 | 9,03 | 275,40 | 415,99 | 1,2436 | 1,6656 |
| 65 | 26,873 | 0,999 | 7,92 | 282,44 | 415,40 | 1,2638 | 1,6570 |
| 70 | 29,833 | 1,032 | 6,92 | 289,85 | 414,35 | 1,2846 | 1,6475 |
| 75 | 33,042 | 1,071 | 6,01 | 297,78 | 412,67 | 1,3066 | 1,6366 |
| 80 | 36,520 | 1,120 | 5,17 | 306,50 | 410,13 | 1,3304 | 1,6238 |
| 85 | 40,290 | 1,185 | 4,38 | 316,43 | 406,22 | 1,3571 | 1,6078 |
| 90 | 44,374 | 1,276 | 3,59 | 328,42 | 399,75 | 1,3889 | 1,5853 |
| 95 | 48,802 | 1,506 | 2,60 | 347,63 | 384,73 | 1,4397 | 1,5405 |
| 96,18 | 49,900 | 1,949 | 1,95 | 366,83 | 366,83 | 1,4913 | 1,4913 |

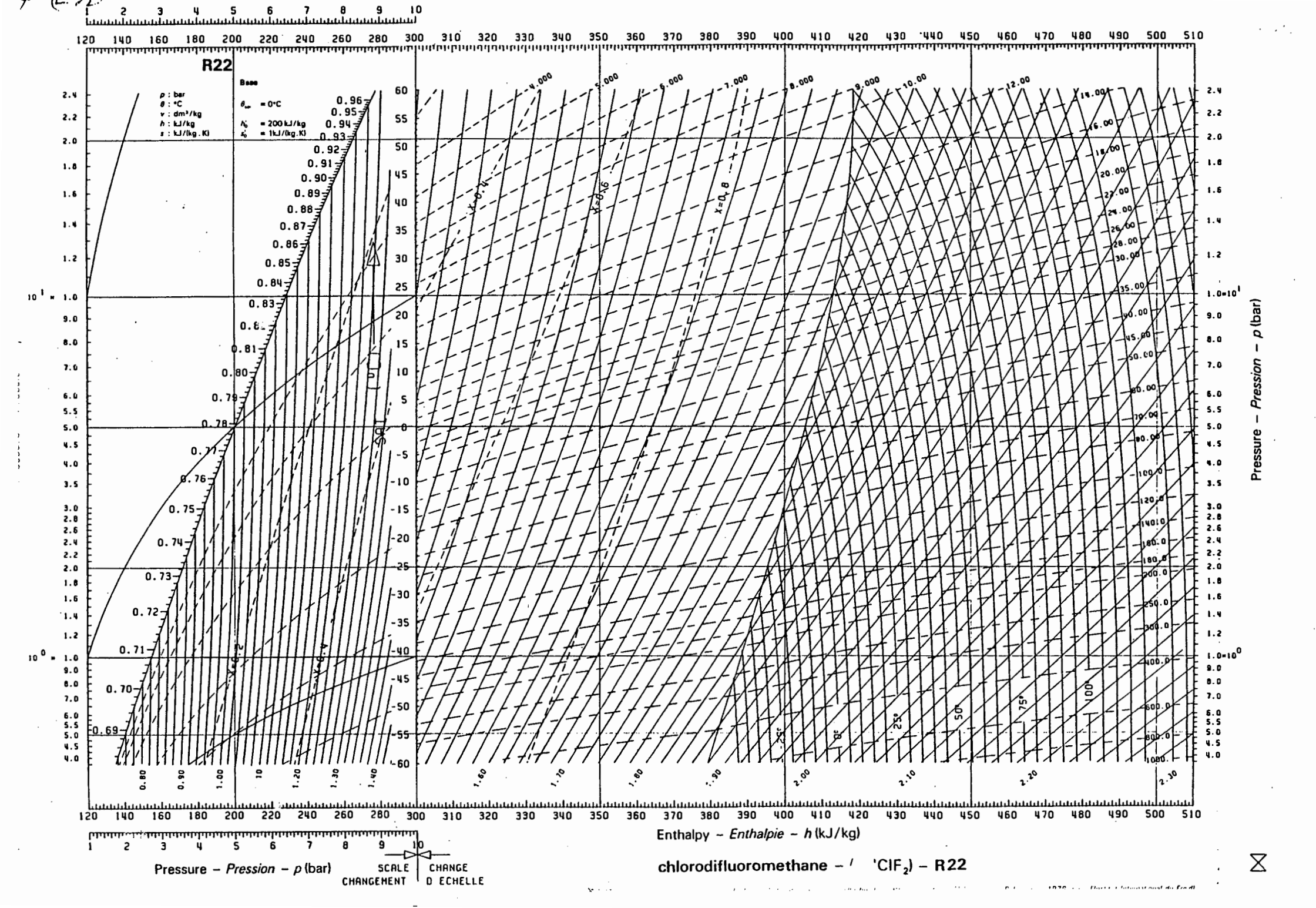
R22
Base
p : bar
θ : °C
v : dm³/kg
h : kJ/kg
s : kJ/(kg.K)
θ = 0°C
h = 200 kJ/kg
s = 1kJ/(kg.K)
Pressure – Pression – p (bar)
Enthalpy – Enthalpie – h (kJ/kg)
Pression – p (bar)
SCALE CHANGE
CHANGEMENT D ECHELLE
chlorodifluoromethane – ('ClF2) – R22

Appendix D

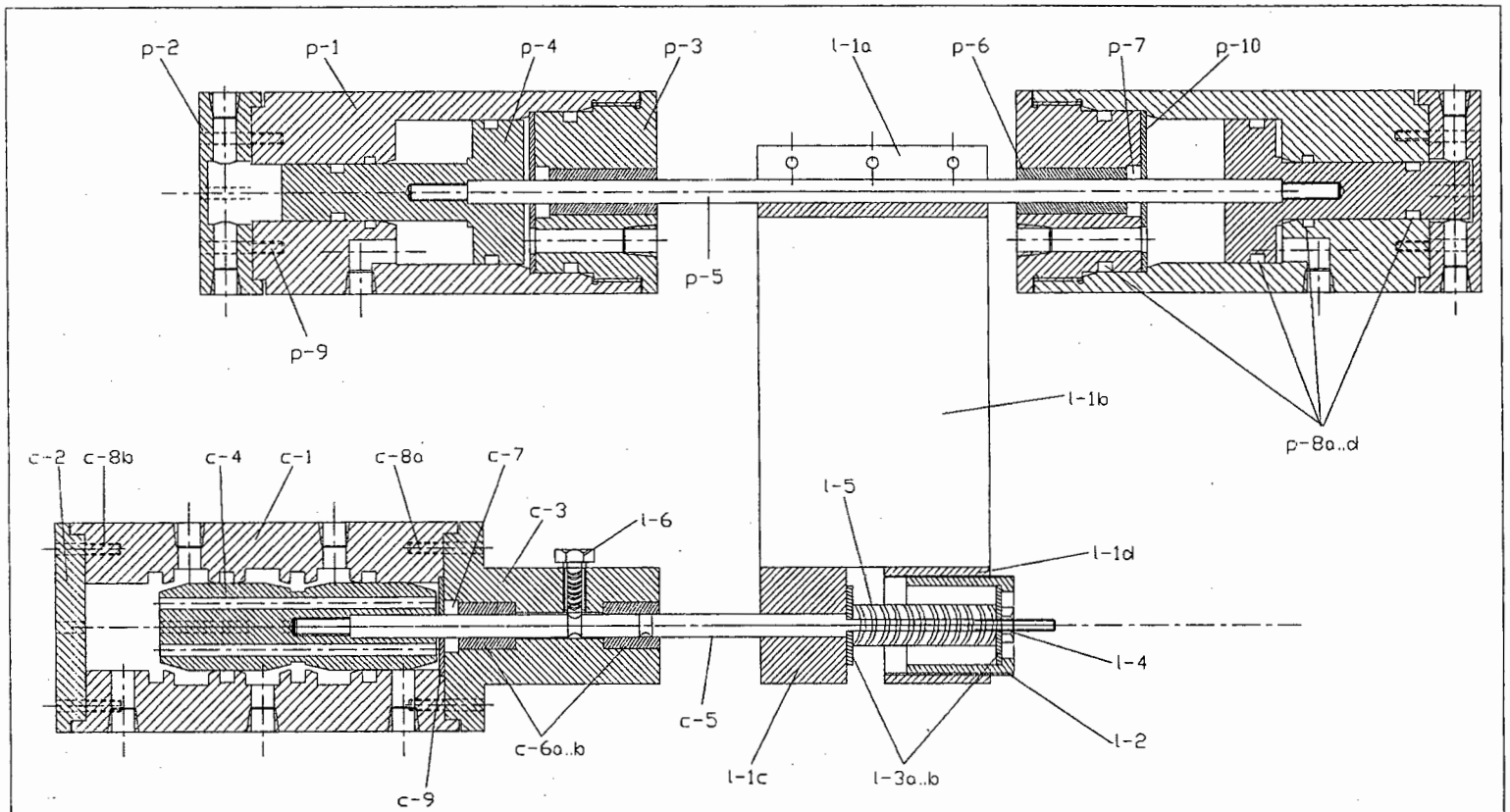


p-1 pump cylinder
p-2 pump cap
p-3 pump end
p-4 pump piston
p-5 pump shaft
p-6 pump bush
p-7 pump lipseal
p-8a..d pump O-rings
p-9 pump cap bolts
p-10 seal holding ring

c-1 control cylinder
c-2 control lid
c-3 control cap
c-4 control core
c-5 control shaft
c-6a..b control bushes
c-7 control lipseal
c-8a..b control cap/lid bolts
c-9 seal holding ring

l-1a pump shaft link
l-1b linking plate
l-1c link bush
l-1d link threaded cylinder
l-2 ring holding cylinder
l-3a..b spring plates
l-4 securing nut
l-5 control spring
l-6 spring plunger

Absorption Refrigeration Pump
University of Cape Town
Mechanical Engineering
Drawn: E Krafft
Date: 5 June 1994

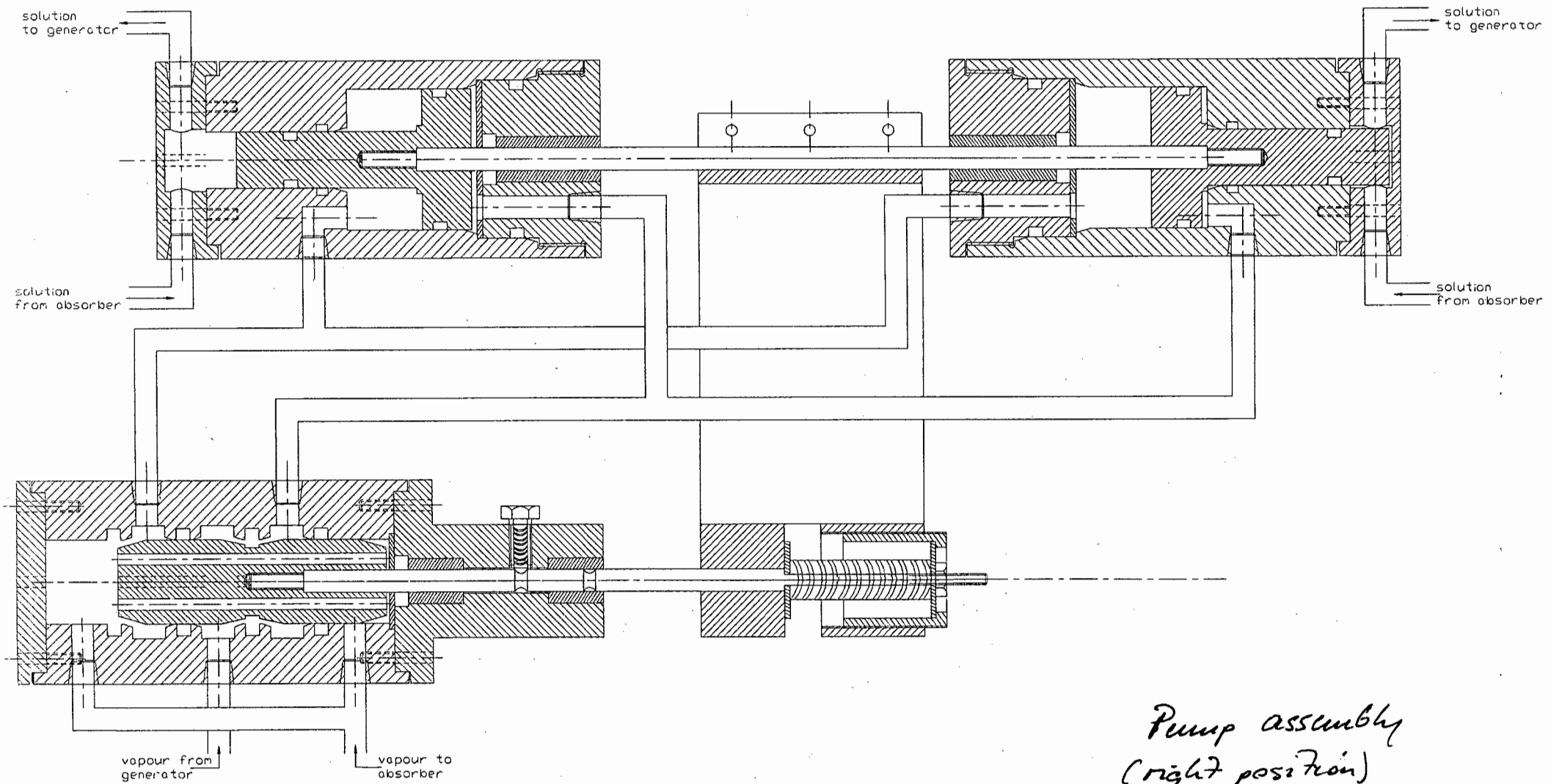


Pump assembly
(right position)

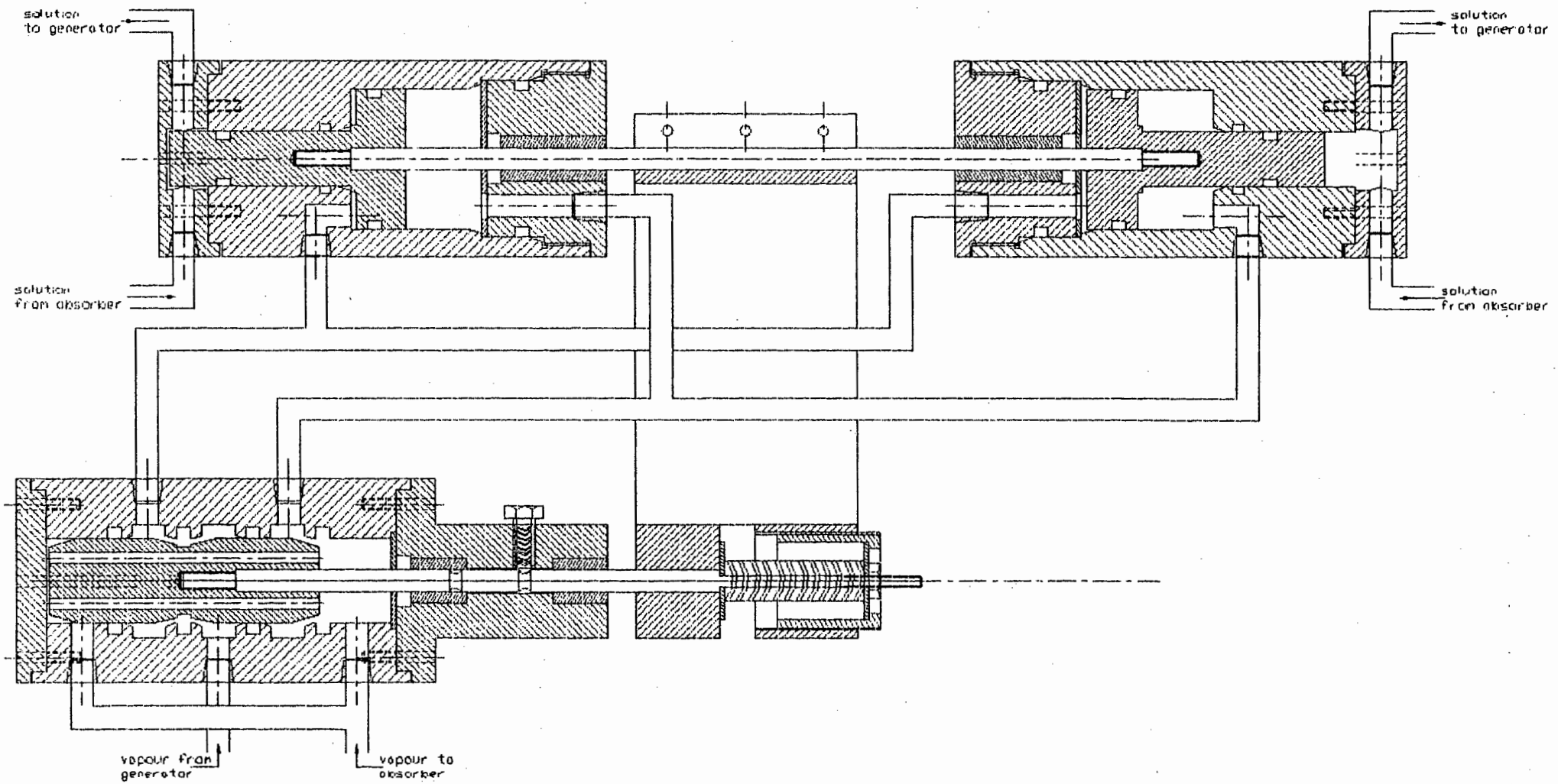


Pump assembly
(left positive)

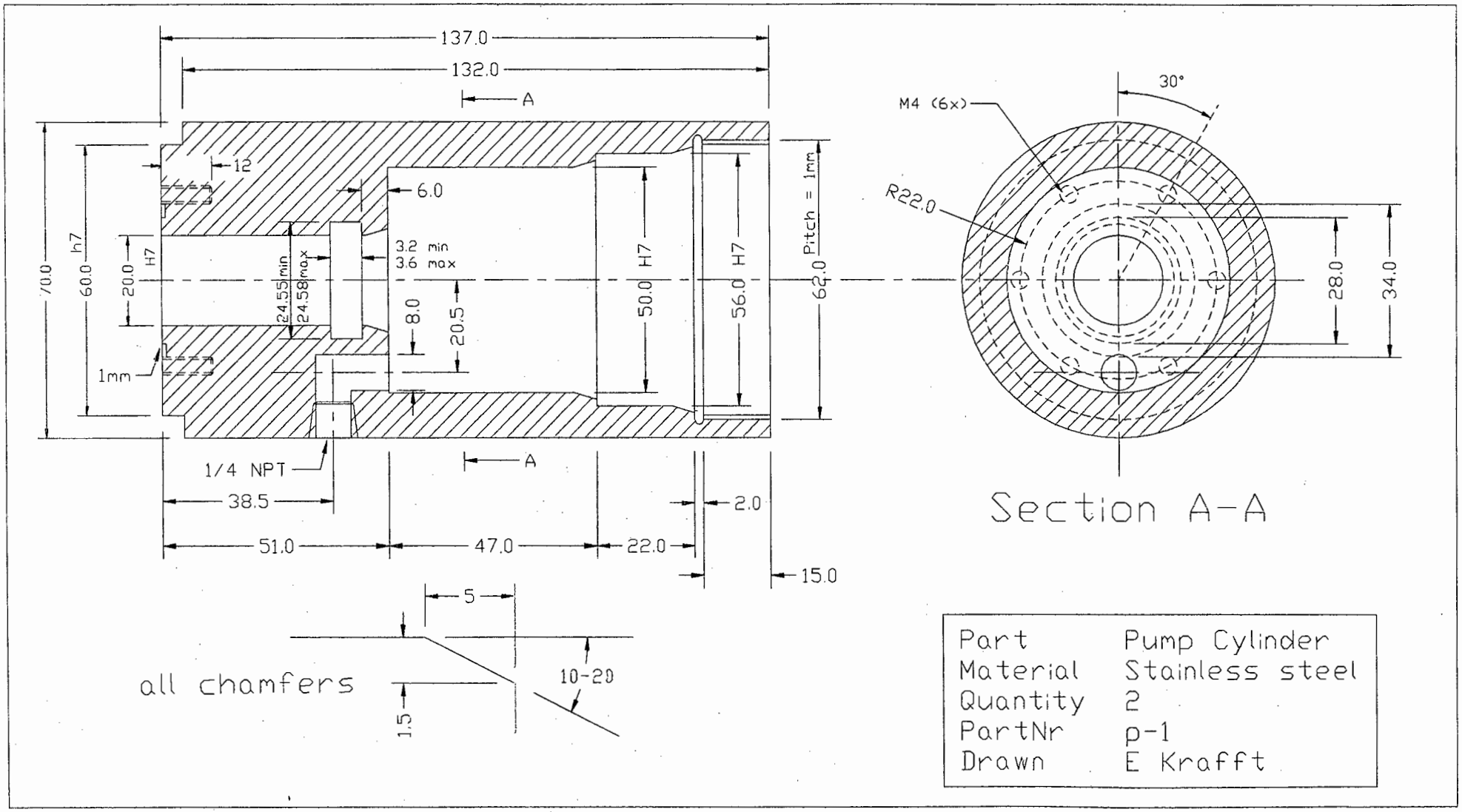
137.0
132.0
A
12
6.0
3.2 min
3.6 max
24.55 min
24.58 max
8.0
20.5
50.0 H7
56.0 H7
62.0
Pitch = 1mm
70.0
60.0 h7
20.0 H7
1mm
1/4 NPT
38.5
51.0
47.0
22.0
2.0
15.0
5
10-20
1.5
all chamfers
M4 (6x)
30°
R22.0
28.0
34.0
Section A-A
Part Pump Cylinder
Material Stainless steel
Quantity 2
PartNr p-1
Drawn E Krafft

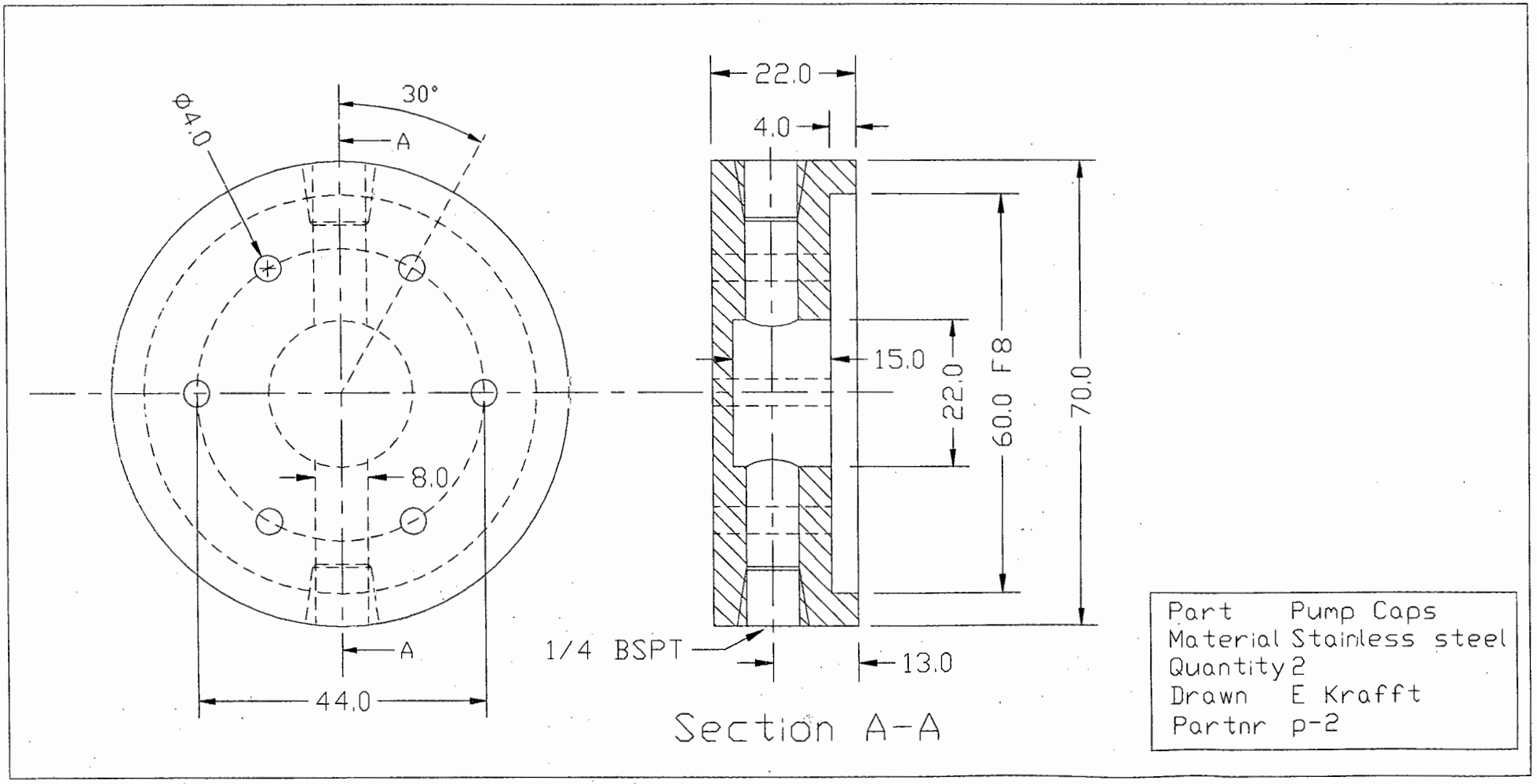
30°
A
ϕ4.0
8.0
A
44.0
22.0
4.0
15.0
22.0
60.0 F8
70.0
1/4 BSPT
13.0
Section A-A
Part Pump Caps
Material Stainless steel
Quantity 2
Drawn E Krafft
Partnr p-2

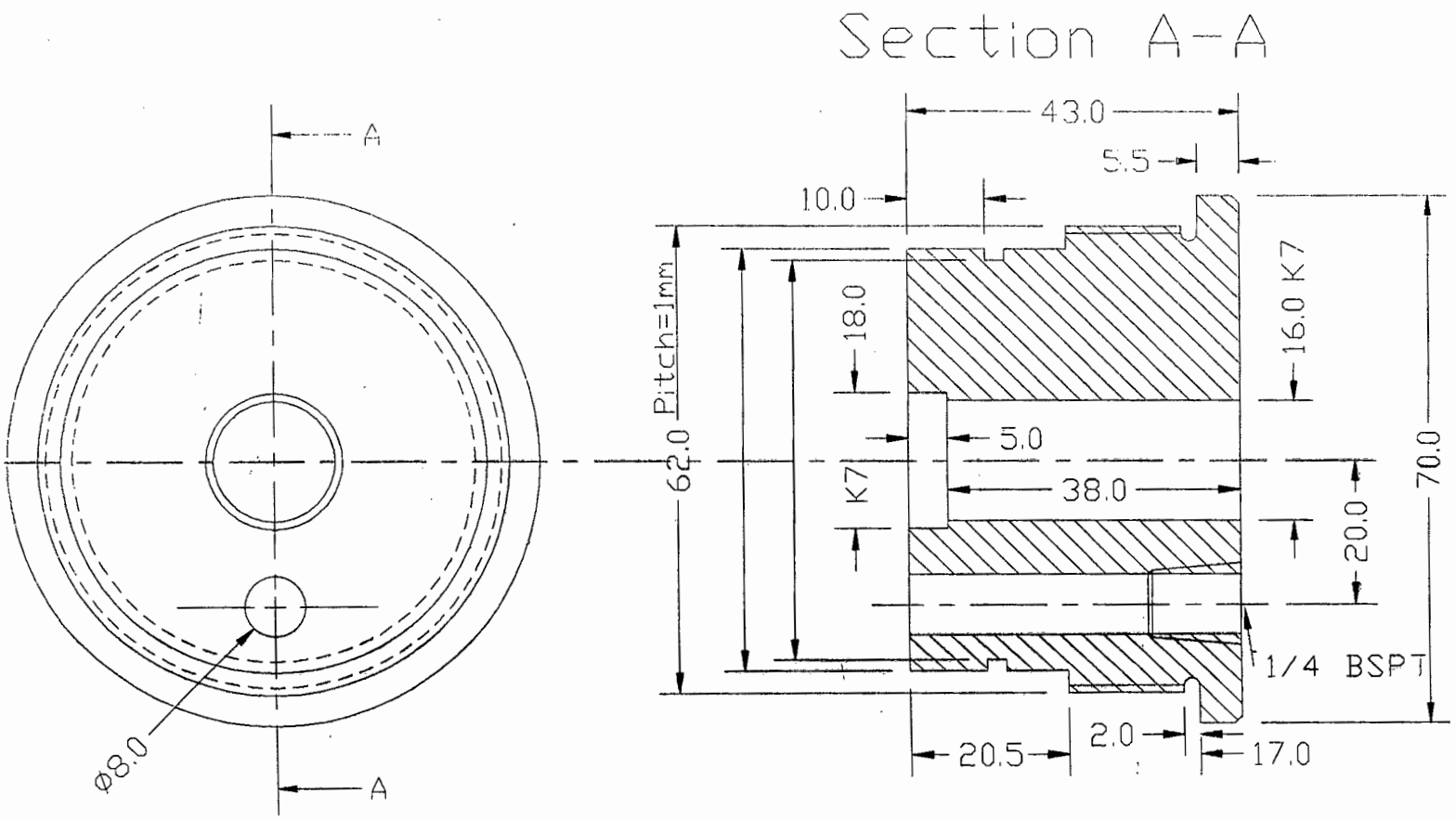


| | |
|---|---|
| Part | Pump Ends |
| Material | Stainless. steel |
| Quantity | 2 |
| PartNr | p-3 |
| Drawn | E Krafft |

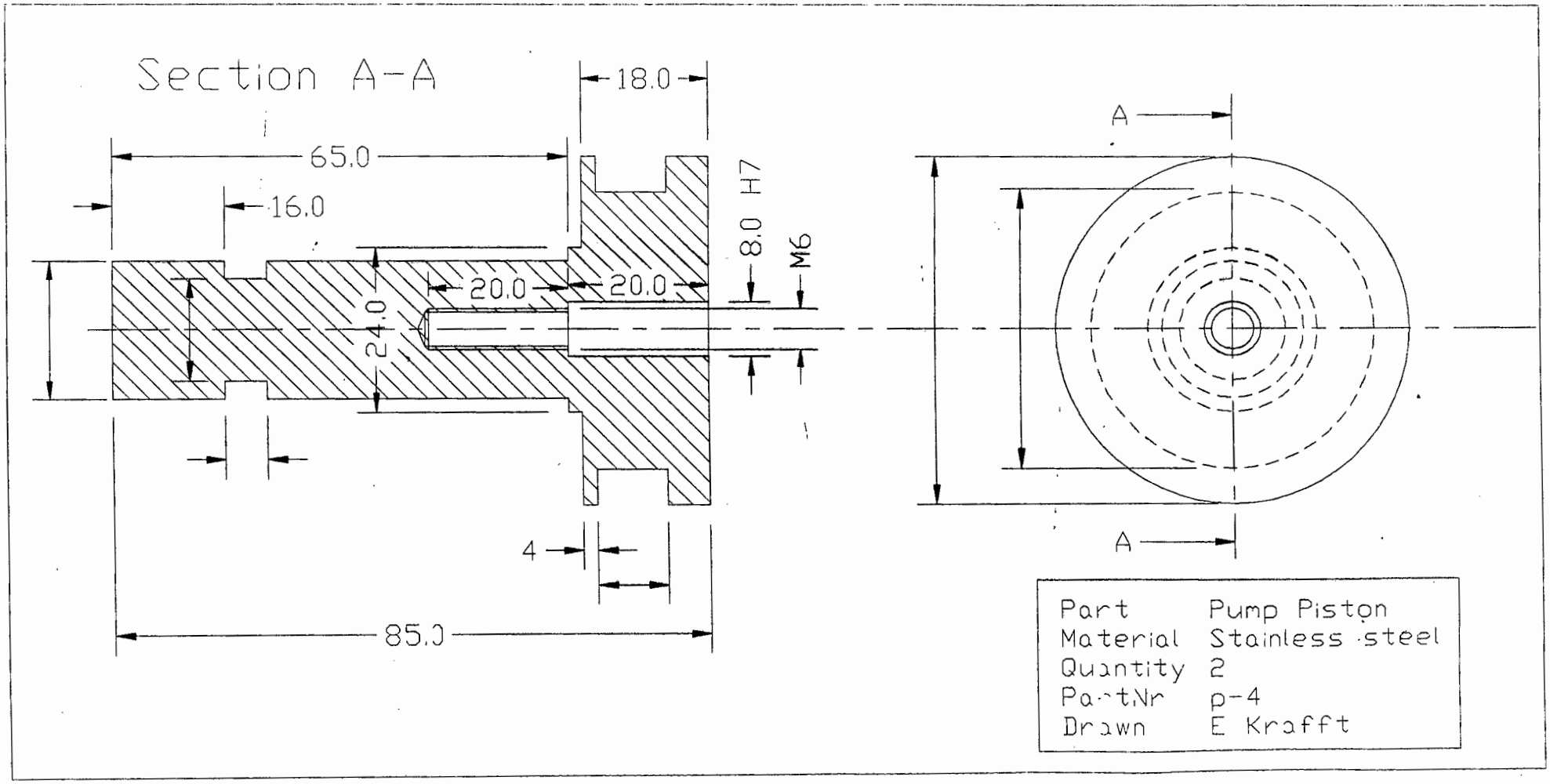
Section A-A
18.0
65.0
16.0
8.0 H7
M6
20.0
20.0
24.0
4
85.0
A
A
Part Pump Piston
Material Stainless steel
Quantity 2
Part Nr p-4
Drawn E Krafft

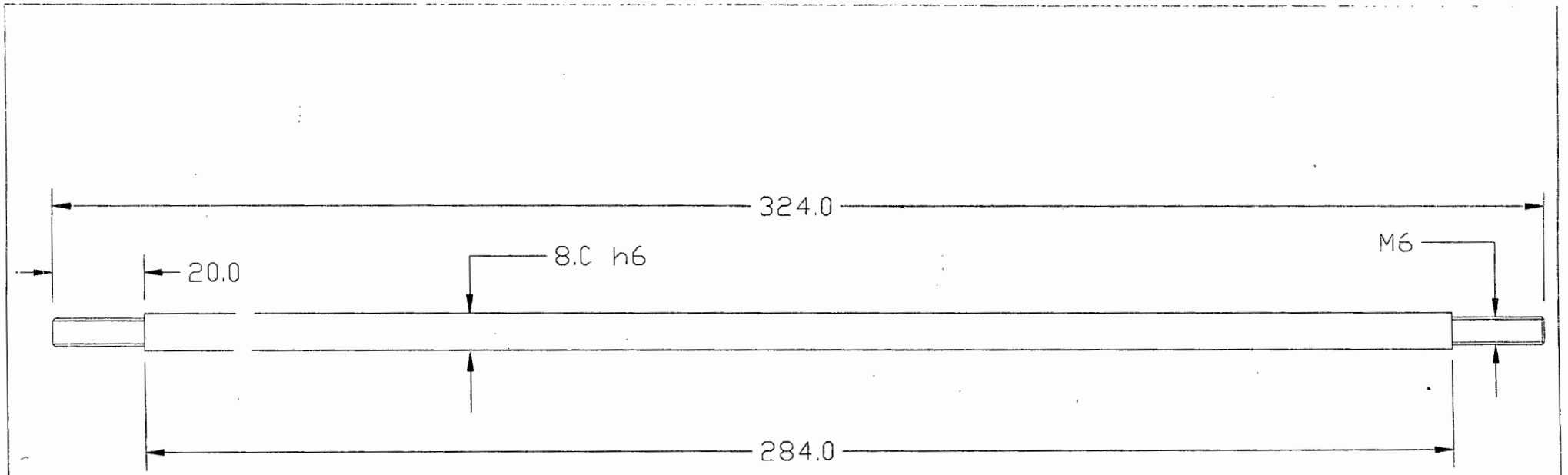


| | |
|---|---|
| Part | Pump Shaft |
| Material | Silver steel (polished) |
| Quantity | 1 |
| PartNr | p-5 |
| Drawr | E Krafft |

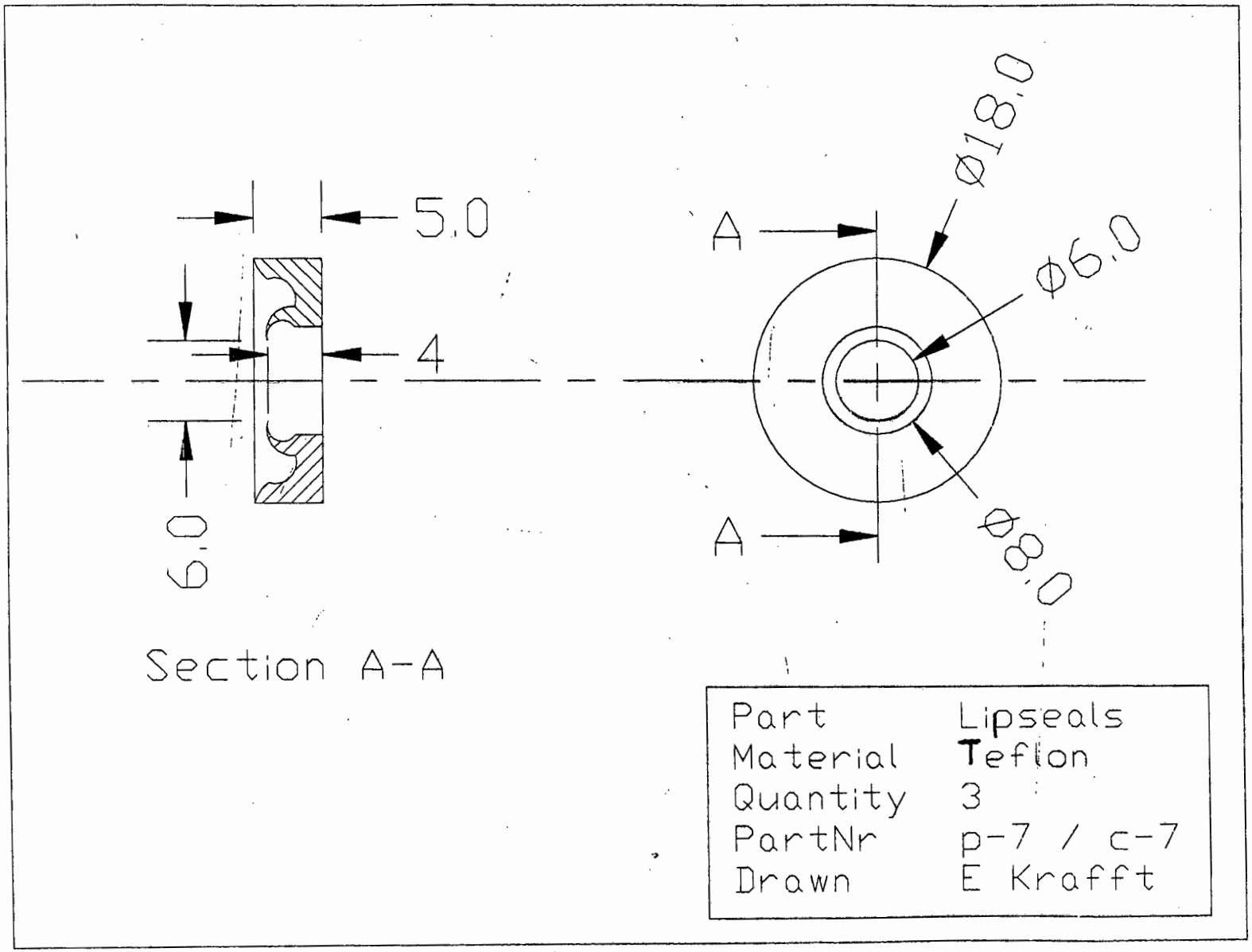
5.0
4
6.0
A
A
Ø18.0
Ø6.0
Ø8.0
Section A-A
Part Lipseals
Material Teflon
Quantity 3
PartNr p-7 / c-7
Drawn E Krafft

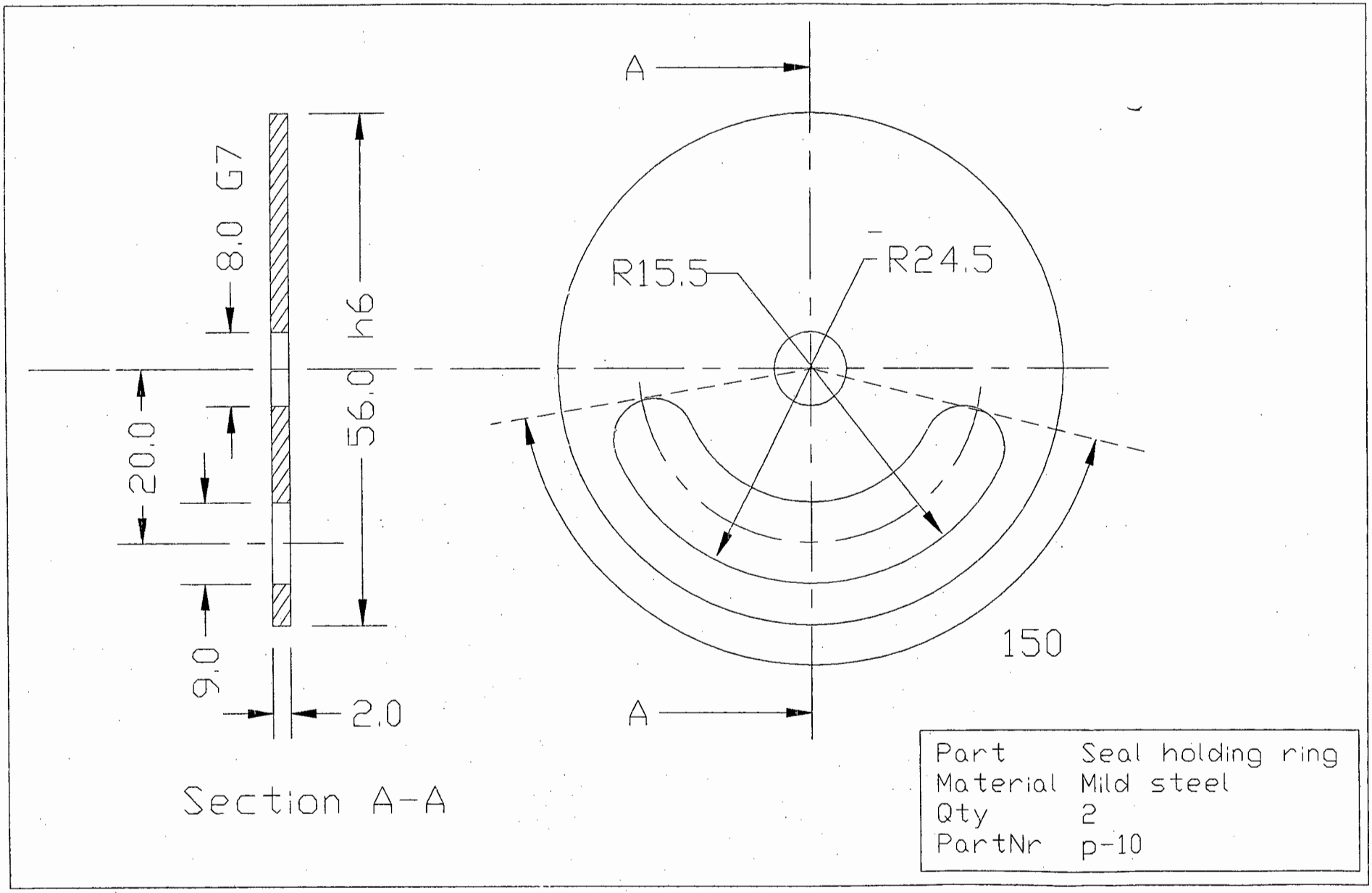
A
R15.5
R24.5
150
A
8.0 G7
h6
56.0
20.0
9.0
2.0
Section A-A
Part Seal holding ring
Material Mild steel
Qty 2
PartNr p-10

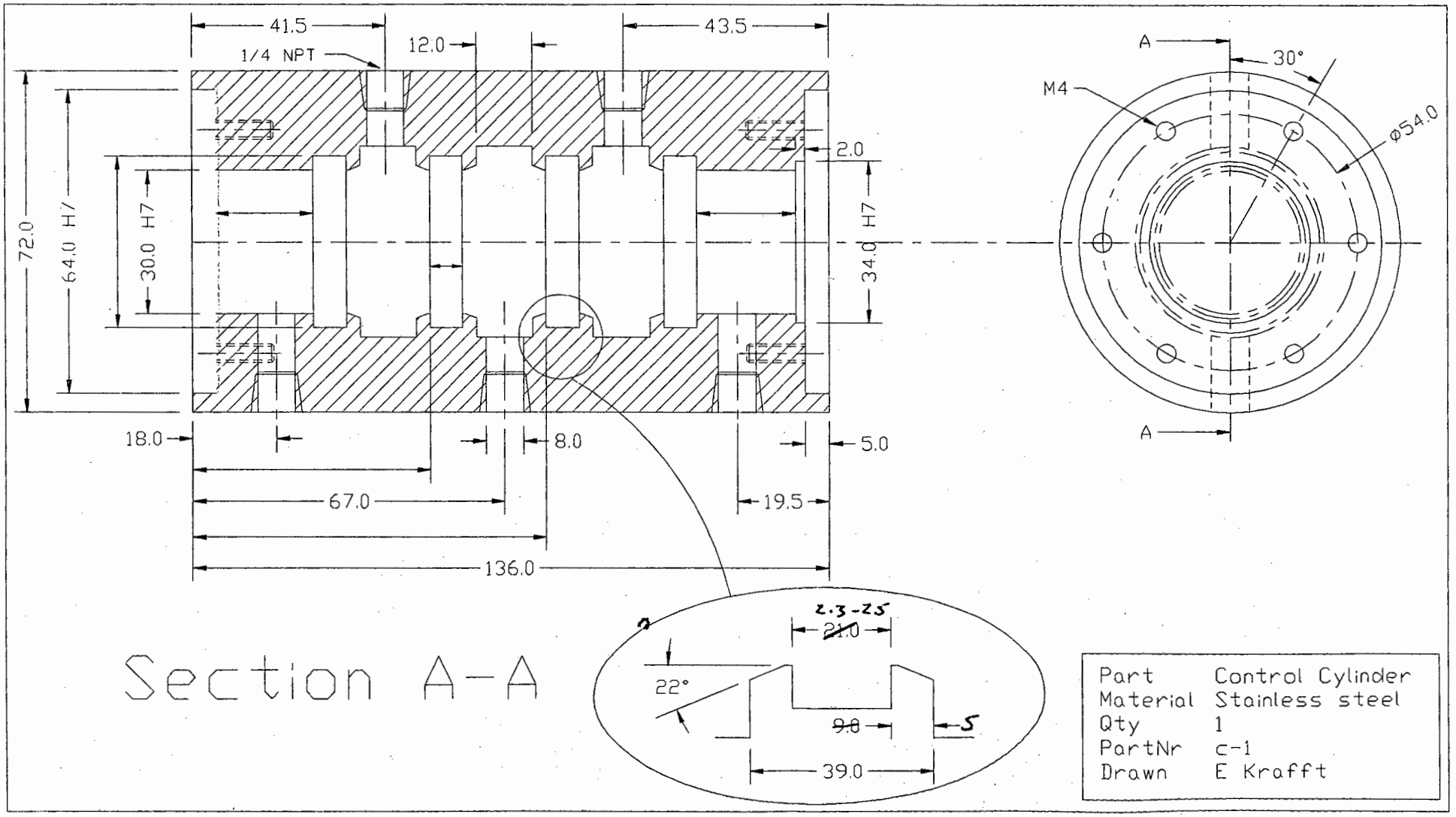
41.5
12.0
43.5
1/4 NPT
72.0
64.0 H7
30.0 H7
2.0
34.0 H7
18.0
8.0
5.0
67.0
19.5
136.0
A
30°
M4
ø54.0
A
Section A-A
2.3-25
21.0
22°
9.8
5
39.0
Part Control Cylinder
Material Stainless steel
Qty 1
PartNr c-1
Drawn E Krafft

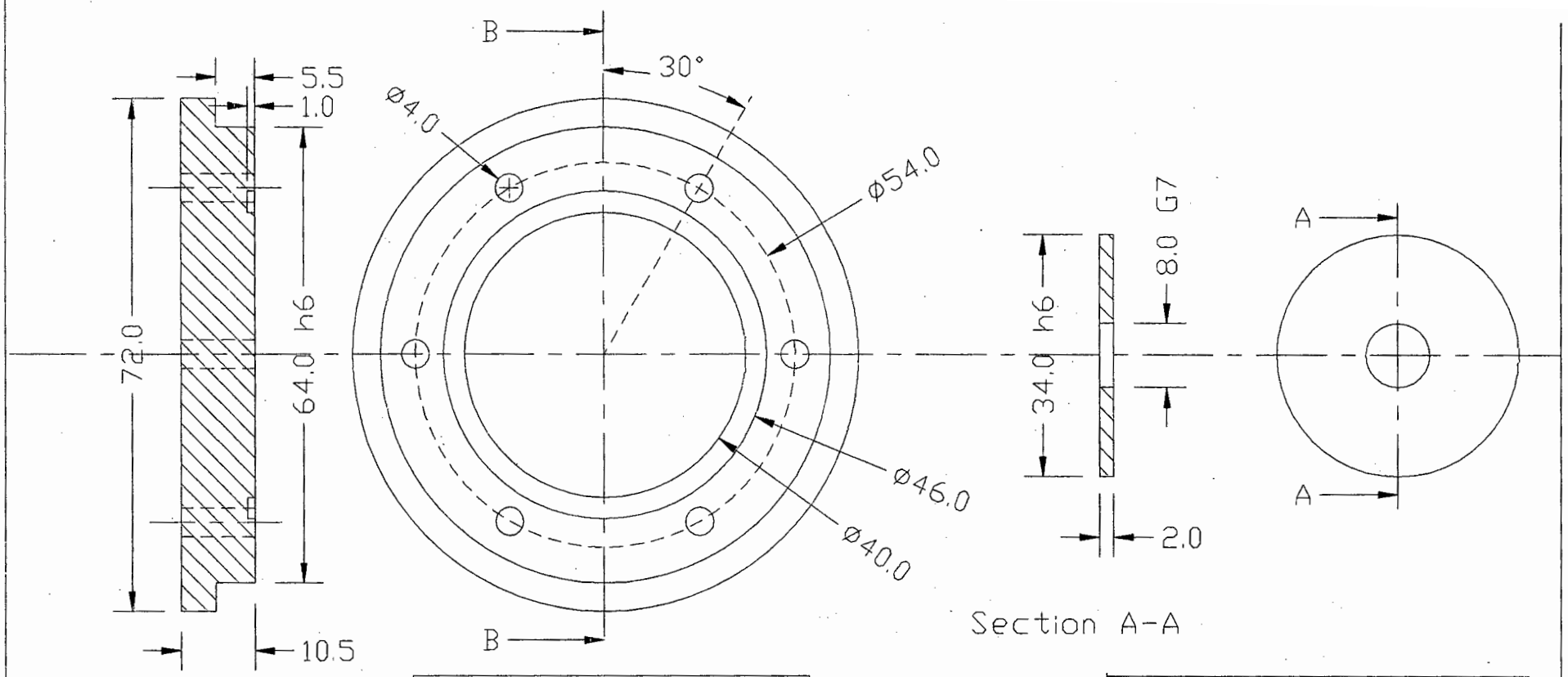


Section B-B

Section A-A

| | |
|---|---|
| Part | Control Lid |
| Material | Mild steel |
| Quantity | 1 |
| PartNr | c-2 |

| | |
|---|---|
| Part | Seal holding ring |
| Material | Mild steel |
| Quantity | 1 |
| PartNr | c-9 |

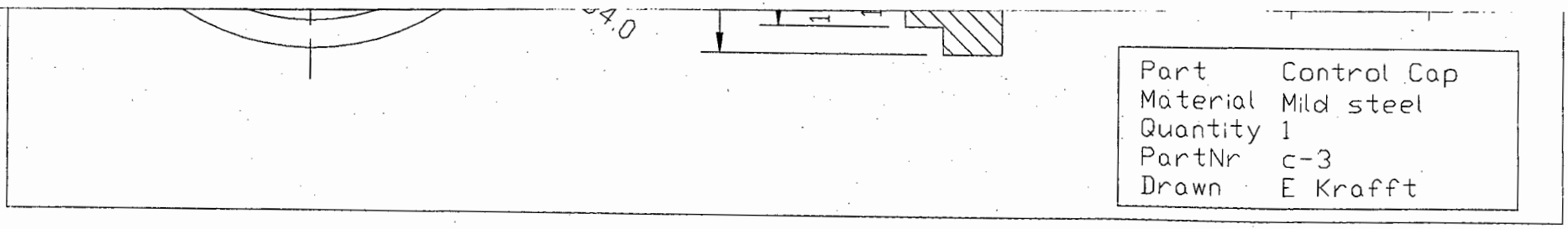

| | |
|---|---|
| Part | Control Cap |
| Material | Mild steel |
| Quantity | 1 |
| PartNr | c-3 |
| Drawn | E Krafft |

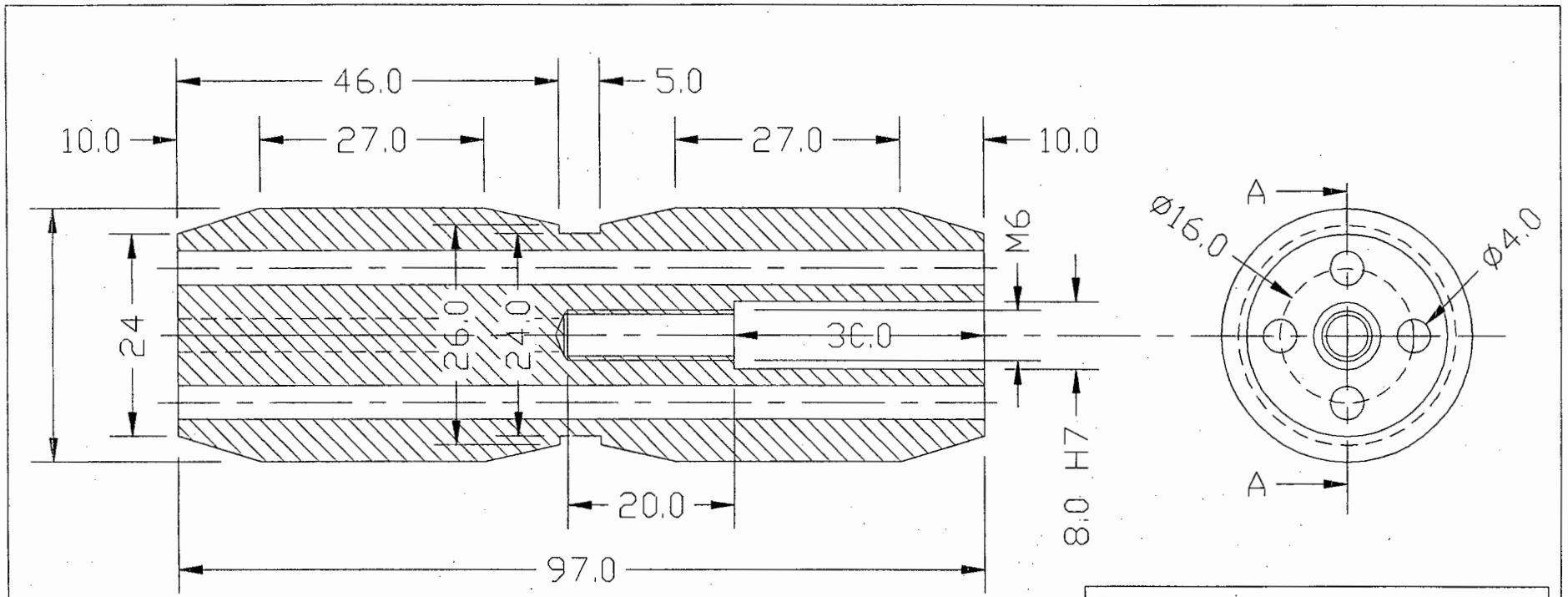


Section A-A

| | |
|---|---|
| Part | Control core |
| Material | Stainless steel |
| Qty | 1 |
| PartNr | c-4 |
| Drawn | E Krafft |

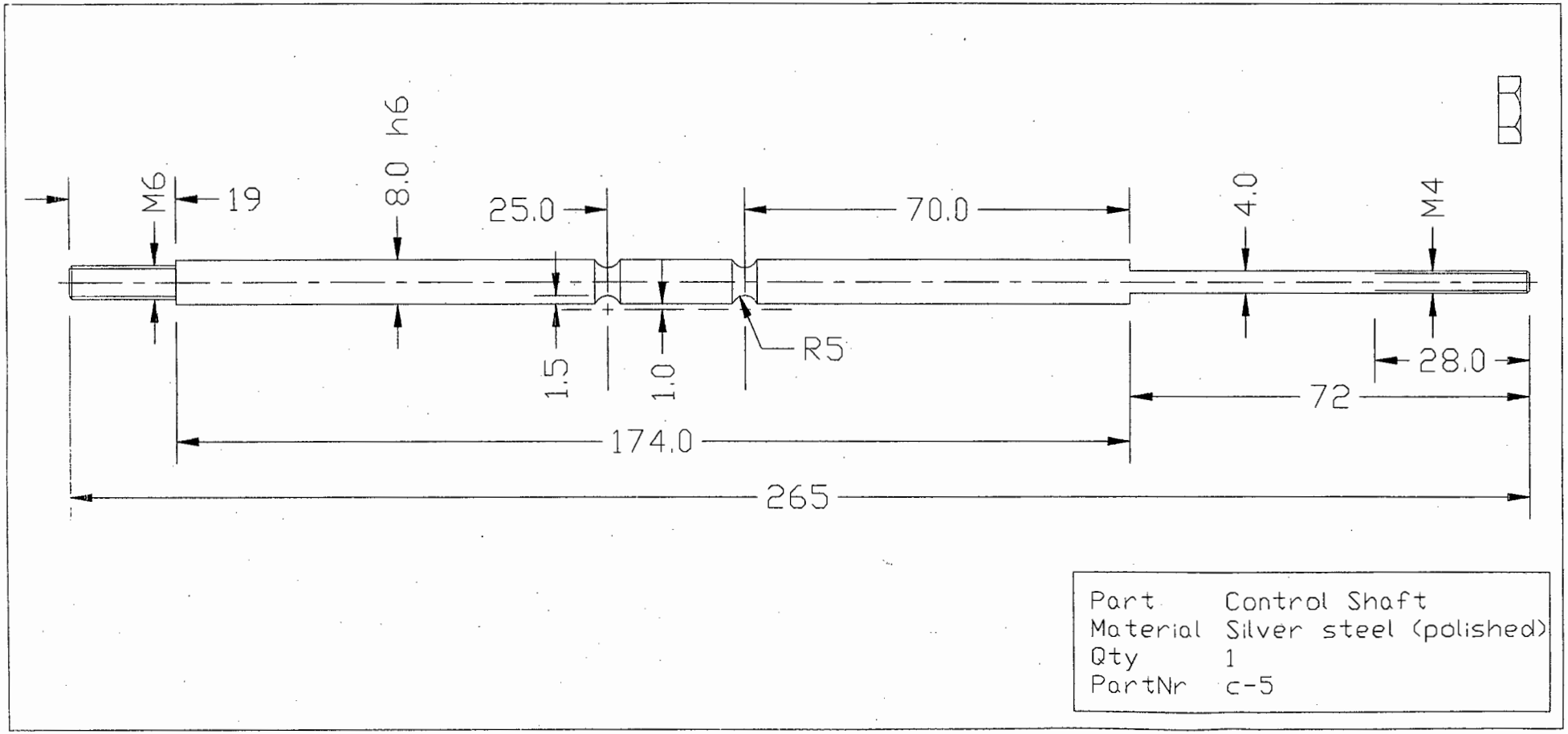
M6
19
8.0 h6
25.0
70.0
4.0
M4
1.5
1.0
R5
28.0
72
174.0
265
Part Control Shaft
Material Silver steel (polished)
Qty 1
PartNr c-5

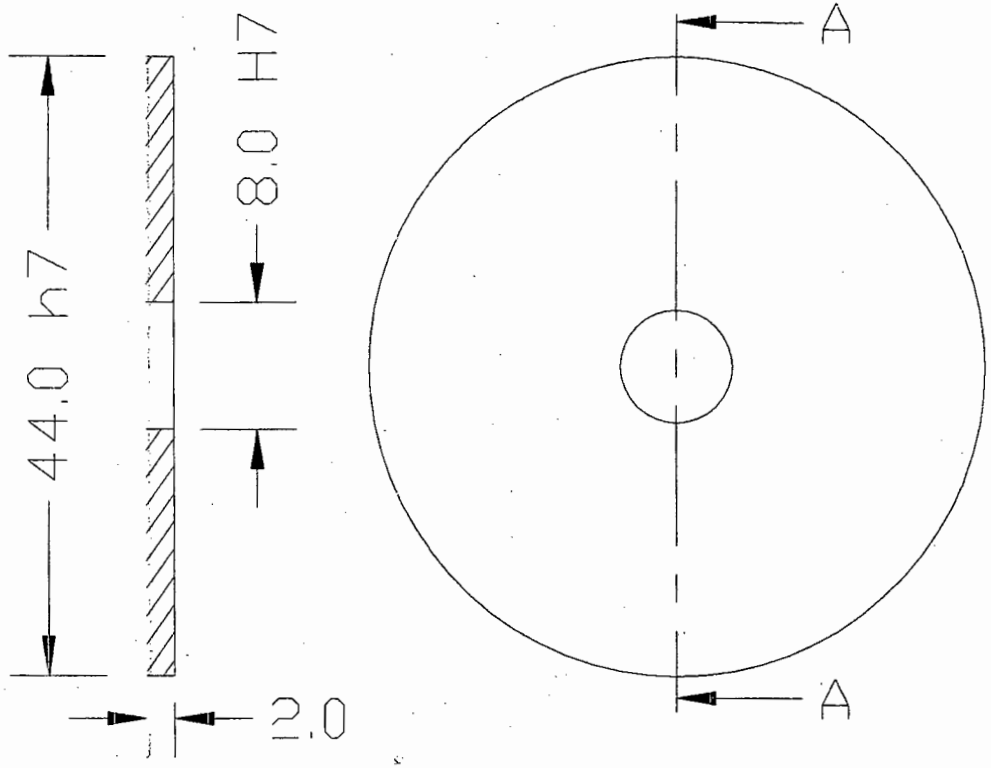


Section A-A

| | |
|---|---|
| Part | Seal holding ring |
| Material | Steel |
| Quantity | 1 |
| PartNr | c-9 |

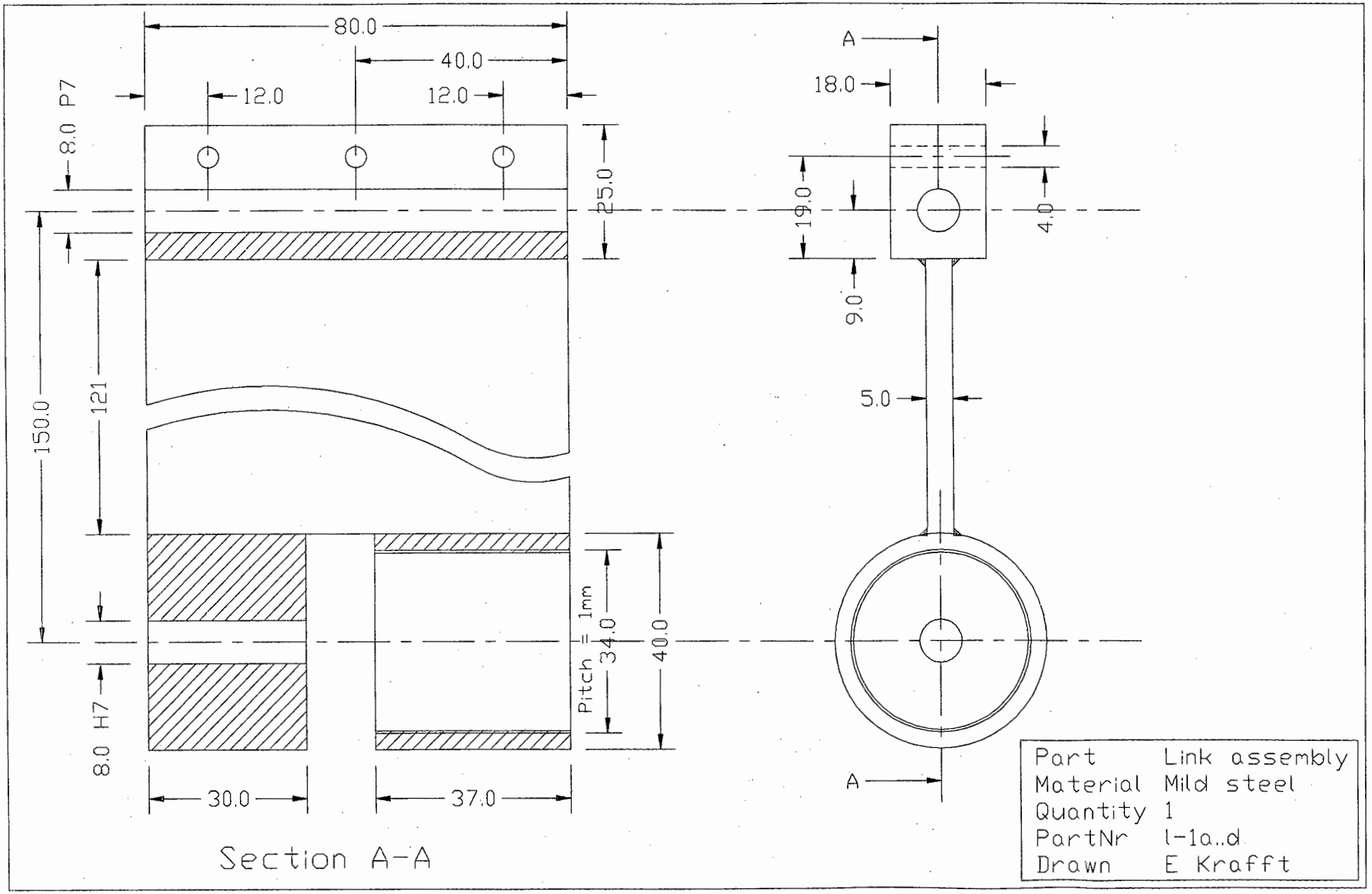
80.0
40.0
12.0
12.0
8.0 P7
25.0
150.0
121
8.0 H7
30.0
37.0
Pitch ± 1mm
34.0
40.0
A
18.0
19.0
9.0
4.0
5.0
A
Section A-A
Part Link assembly
Material Mild steel
Quantity 1
PartNr l-1a..d
Drawn E Krafft

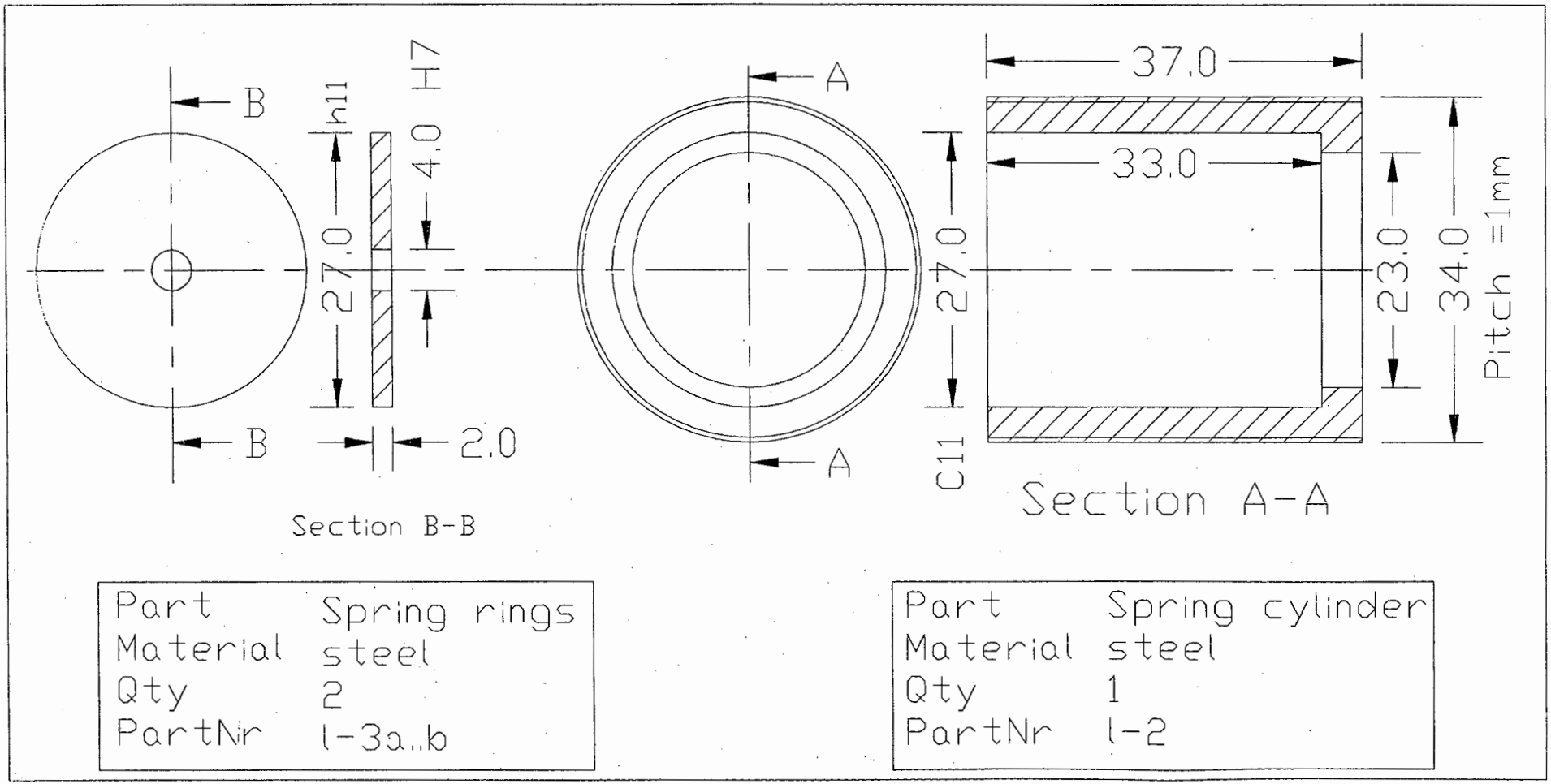


| | |
|---|---|
| Part | Spring rings |
| Material | steel |
| Qty | 2 |
| PartNr | 1-3a..b |

| | |
|---|---|
| Part | Spring cylinder |
| Material | steel |
| Qty | 1 |
| PartNr | 1-2 |

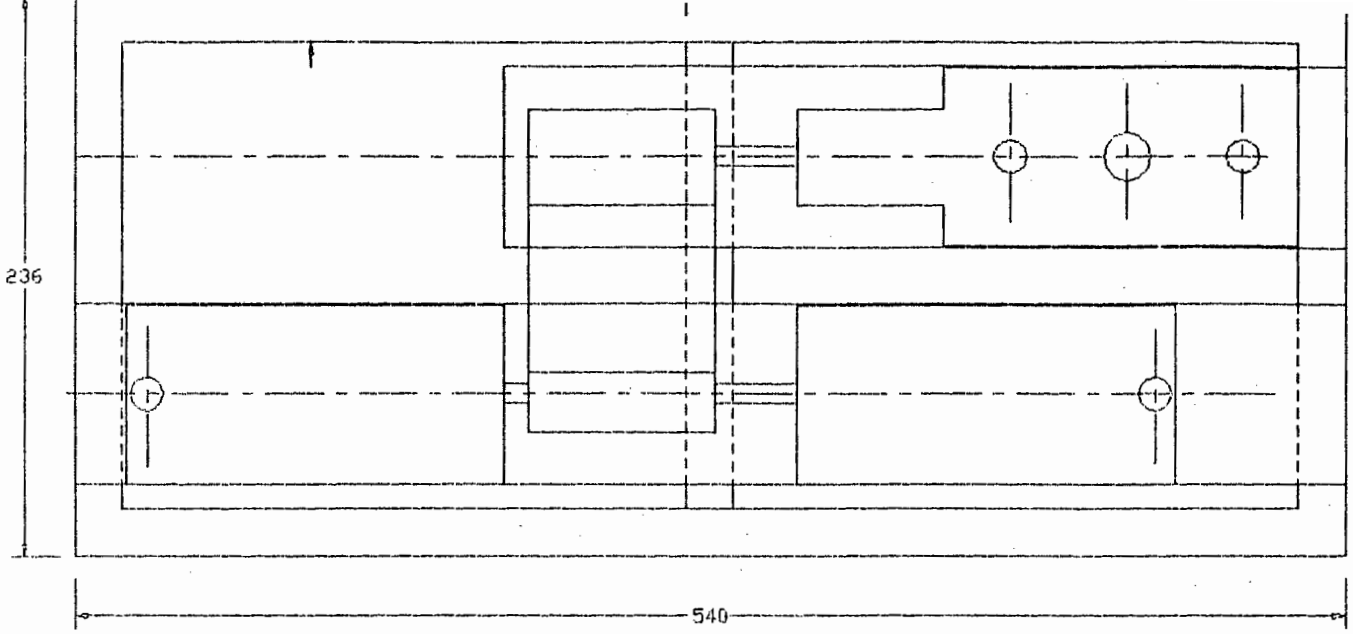


top view

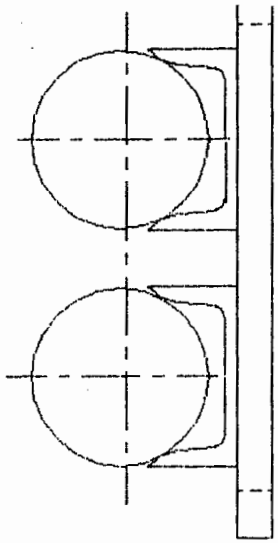

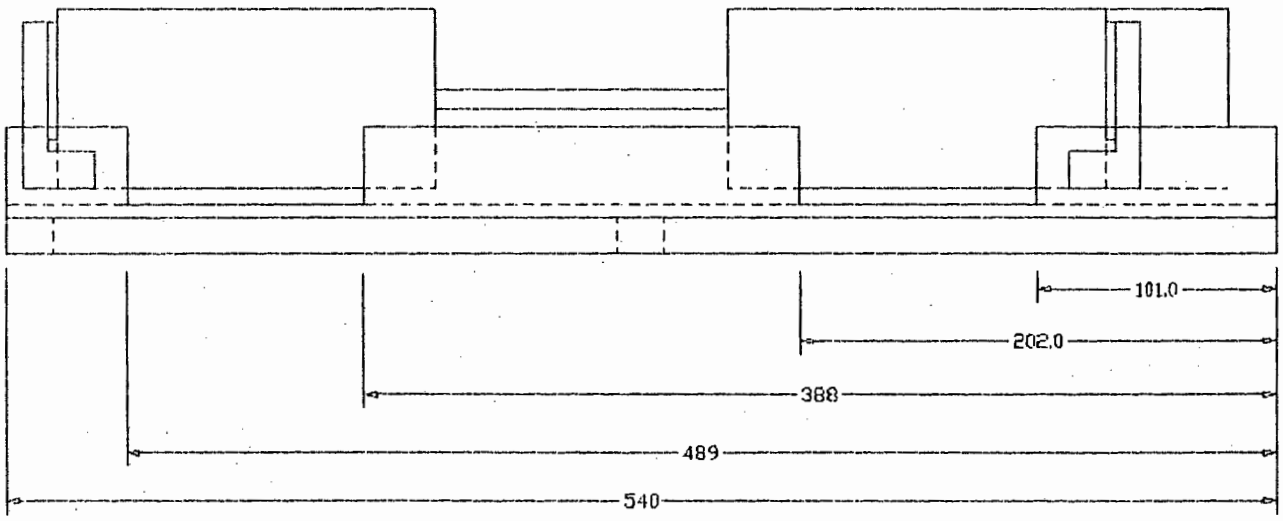


Side view

Base plate - Pump Assembly

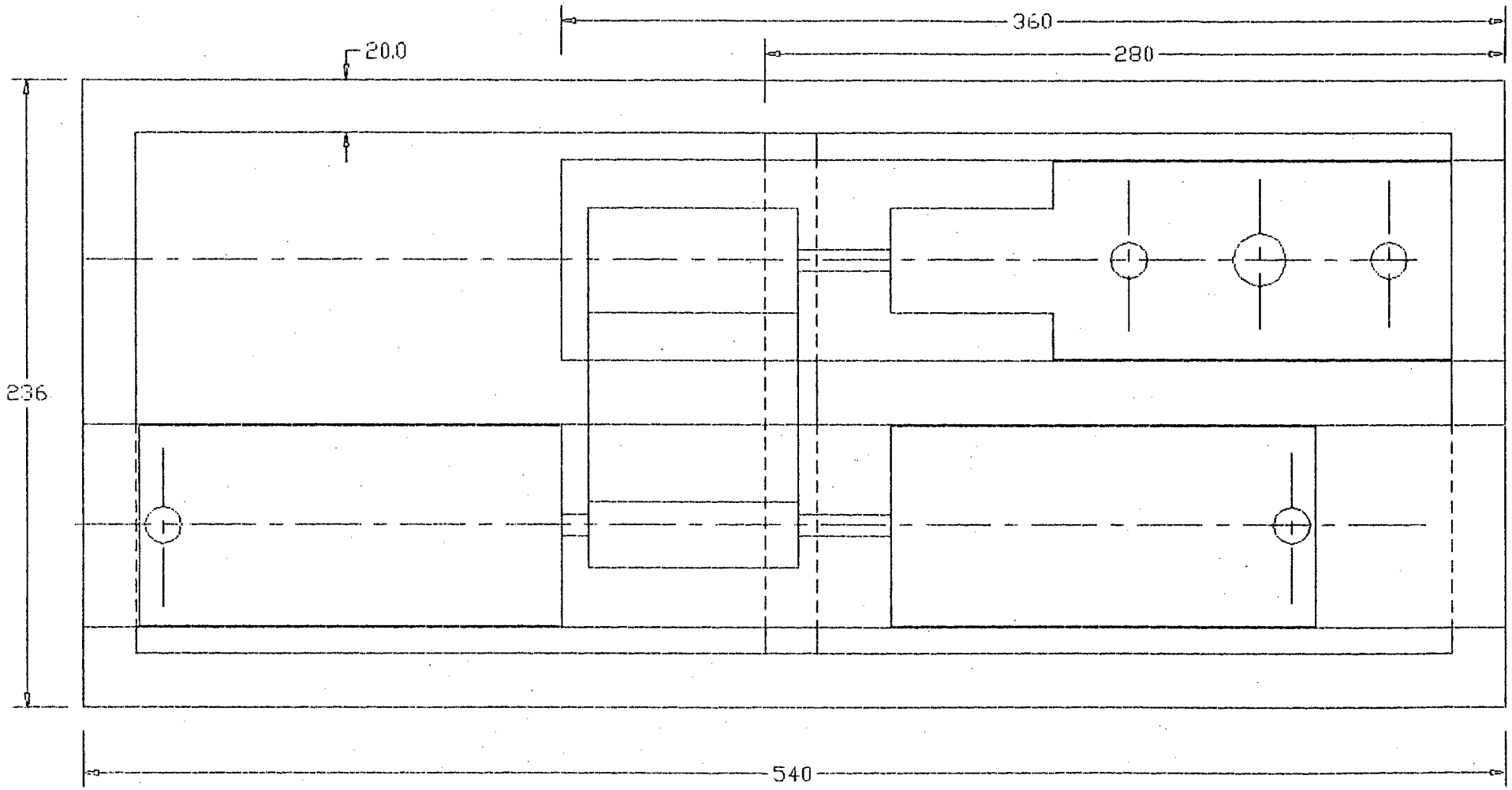


Base Plate - Pump Assembly - top view

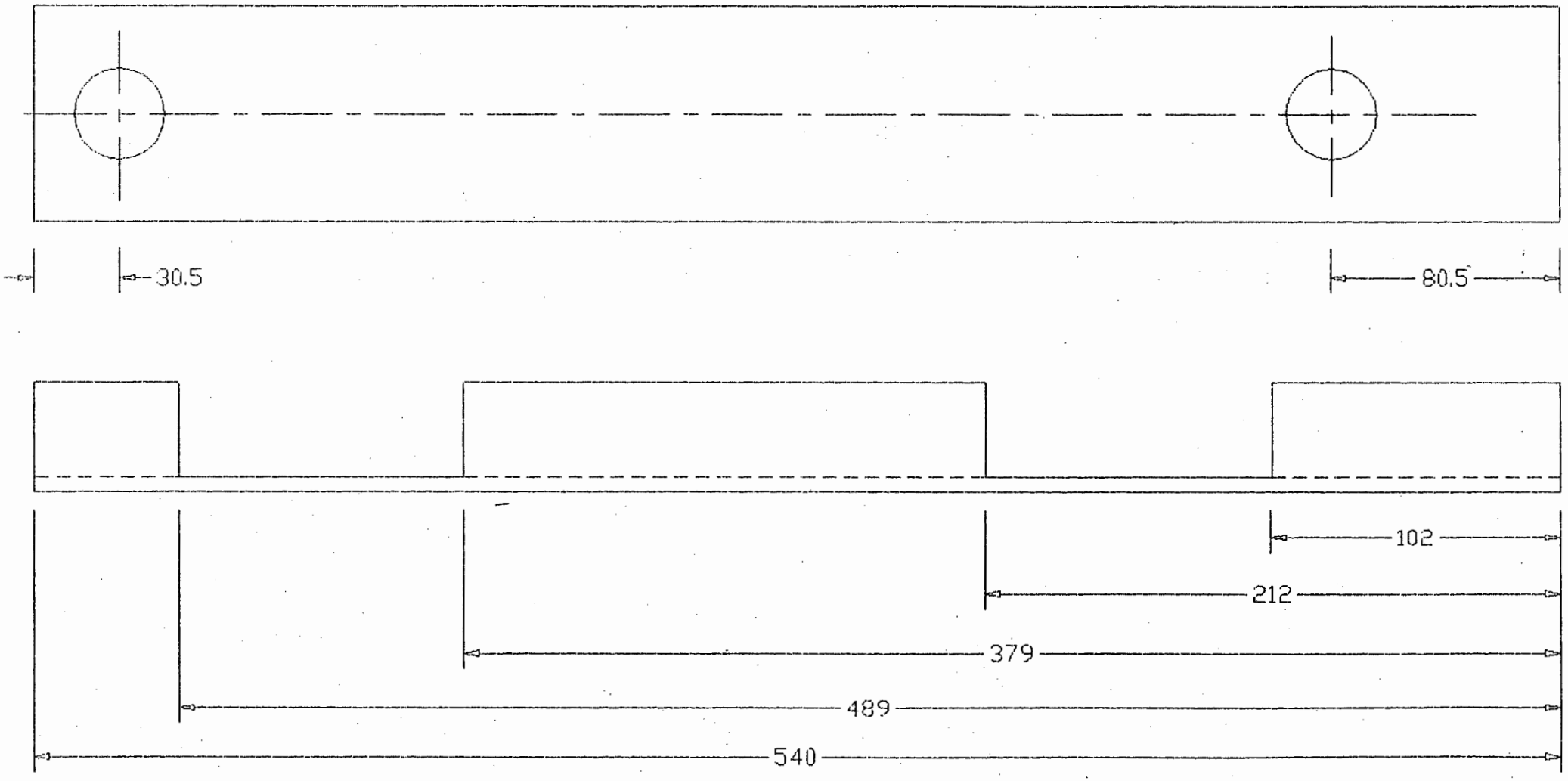


Base plate Channel

# Appendix E

## Seal specifications

Figure E.1 shows the location of seals.

Tables E.1 to E.6 (obtained from Bearing Man, Cape Town) were taken as guidelines for the groove dimensions.

The groove dimensions are calculated as follows:

*for piston grooves*

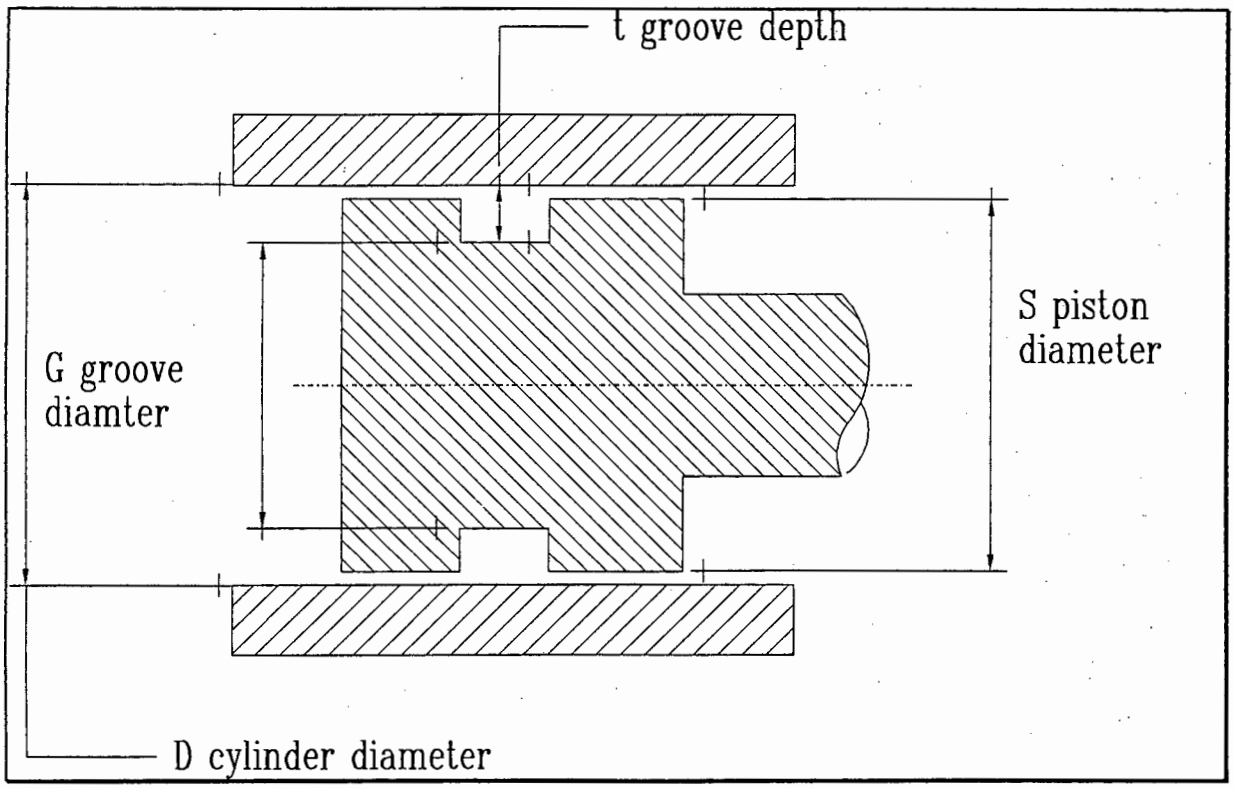


the groove diameter

$$G_{min} = D_{max} - 2t_{max}$$

$$G_{max} = D_{min} - 2t_{min}$$

*and for cylinder grooves*

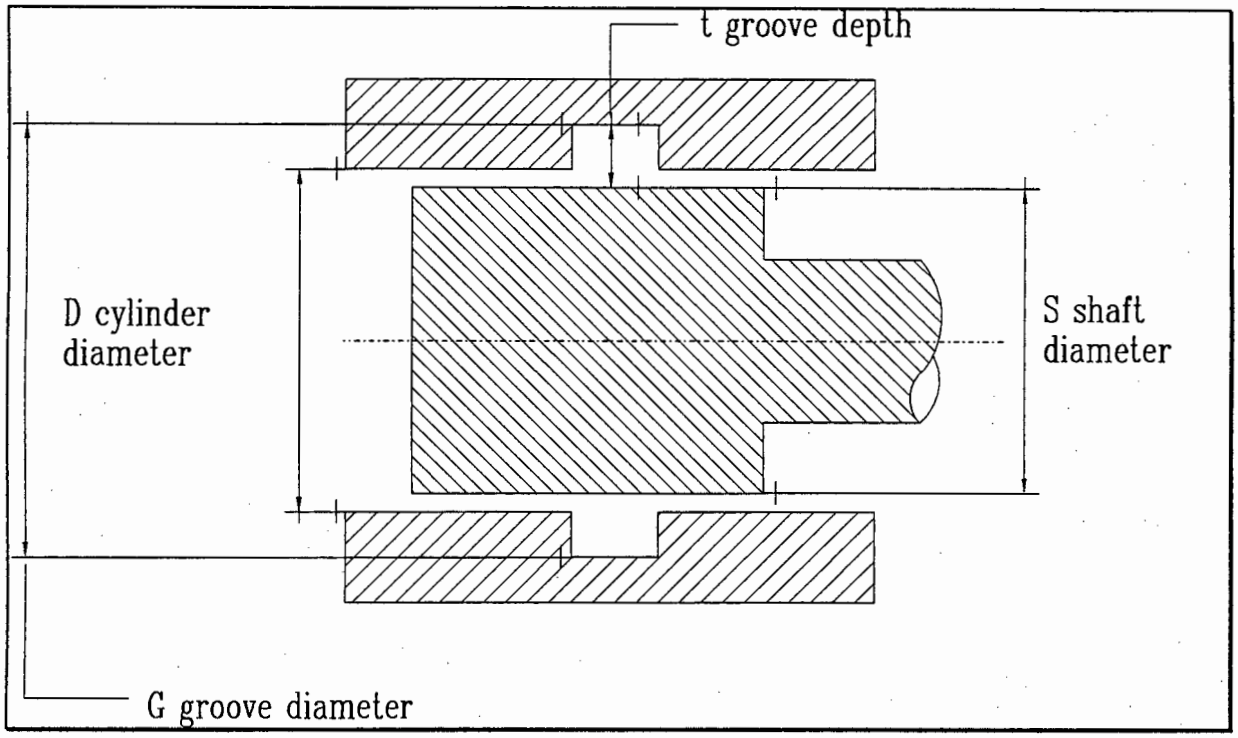


the groove diameter

$$G_{min} = S_{max} + 2t_{min}$$

$$G_{max} = S_{min} + 2t_{max}$$

Only British Standard (BS) O-rings were selected. EPDM seals are not readily available in other sizes. The reference surface (cylinder diameter D in piston grooves and shaft diameter S in cylinder grooves) are specified to a IT7 tolerance grade.

| tolerance grade | nominal size (mm) | tolerance (mm) |
|---|---|---|
| IT7 | 18 - 30 | 0.021 |
| IT7 | 30 - 50 | 0.025 |

Various O-ring handbooks give different guidelines on the diametrical clearance between the moving parts. Generally, the smaller the clearance the smaller the likelihood of ring failure by extrusion. A diametrical clearance of 50 to 150

µm, as specified for the pump, is on the conservative side and satisfies most guidelines. Using above information and tables the seal dimensions were specified as follows.

Seal material: ethylene propylene (EPDM)

| Ring nr | BS nr | ID (mm) | d (mm) | D (mm) | S (mm) | G (mm) | b (mm) | t (mm) |
|---|---|---|---|---|---|---|---|---|
| 1 | 826 | 42.86 | 3.53 | 50.00<br>50.03 | 49.88<br>49.95 | 43.53<br>43.60 | 4.2 | 3.20<br>3.25 |
| 2 | 616 | 15.08 | 2.62 | 20.00<br>20.02 | 19.88<br>19.95 | 15.32<br>15.40 | 3.1 | 2.30<br>2.35 |
| 3 | 136 | 50.47 | 2.62 | 56.00<br>56.03 | 55.90<br>55.95 | 51.60<br>51.80 | 3.4 | 2.10<br>2.22 |
| 4 | 116 | 18.72 | 2.62 | 20.00<br>20.02 | 19.88<br>19.95 | 24.55<br>24.58 | 3.1 | 2.30<br>2.32 |
| 5 | 025 | 29.87 | 1.78 | 30.62<br>30.65 | 30.50<br>30.57 | 33.57<br>33.60 | 2.3 | 1.50<br>1.55 |

Ring nr as indicated on figure E.1
BS = British standard
ID = internal ring diameter
d = ring crosssection diameter
D = cylinder diameter
S = shaft diameter
G = groove diameter
b = groove width
t = groove depth

For the working pressures involved (up to 12 bar) extrusion of the O-rings is unlikely to occur. Should this mode of failure however be observed, back-up rings are required. For no back-up rings a fillet radius in the groove of r = 0.5 max is specified. Where back-up rings are used the groove can have sharp edges and a square profile.

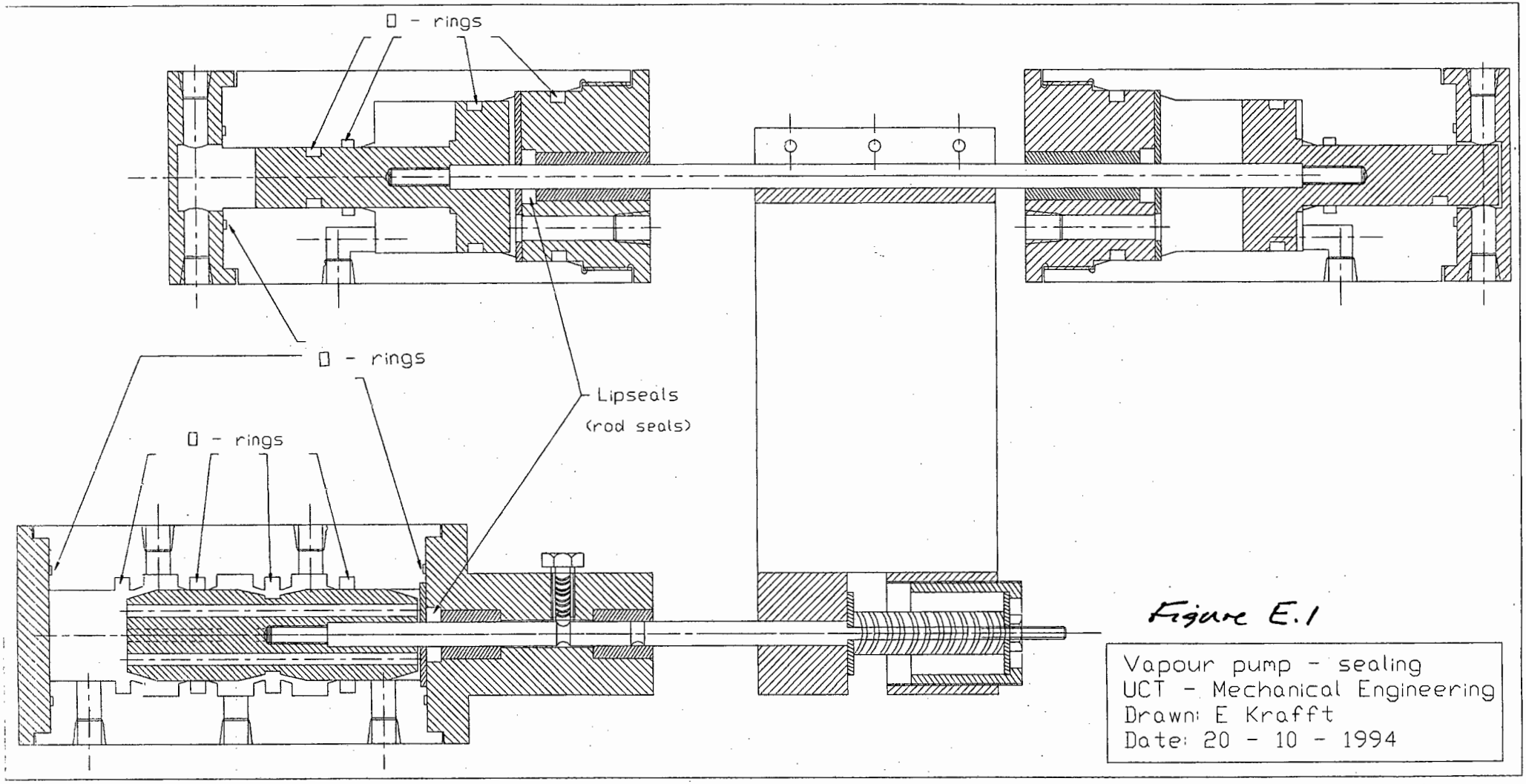


Figure E.1

Vapour pump - sealing
UCT - Mechanical Engineering
Drawn: E Krafft
Date: 20 - 10 - 1994

O-Rings are moulded sealing rings with extremely accurate measurements. Shape, material, hardness, sizes and tolerances are laid down as per DIN-Standards 3770 resp. DIN ISO 3601.

## Indication of sizes

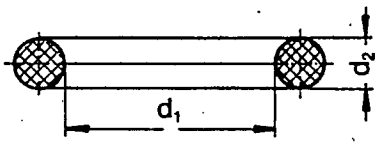


$d_1$ — inside diameter in mm

$d_2$ — section diameter in mm

Compounds and their abbreviations as per DIN

- NB Nitrile-Butadiene-Rubber
- AC Acrylate-Rubber
- SI Silicone-Rubber
- FP Fluorocarbon-Rubber
- EP Ethylene-Propylene-Rubber
- CR Chloroprene-Rubber
- SB Styrol-Butadiene-Rubber
- BU Butyl-Rubber
- NR Natural Rubber
- FS Fluorosilicone-Rubber

Hardness of compounds is either indicated according to Shore A or to IRHD. Standard hardness is 70 Shore A resp. 73 IRHD.

| Hardness Shore A | 60 | 70 | 80 | 90 |
|---|---|---|---|---|
| Hardness IRHD | 63 | 73 | 83 | 92 |
| Allowed deviation ± 5<br>Testing method of hardness acc. to DIN 53 505 resp. DIN 53519 | | | | |

Table E.1

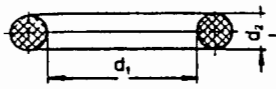


Dimensions of O-Rings have been published in various German and International Standards. Besides, there exists a variety of non-standard sizes (see catalogue pages 17—28).

Approved tolerances reflected in the index shown opposite refer to the compound Nitrile-Butadiene-Rubber in 70 Shore A resp. 73 IRHD.

Other compounds, however, vary considerably in their shrinkage rates and when produced from the same tooling are likely to come out with a wider tolerance. Special tooling can, of course, always be manufactured to produce to exact sizes where application demands such accuracy.

| $d_1$ | ± tolerance | $d_2$ | ± tolerance |
|---|---|---|---|
| - 3 | 0,14 | - 1,8 | 0,08 |
| 3 - 6 | 0,15 | 1,8 - 2,6 | 0,09 |
| 6 - 10 | 0,17 | 2,6 - 3,5 | 0,10 |
| 10 - 18 | 0,20 | 3,5 - 5,3 | 0,13 |
| 18 - 30 | 0,30 | 5,3 - 7 | 0,15 |
| 30 - 50 | 0,40 | 7 - 8 | 0,17 |
| 50 - 80 | 0,65 | 8 - 10 | 0,20 |
| 80 - 100 | 0,85 | 10 - 15 | 0,25 |
| 100 - 120 | 1,0 | | |
| 120 - 150 | 1,2 | | |
| 150 - 180 | 1,4 | | |
| 180 - 250 | 1,8 | | |
| 250 - 300 | 2,1 | | |
| 300 - 350 | 2,5 | | |
| 350 - 400 | 2,8 | | |
| 400 - 500 | 3,4 | | |
| 500 - 650 | 4,3 | | |
| 650 - 800 | 6,5 | | |

TABLE E.2

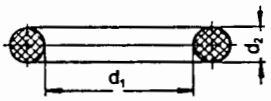


Deficiencies normally experienced with O-Rings are shown in the index. We differentiate between two type characteristics.

Type characteristic N

These O-Rings represent our standard quality which comply with high quality requirements and cover day to day application.

Type characteristic S

These O-Rings find their field of application in cases of extremely high requirements regarding the surface finish, naturally, resulting in higher production and controlling expenses.

Staggered

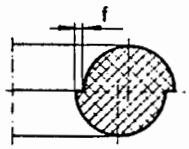


Extent of flash

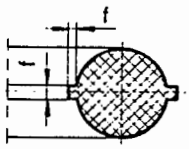


Notches

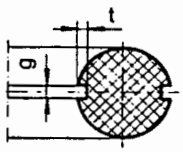


Deburring width

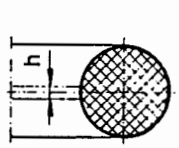


Flow lines

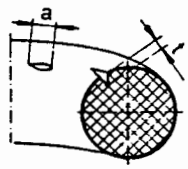


Other deficiencies:

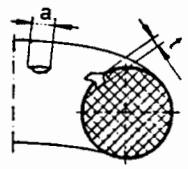


| Deficiency | | | Type characteristics | Permissible extent of deficiency for section $d_2$ | |
|---|---|---|---|---|---|
| | | | | up to 2,65 | >2,65 |
| Staggered partition line, Extent of flash | | f | N<br>S | 0,06<br>0,05 | 0,12<br>0,09 |
| Notches | width<br>depth | g<br>t | N | $0,1 \cdot d_2$<br>0,05 | $0,1 \cdot d_2$<br>0,09 |
| | width<br>depth | g<br>t | S | $0,05 \cdot d_2$<br>0,05 | $0,05 \cdot d_2$<br>0,09 |
| Deburring width (excess amounts permissible, too, provided that tolerance of section is adhered to and surface remains smooth) | | h | N<br>S | 0,4<br>0,4 | 1,2<br>0,7 |
| Flow lines in circumferential direction | thickness<br>depth | a<br>t | N | $0,1 \cdot d_1$<br>0,03 | $0,1 \cdot d_1$<br>0,06 |
| | thickness<br>depth | a<br>t | S | $0,05 \cdot d_1$<br>0,03 | $0,05 \cdot d_1$<br>0,06 |
| Other deficiencies: air-pockets, bubbles, pores, excess rubber, etc. | thickness<br>depth | a<br>t | N | $0,3 \cdot d_2$<br>0,05 | $0,3 \cdot d_2$<br>0,09 |
| | thickness<br>depth | a<br>t | S | $0,1 \cdot d_2$<br>0,03 | $0,1 \cdot d_2$<br>0,06 |
| Surface roughness $R_t$ | | µm | N<br>S | 10<br>5 | 16<br>8 |
| Spots | | | N<br>S | permissible<br>permissible | |

The one and only difference in the two characteristics is the extent of accuracy permissible, whilst tolerances in measurements are identical.

The extent of accuracy as per illustrations determines the extensity of controls in the production and finishing process. This applies to both, the manufacturer and the applicant.

TABLE E.3

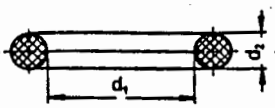


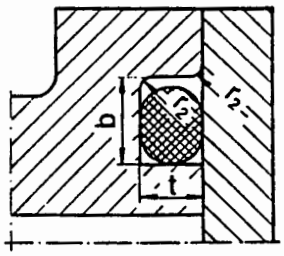


The measurement »b«, which is the width of the O-Ring groove, has to be larger than the deformed O-Ring. Depending upon application the groove may be open on one side. However, the pressure applied to the medium to be sealed must have full access to the O-Ring. The surfaces of the groove and the opposed surfaces should have more or less rounded processing traces to permit peak-to-valley-heights of 44 — 25 $\mu$m.

Groove sizes
Static application

| $d_2$ | t | b |
|---|---|---|
| 1 | 0,8 | 1,3 |
| 1,5 | 1,1 | 1,9 |
| 1,6 | 1,2 | 2,1 |
| 1,78 | 1,3 | 2,3 |
| 1,9 | 1,4 | 2,4 |
| 2 | 1,5 | 2,6 |
| 2,4 | 1,8 | 3,1 |
| 2,5 | 1,9 | 3,2 |
| 2,62 | 2,0 | 3,4 |
| 2,7 | 2,1 | 3,5 |
| 3 | 2,3 | 3,9 |
| 3,5 | 2,7 | 4,5 |
| 3,53 | 2,7 | 4,5 |
| 3,6 | 2,8 | 4,7 |
| 4 | 3,15 | 5,2 |
| 4,5 | 3,6 | 5,8 |

| $d_2$ | t | b |
|---|---|---|
| 5 | 4 | 6,5 |
| 5,33 | 4,3 | 6,9 |
| 5,5 | 4,5 | 7,1 |
| 5,7 | 4,65 | 7,4 |
| 6 | 4,95 | 7,8 |
| 6,5 | 5,4 | 8,4 |
| 6,99 | 5,85 | 9,1 |
| 7 | 5,85 | 9,1 |
| 7,5 | 6,3 | 9,7 |
| 8 | 6,75 | 10,4 |
| 8,4 | 7,15 | 10,9 |
| 8,5 | 7,25 | 11,0 |
| 9 | 7,7 | 11,7 |
| 9,5 | 8,2 | 12,3 |
| 10 | 8,65 | 13 |

In case of applying back-up rings the width of groove »b« is increased by the width of the back-up ring resp. in case of support on either side by the double width of the back-up ring.

TABLE E.4

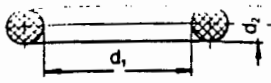


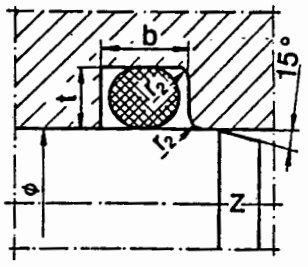


Groove sizes
Dynamic application — Hydraulics

| $d_2$ | t | b | z |
|---|---|---|---|
| 1 | 0,9 | 1,3 | 1 |
| 1,5 | 1,3 | 1,9 | 1 |
| 1,6 | 1,4 | 2 | 1,1 |
| 1,78 | 1,5 | 2,3 | 1,1 |
| 1,9 | 1,6 | 2,4 | 1,2 |
| 2 | 1,7 | 2,4 | 1,2 |
| 2,4 | 2,1 | 2,9 | 1,4 |
| 2,5 | 2,2 | 3 | 1,4 |
| 2,62 | 2,3 | 3,1 | 1,5 |
| 2,7 | 2,4 | 3,2 | 1,5 |
| 3 | 2,6 | 3,6 | 1,6 |
| 3,5 | 3,1 | 4,2 | 1,8 |
| 3,53 | 3,1 | 4,2 | 1,8 |
| 3,6 | 3,2 | 4,3 | 1,8 |
| 4 | 3,5 | 4,8 | 2 |
| 4,5 | 4 | 5,4 | 2,3 |

| $d_2$ | t | b | z |
|---|---|---|---|
| 5 | 4,45 | 6 | 2,5 |
| 5,33 | 4,7 | 6,4 | 2,7 |
| 5,5 | 4,95 | 6,6 | 2,8 |
| 5,7 | 5,1 | 6,9 | 3 |
| 6 | 5,4 | 7,2 | 3,1 |
| 6,5 | 5,8 | 7,8 | 3,3 |
| 6,99 | 6,3 | 8,4 | 3,6 |
| 7 | 6,3 | 8,4 | 3,6 |
| 7,5 | 6,7 | 9 | 3,8 |
| 8 | 7,2 | 9,6 | 4 |
| 8,4 | 7,6 | 10,1 | 4,2 |
| 8,5 | 7,7 | 10,2 | 4,2 |
| 9 | 8,2 | 10,8 | 4,3 |
| 9,5 | 8,6 | 11,4 | 4,4 |
| 10 | 9,1 | 12 | 4,5 |

Groove sizes
Dynamic application — Pneumatics

| $d_2$ | t | b | z |
|---|---|---|---|
| 1 | 0,95 | 1,3 | 1 |
| 1,5 | 1,35 | 1,9 | 1 |
| 1,6 | 1,45 | 2 | 1,1 |
| 1,78 | 1,55 | 2,3 | 1,1 |
| 1,9 | 1,75 | 2,4 | 1,2 |
| 2 | 1,8 | 2,4 | 1,2 |
| 2,4 | 2,15 | 2,9 | 1,4 |
| 2,5 | 2,25 | 3 | 1,4 |
| 2,62 | 2,35 | 3,1 | 1,5 |
| 2,7 | 2,45 | 3,3 | 1,5 |
| 3 | 2,75 | 3,6 | 1,6 |
| 3,5 | 3,25 | 4,2 | 1,8 |
| 3,53 | 3,25 | 4,2 | 1,8 |
| 3,6 | 3,35 | 4,3 | 1,8 |
| 4 | 3,7 | 4,8 | 2 |
| 4,5 | 4,2 | 5,4 | 2,3 |

| $d_2$ | t | b | z |
|---|---|---|---|
| 5 | 4,65 | 6 | 2,5 |
| 5,33 | 4,95 | 6,4 | 2,7 |
| 5,5 | 5,15 | 6,6 | 2,8 |
| 5,7 | 5,35 | 6,9 | 3 |
| 6 | 5,65 | 7,2 | 3,1 |
| 6,5 | 6,1 | 7,8 | 3,3 |
| 6,99 | 6,6 | 8,4 | 3,6 |
| 7 | 6,6 | 8,4 | 3,6 |
| 7,5 | 7,1 | 9 | 3,8 |
| 8 | 7,6 | 9,6 | 4 |
| 8,4 | 7,9 | 10,1 | 4,2 |
| 8,5 | 8 | 10,2 | 4,2 |
| 9 | 8,5 | 10,8 | 4,3 |
| 9,5 | 9 | 11,4 | 4,4 |
| 10 | 9,5 | 12 | 4,5 |

In case of applying back-up rings the width of groove »b« is increased by the width of the back-up ring resp. in case of support on either side by the double width of the back-up ring.

TABLE E.5

Dichtomatik-Compounds for O-Rings

| Elastomer | DIN-Abbrev. | Comp.-No. | Hardn. Shore A | Hardn. IRHD | Colour | Special Field of Application/ Characteristics |
|---|---|---|---|---|---|---|
| Nitrile-Butadiene-Rubber | NB | 0106 | 55 | 57 | black | |
| " | NB | 1015 | 60 | 63 | black | |
| " | NB | 1009 | 70 | 73 | black | |
| " | NB | 1008 | 75 | 78 | black | |
| " | NB | 1023 | 80 | 83 | black | |
| " | NB | 1026 | 90 | 92 | black | |
| " | NB | 1011 | 70 | 73 | grey | food applic. |
| " | NB | 1010 | 70 | 73 | black | low temp. |
| " | NB | 1007 | 70 | 73 | black | non-sulfurous |
| " | NB | 1004 | 70 | 73 | black | super gasoline |
| " | NB | 1019 | 80 | 83 | grey | food applic. |
| " | NB | 1021 | 80 | 83 | black | low temp. |
| " | NB | 1018 | 80 | 83 | black | non-sulfurous |
| " | NB | 1020 | 80 | 83 | black | super gasoline |
| Fluorocarbon-Rubber | FP | 0712 | 60 | 63 | black | |
| " | FP | 7018 | 70 | 73 | black | |
| " | FP | 7027 | 80 | 83 | black | |
| " | FP | 7032 | 90 | 92 | black | |
| " | FP | 7019 | 70 | 73 | green | |
| " | FP | 7028 | 80 | 83 | green | |
| " | FP | 7016 | 75 | 78 | red | |
| " | FP | 7015 | 75 | 78 | brown | with lead oxide |
| Silicone | SI | 0804 | 50 | 52 | red-brown | |
| " | SI | 8007 | 60 | 63 | red-brown | |
| " | SI | 8008 | 70 | 73 | red-brown | |
| " | SI | 8006 | 80 | 83 | red-brown | |
| Ethylene-Propylene-Rubber | EP | 0305 | 75 | 78 | black | |
| " | EP | 3007 | 80 | 83 | black | |
| " | EP | 3004 | 85 | 88 | black | |
| Chloroprene-Rubber | CR | 0207 | 50 | 52 | black | non-sulfurous |
| " | CR | 2005 | 60 | 63 | black | |
| " | CR | 2010 | 70 | 73 | black | |
| " | CR | 2014 | 70 | 73 | black | frigen-resistant |
| " | CR | 2012 | 90 | 92 | black | |
| Natural Rubber | NR | 0404 | 45 | 47 | black | |
| " | NR | 4001 | 65 | 68 | black | |
| " | NR | 4007 | 80 | 83 | black | |
| Butyl-Rubber | BU | 0504 | 65 | 68 | black | |
| Polyethylene-Rubber sulfonated by Chlorine | CSM | 0601 | 65 | 68 | black | |
| " | CSM | 0602 | 75 | 78 | black | |
| Polytetrafluoro-Ethylene | PTFE | 0910 | | | white | |

Normally available ex stock

TABLE E-6

## Appendix F

### Information on spring plungers

Metric sizes [mm]

| D1 | D2 | E | L1 | l2 | spring force | WDS No |
|---|---|---|---|---|---|---|
| M4 | 2.5 | 0.6 | 9 | 0.8 | 10 N | 606-2704 |
| M5 | 3 | 0.8 | 12 | 0.9 | 11 N | 606-2705 |
| M6 | 3.5 | 1 | 14 | 1 | 13 N | 606-2706 |
| M8 | 5 | 1.2 | 16 | 1.5 | 30 N | 606-2708 |
| M10 | 6 | 1.6 | 19 | 2 | 35 N | 606-2710 |
| M12 | 8 | 2 | 22 | 2.5 | 55 N | 606-2712 |
| M16 | 10 | 2.5 | 24 | 3.5 | 125 N | 606-2716 |

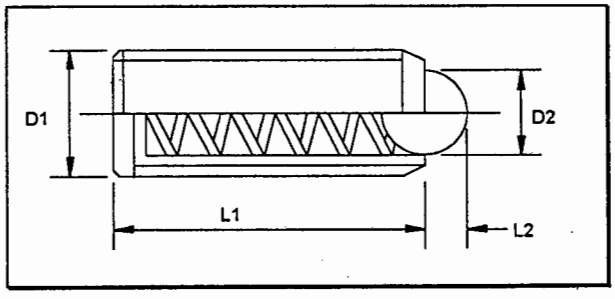

# Appendix G

## Computer generated results as predicted by the simulation

varying evaporator temperature

| Tev, C | -6 | -8 | -10 | -12 | -14 | -16 |
|---|---|---|---|---|---|---|
| Tab, C | 24 | 24 | 24 | 24 | 24 | 24 |
| $T_{Gopt}$, C | 99.6 | 101.2 | 102.8 | 104.5 | 105.2 | 106.4 |
| cop max | 0.488 | 0.480 | 0.472 | 0.465 | 0.457 | 0.447 |
| REF, kW | 1 | 1 | 1 | 1 | 1 | 1 |
| $P_h$, bar | 9.43 | 9.43 | 9.43 | 9.43 | 9.43 | 9.43 |
| $P_l$, bar | 3.21 | 2.96 | 2.72 | 2.50 | 2.30 | 2.10 |
| m6, g/s | 0.88 | 0.87 | 0.86 | 0.85 | 0.85 | 0.84 |
| m7, g/s | 3.49 | 3.64 | 3.82 | 4.01 | 4.32 | 4.61 |
| m8, g/s | 2.44 | 2.60 | 2.78 | 2.97 | 3.28 | 3.56 |
| m16, g/s | 0.17 | 0.17 | 0.18 | 0.19 | 0.20 | 0.21 |
| $x_{we}$, $kg_{ref}/kg_{tot}$ | 0.30 | 0.29 | 0.29 | 0.28 | 0.27 | 0.27 |
| $x_{st}$, $kg_{ref}/kg_{tot}$ | 0.51 | 0.49 | 0.48 | 0.46 | 0.45 | 0.43 |
| Qin, kW | 2.051 | 2.081 | 2.117 | 2.151 | 2.189 | 2.239 |
| H11, kJ/kg | 1448.7 | 1461.0 | 1472.4 | 1481.7 | 1488.8 | 1498.7 |
| Q8, kW | 0.601 | 0.665 | 0.739 | 0.823 | 0.922 | 1.033 |
| Q10, kW | 0.105 | 0.146 | 0.201 | 0.268 | 0.352 | 0.441 |
| Q11, kW | 1.314 | 1.313 | 1.319 | 1.327 | 1.332 | 1.343 |
| Q12, kW | 0.003 | 0.004 | 0.005 | 0.007 | 0.008 | 0.010 |
| Q16, kW | 0.243 | 0.253 | 0.265 | 0.277 | 0.295 | 0.313 |
| Win, kW | 0.0185 | 0.0194 | 0.0214 | 0.0235 | 0.0257 | 0.0279 |
| Wout, kW | 0.0019 | 0.0021 | 0.0023 | 0.0025 | 0.0027 | 0.0030 |
| p-eff, % | 10.6 | 10.6 | 10.7 | 10.7 | 10.9 | 10.9 |
| tp-eff, % | 0.79 | 0.82 | 0.86 | 0.89 | 0.93 | 0.97 |
| $F_{right}$, N | 3458 | 3451 | 3444 | 3437 | 3431 | 3425 |
| $F_{left}$, N | 1439 | 1350 | 1266 | 1187 | 1114 | 1046 |
| $F_{vap}$, N | 2214 | 2304 | 2388 | 2467 | 2541 | 2610 |
| $F_{sol}$, N | 195 | 203 | 211 | 218 | 224 | 230 |
| $F_{net}$, N | 2019 | 2101 | 2178 | 2250 | 2317 | 2379 |
| freq, Hz | 0.163 | 0.169 | 0.177 | 0.185 | 0.198 | 0.210 |
| $D_{vap}$, mm | 50 | 50 | 50 | 50 | 50 | 50 |
| $D_{sol}$, mm | 20 | 20 | 20 | 20 | 20 | 20 |

varying evaporator temperature (cont.)

| Tev, C | -18 | -20 | -22 |
|---|---|---|---|
| Tab, C | 24 | 24 | 24 |
| $T_{Gopt}$, C | 107.7 | 101.2 | 102.8 |
| cop max | 0.434 | 0.480 | 0.472 |
| REF, kW | 1 | 1 | 1 |
| $P_h$, bar | 9.43 | 9.43 | 9.43 |
| $P_l$, bar | 1.92 | 1.76 | 1.60 |
| m6, g/s | 0.84 | 0.84 | 0.83 |
| m7, g/s | 4.93 | 3.71 | 4.01 |
| m8, g/s | 3.87 | 2.70 | 2.99 |
| m16, g/s | 0.22 | 0.17 | 0.18 |
| $x_{we}$, $kg_{ref}/kg_{tot}$ | 0.26 | 0.19 | 0.19 |
| $x_{st}$, $kg_{ref}/kg_{tot}$ | 0.42 | 0.40 | 0.39 |
| Qin, kW | 2.302 | 2.346 | 2.398 |
| H11, kJ/kg | 1510.7 | 1564.2 | 1573.4 |
| Q8, kW | 1.160 | 1.100 | 1.214 |
| Q10, kW | 0.537 | 0.453 | 0.546 |
| Q11, kW | 1.357 | 1.458 | 1.472 |
| Q12, kW | 0.012 | 0.024 | 0.027 |
| Q16, kW | 0.333 | 0.266 | 0.285 |
| Win, kW | 0.0301 | 0.0245 | 0.0266 |
| Wout, kW | 0.0033 | 0.0026 | 0.0028 |
| p-eff, % | 11.1 | 10.5 | 10.6 |
| tp-eff, % | 1.0 | 0.96 | 0.99 |
| $F_{right}$, N | 3420 | 3415 | 3410 |
| $F_{left}$, N | 982 | 922 | 867 |
| $F_{vap}$, N | 2674 | 2733 | 2789 |
| $F_{sol}$, N | 236 | 241 | 246 |
| $F_{net}$, N | 2428 | 2492 | 2543 |
| freq, Hz | 0.223 | 0.177 | 0.190 |
| $D_{vap}$, mm | 50 | 50 | 50 |
| $D_{sol}$, mm | 20 | 20 | 20 |

varying absorber (condenser temperature)

| Tev, C | -10 | -10 | -10 | -10 | -10 |
|---|---|---|---|---|---|
| Tab, C | 20 | 22 | 24 | 26 | 28 |
| $T_{Gopt}$, C | 95.1 | 98.2 | 102.8 | 107.5 | 110.6 |
| cop max | 0.506 | 0.488 | 0.472 | 0.458 | 0.443 |
| REF, kW | 1 | 1 | 1 | 1 | 1 |
| $P_h$, bar | 8.28 | 8.84 | 9.43 | 10.04 | 10.68 |
| $P_l$, bar | 2.72 | 2.72 | 2.72 | 2.72 | 2.72 |
| m6, g/s | 0.86 | 0.86 | 0.86 | 0.86 | 0.86 |
| m7, g/s | 3.38 | 3.65 | 3.82 | 4.00 | 4.32 |
| m8, g/s | 2.38 | 2.62 | 2.78 | 2.94 | 3.24 |
| m16, g/s | 0.15 | 0.16 | 0.18 | 0.20 | 0.22 |
| $x_{we}$, $kg_{ref}/kg_{tot}$ | 0.30 | 0.29 | 0.29 | 0.28 | 0.27 |
| $x_{st}$, $kg_{ref}/kg_{tot}$ | 0.50 | 0.49 | 0.48 | 0.46 | 0.45 |
| Qin, kW | 1.978 | 2.047 | 2.117 | 2.184 | 2.256 |
| H11, kJ/kg | 1440.1 | 1454.3 | 1472.4 | 1486.9 | 1499.6 |
| Q8, kW | 0.539 | 0.634 | 0.739 | 0.856 | 0.994 |
| Q10, kW | 0.035 | 0.111 | 0.201 | 0.303 | 0.430 |
| Q11, kW | 1.266 | 1.289 | 1.319 | 1.348 | 1.374 |
| Q12, kW | 0.002 | 0.003 | 0.005 | 0.008 | 0.010 |
| Q16, kW | 0.212 | 0.240 | 0.265 | 0.291 | 0.328 |
| Win, kW | 0.0165 | 0.0183 | 0.0214 | 0.0247 | 0.0281 |
| Wout, kW | 0.0017 | 0.0020 | 0.0023 | 0.0026 | 0.0030 |
| p-eff, % | 10.4 | 10.6 | 10.7 | 10.8 | 11.0 |
| tp-eff, % | 0.79 | 0.83 | 0.86 | 0.89 | 0.93 |
| $F_{right}$, N | 3037 | 3235 | 3444 | 3662 | 3892 |
| $F_{left}$, N | 1230 | 1248 | 1266 | 1285 | 1305 |
| $F_{vap}$, N | 1981 | 2180 | 2388 | 2607 | 2836 |
| $F_{sol}$, N | 175 | 192 | 211 | 230 | 250 |
| $F_{net}$, N | 1807 | 1988 | 2178 | 2377 | 2586 |
| freq, Hz | 0.161 | 0.171 | 0.177 | 0.183 | 0.194 |
| $D_{vap}$, mm | 50 | 50 | 50 | 50 | 50 |
| $D_{sol}$, mm | 20 | 20 | 20 | 20 | 20 |

varying generator temperature -vapour pump

| | | | | | | | |
|---|---|---|---|---|---|---|---|
| Tev, C | -10 | -10 | -10 | -10 | -10 | -10 | -10 |
| Tab, C | 24 | 24 | 24 | 24 | 24 | 24 | 24 |
| $T_{gen}$, C | 64.8 | 74.3 | 78.8 | 83.3 | 87.8 | 92.3 | 96.8 |
| cop | 0.000 | 0.377 | 0.424 | 0.448 | 0.459 | 0.465 | 0.470 |
| REF, kW | 1 | 1 | 1 | 1 | 1 | 1 | 1 |
| $P_h$, bar | 9.43 | 9.43 | 9.43 | 9.43 | 9.43 | 9.43 | 9.43 |
| $P_l$, bar | 2.72 | 2.72 | 2.72 | 2.72 | 2.72 | 2.72 | 2.72 |
| m6, g/s | 0.86 | 0.86 | 0.86 | 0.86 | 0.86 | 0.86 | 0.86 |
| m7, g/s | 3.85 | 15.67 | 9.98 | 7.43 | 5.99 | 5.08 | 4.44 |
| m8, g/s | 2.78 | 14.13 | 8.65 | 6.19 | 4.82 | 3.95 | 3.342 |
| m16, g/s | 0.18 | 0.56 | 0.40 | 0.32 | 0.26 | 0.23 | 0.20 |
| $x_{we}$, $kg_{ref}/kg_{tot}$ | 0.48 | 0.42 | 0.40 | 0.38 | 0.36 | 0.33 | 0.31 |
| $x_{st}$, $kg_{ref}/kg_{tot}$ | 0.48 | 0.48 | 0.48 | 0.48 | 0.48 | 0.48 | 0.48 |
| Qin, kW | | 2.655 | 2.358 | 2.231 | 2.178 | 2.150 | 2.129 |
| H11, kJ/kg | 1472 | 1421 | 1426 | 1431 | 1438 | 1447 | 1448 |
| Q8, kW | 0.739 | 1.440 | 1.066 | 0.913 | 0.847 | 0.805 | 0.769 |
| Q10, kW | 0.201 | 0.816 | 0.520 | 0.387 | 0.312 | 0.264 | 0.231 |
| Q11, kW | 1.319 | 1.235 | 1.244 | 1.254 | 1.265 | 1.280 | 1.297 |
| Q12, kW | 0.005 | 0.001 | 0.001 | 0.002 | 0.002 | 0.003 | 0.004 |
| Q16, kW | 0.265 | 0.796 | 0.570 | 0.452 | 0.380 | 0.332 | 0.298 |
| p-eff, % | 10.7 | 14.6 | 13.0 | 12.1 | 11.6 | 11.2 | 10.9 |
| tp-eff, % | 0.86 | 1.2 | 1.0 | 0.97 | 0.93 | 0.91 | 0.91 |
| $F_{right}$, N | 3444 | 3444 | 3444 | 3444 | 3444 | 3444 | 3444 |
| $F_{left}$, N | 1266 | 1266 | 1266 | 1266 | 1266 | 1266 | 1266 |
| $F_{vap}$, N | 2388 | 2388 | 2388 | 2388 | 2388 | 2388 | 2388 |
| $F_{sol}$, N | 211 | 211 | 211 | 211 | 211 | 211 | 211 |
| $F_{net}$, N | 2178 | 2178 | 2178 | 2178 | 2178 | 2178 | 2178 |
| freq, Hz | 0.177 | 0.525 | 0.377 | 0.301 | 0.254 | 0.222 | 0.199 |
| $D_{vap}$, mm | 50 | 50 | 50 | 50 | 50 | 50 | 50 |
| $D_{sol}$, mm | 20 | 20 | 20 | 20 | 20 | 20 | 20 |

varying generator temperature -vapour pump (cont.)

| | | | | | | | |
|---|---|---|---|---|---|---|---|
| Tev, C | -10 | -10 | -10 | -10 | -10 | -10 | -10 |
| Tab, C | 24 | 24 | 24 | 24 | 24 | 24 | 24 |
| $T_{gen}$, C | 101.3 | 105.8 | 110.3 | 114.8 | 119.3 | 123.8 | 128.3 |
| cop | 0.472 | 0.471 | 0.469 | 0.466 | 0.464 | 0.463 | 0.460 |
| REF, kW | 1 | 1 | 1 | 1 | 1 | 1 | 1 |
| $P_h$, bar | 9.43 | 9.43 | 9.43 | 9.43 | 9.43 | 9.43 | 9.43 |
| $P_l$, bar | 2.72 | 2.72 | 2.72 | 2.72 | 2.72 | 2.72 | 2.72 |
| m6, g/s | 0.86 | 0.86 | 0.86 | 0.86 | 0.86 | 0.86 | 0.86 |
| m7, g/s | 3.978 | 3.627 | 3.351 | 3.128 | 2.944 | 2.79 | 2.66 |
| m8, g/s | 2.902 | 2.569 | 2.307 | 2.096 | 1.922 | 1.776 | 1.651 |
| m16, g/s | 0.19 | 0.17 | 0.16 | 0.15 | 0.14 | 0.13 | 0.13 |
| $x_{we}$, $kg_{ref}/kg_{tot}$ | 0.29 | 0.27 | 0.25 | 0.23 | 0.21 | 0.19 | 0.17 |
| $x_{st}$, $kg_{ref}/kg_{tot}$ | 0.48 | 0.48 | 0.48 | 0.48 | 0.48 | 0.48 | 0.48 |
| Qin, kW | 2.118 | 2.121 | 2.134 | 2.146 | 2.153 | 2.161 | 2.176 |
| H11, kJ/kg | 1469 | 1478 | 1486 | 1495 | 1507 | 1518 | 1528 |
| Q8, kW | 0.744 | 0.735 | 0.736 | 0.734 | 0.725 | 0.715 | 0.714 |
| Q10, kW | 0.207 | 0.189 | 0.175 | 0.163 | 0.153 | 0.145 | 0.138 |
| Q11, kW | 1.314 | 1.330 | 1.345 | 1.362 | 1.382 | 1.403 | 1.423 |
| Q12, kW | 0.005 | 0.006 | 0.008 | 0.009 | 0.011 | 0.013 | 0.016 |
| Q16, kW | 0.272 | 0.251 | 0.235 | 0.221 | 0.210 | 0.201 | 0.193 |
| p-eff, % | 10.7 | 10.6 | 10.5 | 10.3 | 10.3 | 10.2 | 10.1 |
| tp-eff, % | 0.87 | 0.86 | 0.85 | 0.84 | 0.83 | 0.82 | 0.82 |
| $F_{right}$, N | 3444 | 3444 | 3444 | 3444 | 3444 | 3444 | 3444 |
| $F_{left}$, N | 1266 | 1266 | 1266 | 1266 | 1266 | 1266 | 1266 |
| $F_{vap}$, N | 2388 | 2388 | 2388 | 2388 | 2388 | 2388 | 2388 |
| $F_{sol}$, N | 211 | 211 | 211 | 211 | 211 | 211 | 211 |
| $F_{net}$, N | 2178 | 2178 | 2178 | 2178 | 2178 | 2178 | 2178 |
| freq, Hz | 0.182 | 0.168 | 0.157 | 0.148 | 0.141 | 0.134 | 0.129 |
| $D_{vap}$, mm | 50 | 50 | 50 | 50 | 50 | 50 | 50 |
| $D_{sol}$, mm | 20 | 20 | 20 | 20 | 20 | 20 | 20 |

varying the generator temperature -electrical pump

| | | | | | | | |
|---|---|---|---|---|---|---|---|
| Tev, C | -10 | -10 | -10 | -10 | -10 | -10 | -10 |
| Tab, C | 24 | 24 | 24 | 24 | 24 | 24 | 24 |
| $T_{gen}$, C | 64.8 | 69.3 | 73.8 | 78.3 | 82.8 | 87.3 | 91.8 |
| cop | 0.000 | 0.616 | 0.615 | 0.615 | 0.609 | 0.596 | 0.585 |
| REF, kW | 1 | 1 | 1 | 1 | 1 | 1 | 1 |
| $P_h$, bar | 9.43 | 9.43 | 9.43 | 9.43 | 9.43 | 9.43 | 9.43 |
| $P_l$, bar | 2.72 | 2.72 | 2.72 | 2.72 | 2.72 | 2.72 | 2.72 |
| m6, g/s | 0.86 | 0.86 | 0.86 | 0.86 | 0.86 | 0.86 | 0.86 |
| m7, g/s | 27.21 | 18.58 | 9.912 | 7.001 | 5.534 | 4.645 | 4.049 |
| m8, g/s | 26.35 | 17.72 | 9.053 | 6.141 | 4.674 | 3.785 | 3.189 |
| $x_{we}$, $kg_{ref}/kg_{tot}$ | 0.476 | 0.451 | 0.427 | 0.404 | 0.381 | 0.359 | 0.337 |
| $x_{st}$, $kg_{ref}/kg_{tot}$ | 0.476 | 0.476 | 0.476 | 0.476 | 0.476 | 0.476 | 0.476 |
| Qin, kW | | 1.609 | 1.617 | 1.619 | 1.638 | 1.673 | 1.706 |
| H11, kJ/kg | 1411 | 1413 | 1420 | 1425 | 1430 | 1437 | 1446 |
| Q8, kW | 1.797 | 1.353 | 0.901 | 0.742 | 0.676 | 0.653 | 0.641 |
| Q10, kW | 1.417 | 0.967 | 0.512 | 0.365 | 0.288 | 0.242 | 0.211 |
| Q11, kW | 1.219 | 1.223 | 1.234 | 1.243 | 1.253 | 1.264 | 1.278 |
| Q12, kW | 0.000 | 0.000 | 0.001 | 0.001 | 0.002 | 0.002 | 0.003 |

| | | | | | | | |
|---|---|---|---|---|---|---|---|
| Tev, C | -10 | -10 | -10 | -10 | -10 | -10 | -10 |
| Tab, C | 24 | 24 | 24 | 24 | 24 | 24 | 24 |
| $T_{gen}$, C | 96.3 | 100.8 | 105.3 | 109.8 | 114.3 | 118.8 | 123.3 |
| cop | 0.579 | 0.570 | 0.560 | 0.550 | 0.542 | 0.535 | 0.529 |
| REF, kW | 1 | 1 | 1 | 1 | 1 | 1 | 1 |
| $P_h$, bar | 9.43 | 9.43 | 9.43 | 9.43 | 9.43 | 9.43 | 9.43 |
| $P_l$, bar | 2.72 | 2.72 | 2.72 | 2.72 | 2.72 | 2.72 | 2.72 |
| m6, g/s | 0.86 | 0.86 | 0.86 | 0.86 | 0.86 | 0.86 | 0.86 |
| m7, g/s | 3.620 | 3.298 | 3.047 | 2.847 | 2.683 | 2.546 | 2.429 |
| m8, g/s | 2.760 | 2.438 | 2.188 | 1.987 | 1.823 | 1.686 | 1.569 |
| $x_{we}$, $kg_{ref}/kg_{tot}$ | 0.316 | 0.295 | 0.274 | 0.253 | 0.233 | 0.214 | 0.194 |
| $x_{st}$, $kg_{ref}/kg_{tot}$ | 0.476 | 0.476 | 0.476 | 0.476 | 0.476 | 0.476 | 0.476 |
| Qin, kW | 1.730 | 1.753 | 1.782 | 1.814 | 1.844 | 1.868 | 1.889 |
| H11, kJ/kg | 1457 | 1468 | 1477 | 1485 | 1494 | 1505 | 1517 |
| Q8, kW | 0.628 | 0.618 | 0.618 | 0.627 | 0.633 | 0.631 | 0.627 |
| Q10, kW | 0.189 | 0.172 | 0.159 | 0.148 | 0.140 | 0.133 | 0.126 |
| Q11, kW | 1.295 | 1.312 | 1.328 | 1.343 | 1.360 | 1.380 | 1.401 |
| Q12, kW | 0.004 | 0.005 | 0.006 | 0.007 | 0.009 | 0.011 | 0.013 |

# Appendix H

## The pneumatic circuit to drive the control shaft

The circuit employed to drive the control shaft is shown in figure H.1. The double acting cylinder performs reciprocating movements without using limit switches. Instead, time elements are used to effect reversal. The frequency of the stroke can be changed time-dependently.

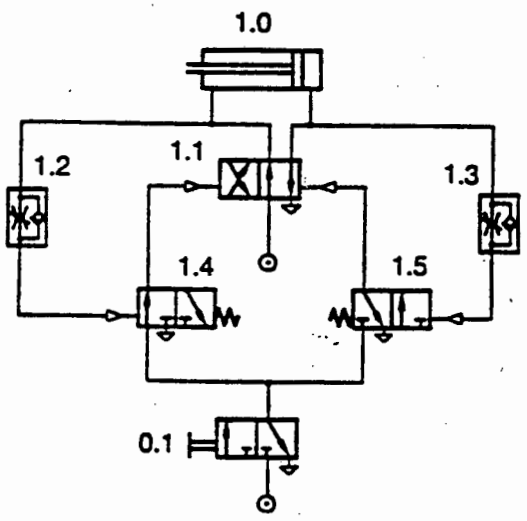


**Figure H.1** The pneumatic circuit for a reciprocating cylinder

with the symbols in figure H.1 representing the following components:

| | |
|---|---|
| 1.0 | differential cylinder with single-ended piston rod |
| 1.1 | 4/2 way valve |
| 1.2 | throttle relief valve, adjustable |
| 1.3 | throttle relief valve, adjustable |
| 1.4 | spring activated 3/2 way valve |
| 1.5 | spring activated 3/2 way valve |
| 0.1 | 3/2 way valve, neutral postion closed |

The two time switches were set and the following stroke frequencies recorded.

| time switch setting left | time setting setting right | time for 10 return strokes [sec] | frequency [Hz] |
|---|---|---|---|
| 8.40 | 8.40 | 34.3 | 0.292 |
| 8.60 | 8.60 | 38.2 | 0.262 |
| 8.80 | 8.80 | 43.5 | 0.230 |
| 9.00 | 9.00 | 49.0 | 0.204 |
| 9.20 | 9.20 | 55.7 | 0.180 |
| 9.40 | 9.40 | 66.1 | 0.151 |
| 9.00 | 4.00 | 29.8 | 0.336 |
| 9.00 | 7.00 | 34.5 | 0.290 |
| 9.50 | 4.00 | 38.7 | 0.258 |
| 9.50 | 4.50 | 39.4 | 0.254 |
| 9.50 | 5.00 | 39.9 | 0.251 |
| 9.80 | 5.00 | 48.5 | 0.206 |
| 9.90 | 5.00 | 57.1 | 0.175 |
| 10.00 | 5.00 | 63.0 | 0.159 |

**Table H.1** stroke frequency as a function of time delay valve setting

# Appendix I

## The composition of the burner fuel gas

The gas used in the burner is supplied by the Capegas gas works, Woodstock. The composition of the gas is as follows:

| *Compound* | *Chemical formula* | *percentage* |
|---|---|---|
| Carbon dioxide | $CO_2$ | 4.2 |
| Oxygen | $O_2$ | 0.6 |
| Carbon monoxide | CO | 19.0 |
| Methan | $CH_4$ | 19.0 |
| Hydrogen | $H_2$ | 45.0 |
| Nitrogen | $N_2$ | 9.0 |
| Heavy hydrocarbons | | 3.2 |

The calorific value (heat of combustion) of the gas is given as 16.76 $MJ/m^3$.

# Appendix J

## The fuel energy conversion factor

The heat input to the generator depends on the gas flow rate through the burner and upon the temperature of the solution in the generator. Vicatos [24] has in his experiments calculated the heat input as a function of the solution temperature, heat transfer coefficient and gas temperature difference. The calculated heat input devided by the calorific value of the gas is defined as the energy conversion factor. Using Vicatos' data a polynomial was created that gives the conversion factor as a function of the gas flow rate and solution temperature.

| *gas flow rate* | *calorific value* | *solution temperature* | *heat input* | *conversion factor* |
|---|---|---|---|---|
| *l/sec* | *kW* | *C* | *kW* | |
| 0.52 | 8.72 | 69.0 | 2.17 | 0.249 |
| 0.53 | 8.88 | 71.0 | 2.17 | 0.244 |
| 0.54 | 9.05 | 79.4 | 2.14 | 0.237 |
| 0.59 | 9.89 | 87.5 | 2.24 | 0.227 |
| 0.72 | 12.07 | 93.6 | 2.58 | 0.214 |
| 0.80 | 13.41 | 103.8 | 2.73 | 0.203 |
| 0.84 | 14.08 | 111.4 | 2.76 | 0.196 |
| 0.88 | 14.75 | 117.4 | 2.82 | 0.191 |
| 1.10 | 18.44 | 126.7 | 3.29 | 0.179 |
| 1.16 | 19.44 | 131.4 | 3.39 | 0.174 |
| 1.28 | 21.45 | 133.2 | 3.65 | 0.170 |
| 1.50 | 25.14 | 135.9 | 4.11 | 0.163 |

The polynomial $\eta = a\dot{V} + \frac{b}{\dot{V}} + cT + \frac{d}{T}$ accurately evaluates the conversion efficiency. A regression was performed to obtain the coefficients:

Regression output:

| | | |
|---|---|---|
| Constant | : | 0.192276 |
| Std err of y est | : | 0.000782 |
| R squared | : | 0.999566 |
| No of observations | : | 12 |
| Degrees of freedom | : | 7 |

| | | |
|---|---|---|
| X coefficients | : -0.01208 | a |
| | 0.021506 | b |
| | -0.00035 | c |
| | 3.111921 | d |

## Appendix K

### Analysis of causes for the failure of the link mechanism

The spring fails in either of three ways:

*type 1 failure:* The pump pistons have travelled the full stroke of 25 mm, yet the compressed spring has not released the spring plunger. The precompression of the spring can be increased to the maximum allowed by the dimensions of the link mechanism. If the spring still fails to move the control shaft, the spring stiffness is to low. One method to overcome this problem is shown in figure K.1.

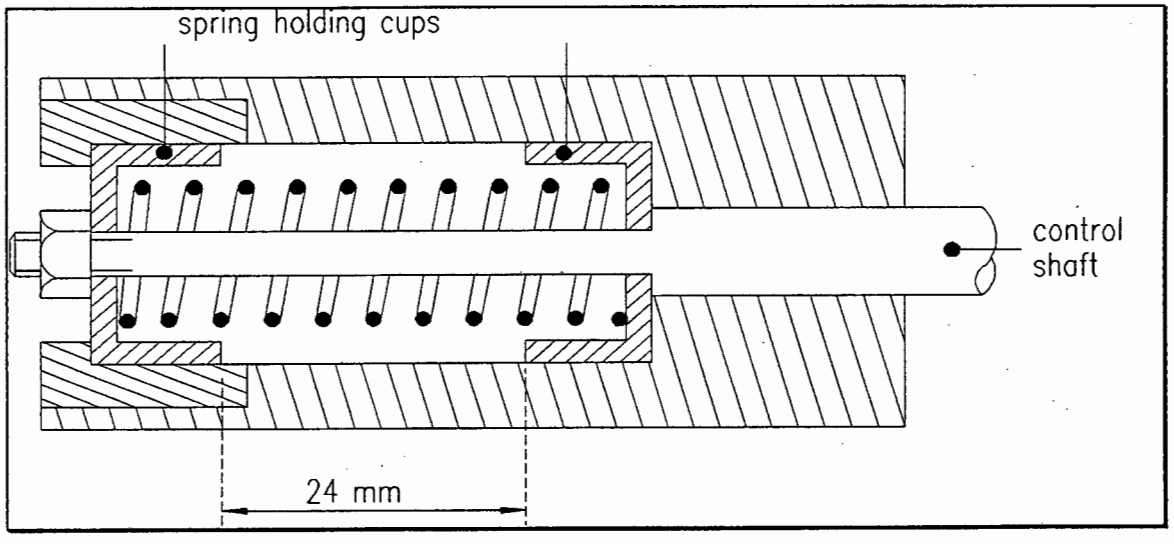


**Figure K.1** Spring chamber with spring holding cups

A holding cup at either end holds the spring in place. The cups are dimensioned so that they are apart a distance just less than the stroke length. Just before the pump pistons

reach the end of their stroke the two holding cups come into solid contact and force the spring plunger to release the control shaft from its end position. Once released, the spring might now push the control shaft to the opposite end position or might end up as a type 2 failure.

*type 2 failure:* The pump pistons have travelled the full stroke of 25 mm and the spring plunger has released the control shaft, either because the spring in the link has exerted a force big enough to overcome the resistance of the spring plunger, or by means of the holding cup method. The control shaft, however, does not move all the way to the opposite end position. As a result the pressure ports are not switched over and the pumps stop motion. Nothing can be done to remedy this situation. Precompressing the spring further would result in releasing the spring plunger to early (type 3 failure).

*type 3 failure:* The spring plunger releases the control shaft before the pump pistons reach the end of the stroke. The control shaft cuts of the high pressure line while the pump pistons are still in motion. As a result the pump pistons stop movement and in turn prevent the control shaft from reaching the opposite end position (the control shaft can only move as far as the link mechanism and pump shaft assembly). With the control shaft not being able to move the required 25 mm necessary to open the return high pressure line, movement of pumps and control shaft ceases altogether. The strength of the spring plunger can now be increased to retard the moment of releasing the control shaft. Three spring plungers equally spaced at 120 degrees to each other, instead of the original one, were experimented with.

Numerous springs were experimented with, taking into account all of above considerations. Since the spring can only operate on the fine line between releasing to early (type 3 failure) and not releasing at all (type 1 failure) the spring needs very accurate adjustment of the amount of precompression. The inherent inconstancies of the system, be it because of misalignment, inaccuracies in the manufacture or asymmetry, proved to be greater than allowed by the successful spring operation. The force required for the forward stroke of the control shaft does not equal that one of the return stroke. Sometimes even the exact same setting of the spring would work for one forward stroke, but not for the next. The spring mechanism never worked reliably, and it was consequently decided to simulate the mechanism by a pneumatic system.